Advanced Relaying Methods for One-Way and Two-Way Communication

Vom Fachbereich 18 Elektrotechnik und Informationstechnik
der Technischen Universität Darmstadt
zur Erlangung der Würde eines Doktor-Ingenieurs (Dr.-Ing.) genehmigte

Dissertation

von
Dipl. Ing. Dipl. Math. Adrian Schad,
geboren am 27 Juli 1982 in Schweinfurt, Deutschland.

Referent:	Prof. Dr. Marius Pesavento
Korreferent:	Prof. Dr. Sergiy A. Vorobyov
Tag der Einreichung:	16. Oktober 2014
Tag der mündlichen Prüfung:	29. Oktober 2014

D17
Darmstadt 2015

Acknowledgments

First, I would like to thank Professor Marius Pesavento for supervising and supporting this thesis. His advices helped me a lot during my time as a research assistant.

I am especially indebted to Professor Alex Gershman, who brought me to his research group. May he rest in peace.

I am grateful to Haihua Chen for her support during my first year. Also, I want to give thanks to Edwin Mabande and Walter Kellermann, who introduced me to the field of beamforming.

Moreover, I want to give thanks to Dana Ciochina, Ka Lung Law, Nastasja Kolb, Oscar Ramos, Pouyan Parvazi, Samer Alabed, Xin Wen, Xin Zhang, and Yong Cheng for proofreading an earlier version of this thesis. Furthermore, I would like to thank everyone in our group for the good time.

Above all, I am thankful to my family for their love and encouragement.

Zusammenfassung

Relais werden in drahtlosen Kommunikationssystemen verwendet, um Sendesignale zu empfangen und weiterzuleiten. Sie können die Netzabdeckung im Mobilfunk erhöhen und machen die Funkkommunikation robust gegenüber Schwankungen der Empfangsfeldstärke, indem sie zusätzliche Signalpfade schaffen.

In dieser Dissertation werden neuartige Verfahren für die Einweg-Kommunikation und Zweiweg-Kommunikation in drahtlosen Relais-Netzwerken vorgeschlagen. Zudem werden für diese Verfahren die bestmöglichen Relais-Parameter gesucht, die bestimmte Optimierungsziele erfüllen. Ein Optimierungsziel ist, bei kleinstmöglicher Sendeleistung eine ausreichend hohe Signalqualität bei den Empfängern zu erreichen. Ein weiteres Ziel ist die Signalqualität zu maximieren, während die Sendeleistung begrenzt ist.

Für die Einweg-Übertragung werden Systeme zur Kommunikation über frequenzselektive Funkkanäle vorgestellt, welche zu Intersymbolinterferenzen (ISI) führen. Zunächst wird eine Informationsquelle betrachtet, die über Relais Signale an mehrere Empfänger sendet. Hierbei erhält jeder Empfänger unterschiedliche Daten. Sowohl die Informationsquelle als auch die Relais sind mit mehreren Antennen ausgerüstet. Durch lineare Filter an den Relais können in diesem System sowohl ISI als auch Interferenzen der verschiedenen Sendesignale abgeschwächt werden. Außerdem wird gezeigt, wie eine lineare Vorverarbeitung an der Informationsquelle die Signalqualität an den Empfängern verbessert. Aus dem Relais-System mit einer einzelnen Informationsquelle und mehreren Empfängern wird ein Peer-to-peer-System abgeleitet. In diesem senden mehrere Informationsquellen Daten über ein Relais-Netzwerk an mehrere Empfänger. Durch Vergrößern der Relais-Filterlänge wird die Signalqualität an den Empfängern deutlich verbessert.

Für Relais-Netzwerke, in denen die Funkkanäle einen flachen Frequenzgang aufweisen, wird ein neuartiges Multicast-Verfahren vorgestellt. In diesem Verfahren werden dieselben Daten an mehrere Empfänger gesendet. Die Relais verwenden das Amplify-and-forward-Protokol, um ihre Empfangssignale mit Gewichtsfaktoren zu skalieren und deren Phasen anzupassen. Um die Anzahl der Freiheitsgrade zu erhöhen, wird eine Rang-Zwei-Strahlformungsmethode eingesetzt. Mit dieser Methode werden zwei Kommunikationskanäle von der Informationsquelle zu jedem Empfänger er-

zeugt. Mit einem iterativen Algorithmus werden sowohl die Relais-Gewichtsfaktoren als auch die optimalen Sendeleistungen der Informationsquelle und der Relais berechnet.

Anschließend wird die bidirektionale Zweiweg-Kommunikation eines einzelnen Benutzerpaares unter der Verwendung von Amplify-and-forward Relais betrachtet. Es werden drei verschiedene bidirektionale Übertragungsmethoden anhand ihrer maximalen Übertragungsrate verglichen.

Danach wird die bidirektionale Kommunikation eines einzelnen Benutzerpaares auf mehrere Paare verallgemeinert. Um die Interferenzen im Netzwerk, die aufgrund der Mehrbenutzerkommunikation auftreten, gering zu halten, werden Vielfachzugriffsverfahren eingeführt.

Für die bidirektionale Kommunikation eines einzelnen Benutzerpaares über ein Amplify-and-forward-Relais wird ein differenzielles Verfahren zur Bestimmung der Gewichtsfaktoren vorgeschlagen. Dieses Verfahren benötigt keine expliziten Informationen über die Funkkanäle, ist einfach zu implementieren und kann leicht an andere Relais-Protokolle angepasst werden.

Abstract

In wireless communication, relays are devices that receive and forward radio signals. Relays are attractive as they can increase the coverage of cellular networks. Moreover, relays improve the robustness of the wireless radio communication as they create additional signal paths.

In this thesis, we propose novel schemes for one- and two-way communication in wireless relay networks. We aim to select the optimum relaying parameters by meeting two different design goals. The first goal is to minimize the transmit power where we assume constraints on the signal quality at the receivers. The second goal is to maximize the signal quality where we assume that the transmit power is limited.

For one-directional communication, we propose schemes for communication over frequency selective radio channels that lead to inter-symbol- interference (ISI). First, we consider a multi-antenna source that transmits individual data streams to multiple destinations via multi-antenna relays. The proposed relaying scheme mitigates ISI as well as multi-user interference by using linear filters at the relays. Moreover, we demonstrate that linear precoding at the source efficiently improves the signal quality at the destinations. Then, we show that the latter scheme with a single source and multiple destinations includes the multi-user peer-to-peer (p2p) relaying scheme as a special case. In the p2p scheme, multiple source terminals transmit messages to multiple destination terminals via a network of relays. The simulation results demonstrate that increasing the relay filter length substantially improves the signal quality at the destinations.

For relay networks with frequency-flat channels, we propose a novel multicasting scheme where a single source transmits common information to multiple destinations. The relays use the amplify-and-forward (AF) protocol to scale and adjust the phases of their received signals by using weight coefficients. To increase the number of degrees of freedom in the system, a rank-two beamforming method is used to create two communication links from the source to each destination. We propose an iterative algorithm that computes the relay weights and the optimal transmit power of the source and the relays.

For bi-directional two-way AF relay communication, we first consider a single user pair. We analytically compare three different bi-directional schemes by their maximum rate.

Then, we generalize the bi-directional communication of a single user pair to multiple pairs using an AF relay network. To limit the multi-user interference in the network, we propose to use novel multiple access schemes.

For the bi-directional communication of a single user pair via a multi-antenna relay, a new differential scheme is proposed that allows to compute the relay weights without explicit knowledge of the communication channels. The proposed scheme is easy to implement and can be adapted to other relaying protocols.

Table of Contents

Acknowledgments i

Zusammenfassung iii

Abstract v

Table of Contents vii

List of Figures ix

Notation xiii

Acronyms xvii

1 Introduction 1
- 1.1 Applications of relays . . . 1
  - 1.1.1 Relays in modern cellular networks . . . 2
  - 1.1.2 Cooperative relaying in ad hoc networks . . . 3
- 1.2 Relaying modes and protocols . . . 4
  - 1.2.1 Relaying modes . . . 4
  - 1.2.2 Relaying protocols in the LTE standard . . . 5
- 1.3 Scope and vision of this work . . . 6
- 1.4 Background and contributions . . . 7

2 Signal models and network optimization 13
- 2.1 SISO channel models . . . 13
- 2.2 AF relaying . . . 14
  - 2.2.1 One-directional AF relaying . . . 14
  - 2.2.2 Bi-directional AF relaying . . . 15
- 2.3 Network optimization using CSI . . . 17
- 2.4 Mathematical optimization methods . . . 21

3 Multi-user Filter-and-forward relaying 25
- 3.1 Introduction . . . 25
- 3.2 Multi-user downlink transmissions with precoding and channel equalization . . . 27
  - 3.2.1 Signal model . . . 27

3.2.2 SINR maximization . . . 31
3.2.3 Simulation results . . . 37
3.3 Peer-To-Peer Relay Beamforming . . . 40
3.3.1 Relay sum power minimization . . . 41
3.3.2 SINR maximization . . . 42
3.3.3 Simulation results . . . 43
3.4 Conclusion . . . 49

4 Rank-Two Beamforming and Power Allocation in Multicasting Relay Networks 51
4.1 Introduction . . . 51
4.2 Signal model . . . 53
4.3 Beamformer design and power allocation . . . 59
4.3.1 Rank-two property and relation of the Rank-2-AFMS to the Rank-1-AFMS . 60
4.3.2 Convex inner approximation technique . . . 63
4.4 Simulation results . . . 66
4.5 Conclusion . . . 69

5 Rate maximization in one- and bi-directional single-user networks 73
5.1 Introduction . . . 73
5.2 The one-directional scheme . . . 74
5.3 The bi-directional two time slot scheme . . . 77
5.4 The bi-directional four time slot scheme . . . 78
5.5 The bi-directional three time slot scheme . . . 79
5.6 Numerical results . . . 81
5.7 Conclusion . . . 81

6 Multiuser bi-directional relay networks 85
6.1 Introduction . . . 85
6.2 Signal model . . . 86
6.3 SINR maximization . . . 88
6.3.1 Solution to the max-min fairness problem for $N < M$ . . . 90
6.3.2 Solution to the max-min fairness problem for $N = M$ . . . 91
6.4 Simulation results . . . 92
6.5 Conclusion . . . 95

7 Differential beamforming 97
7.1 Introduction . . . 97
7.2 Signal model . . . 98
7.3 The differential beamforming scheme . . . 100
7.4 Analysis for the high power regime and power allocation . . . 103
7.5 Simulation Results . . . 105
7.6 Conclusion . . . 107

8 Conclusions and future work 109
8.1 Conclusions . . . 109
8.2 Future work . . . 112

A DC programming theorem **115**

B Convolution matrices **117**

C Power and matrix calculation **121**
C.1 Power and matrix calculation for Chapter 3 121
C.1.1 Relay transmit power as a function of the filter weight vector 121
C.1.2 Relay transmit power as a function of the precoding weights 122
C.1.3 Covariance matrices for the destination filter weights 123
C.1.4 Covariance matrices for the precoding filter weights 123
C.2 Power and matrix calculation for Chapter 4 124

Bibliography **126**

Résumé **141**

List of Figures

1.1 Bi-directional transmission schemes: (a) Four time slot transmission, (b) two time slot transmission, (c) three time slot transmission, •: Transceiver, ○: Relay. 8
1.2 Single user pair communication. Blue: Relay network. Green: User pair. 8
1.3 Multi-user p2p communication. Blue: Relay network. Else: User pairs. 8
1.4 Multi-user downlink communication. Blue: Relay network. Red: Source. Else: Destinations. 8
1.5 Single-group multicasting. Blue: Relay network. Red: Source. Green: Destinations. 9

2.1 The relay network. ⊗: Source, ○: Relay, •: Destination. 16

3.1 Setup of the network; ⊗: Source, ○: Relay, •: Destination. 38
3.2 SINR versus the destination filter length L_u. 39
3.3 SINR versus the relay filter length L_w. 39
3.4 SINR versus the source filter length L_a. 40
3.5 Filter-and-forward relay network. 41
3.6 Relay sum power P_{R} versus required SINR; first example. 46
3.7 Relay sum power P_{R} versus relay filter length L_w; first example. 46
3.8 SINR versus the maximum individual relay transmit power $p_{\max}$; second example. . 47
3.9 SINR versus relay filter length L_w; second example. 47
3.10 SINR versus the maximum relay sum power $P_{\mathrm{R,max}}$; third example. 48
3.11 SINR versus relay filter length L_w; third example. 48
3.12 SINR versus the relay filter length L_w; fourth example. 49

4.1 Multicasting via a relay network; ⊗: Source, ○: Relay, •: Destination. 53
4.2 Proposed Alamouti Coded AFMS; ⊗: Source $\mathcal{S}$, ○: Relays, •: Destinations. 54
4.3 Setup of the network; ⊗: source, ○: relay, •: destination. 68
4.4 Minimum rate versus total power $P_{T,\max}$, first example. 70
4.5 Minimum rate versus total power $P_{T,\max}$, first example. 70

4.6 Minimum rate versus number of destinations M, first example. 71
4.7 Minimum rate versus number of destinations M, first example. 71
4.8 Minimum SNR versus number of iterations. 72

5.1 Rate versus the total available power. 82
5.2 Rate versus the total number of relays. 82
5.3 Rate versus σ_f^2. 83

6.1 Example: $M = 3$, $N = 2$, $\mathcal{Q}_1 = \{1, 3, 4, 6\}, \mathcal{Q}_2 = \{2, 5\}$, $\circ$: Relay, $\bullet$: Transceiver. . . 87
6.2 First example, $N = 1$. Minimal rate versus the available relay transmit power. . . . 93
6.3 First example, $N = 1$. Minimal SINR versus the number of transceiver pairs M. . . 93
6.4 Second example. Minimal rate versus the relay transmit power. 94

7.1 BER versus transmit power P for differential and non-differential schemes using QPSK in an urban micro scenario, v =0 km/h. 105
7.2 BER versus velocity v for differential and non-differential schemes using QPSK in an urban micro scenario, $P = 17$dBm. 106

Notation

$\delta(\cdot)$	Dirac function
$\mathrm{E}\{\cdot\}$	statistical expectation operation
arg	phase of a complex number
$\|\cdot\|_F$	Frobenius norm of a matrix
$\|\cdot\|$	Euclidean norm of a vector
$\|\cdot\|$	absolute value
δ_{ij}	Kronecker delta
$\mathbf{I}$	identity matrix
$\mathbf{I}_n$	$n \times n$ identity matrix
$\mathrm{tr}(\cdot)$	trace of a matrix
$[\mathbf{v}]_i$	ith entry of vector $\mathbf{v}$
$[\mathbf{A}]_{i,:}$	ith row of matrix $\mathbf{A}$
$[\mathbf{A}]_{:,j}$	jth column of matrix $\mathbf{A}$
$[\mathbf{A}]_{ij}$	(i,j)th entry of matrix $\mathbf{A}$
$\mathbf{0}$	zero vector
$\mathbf{0}_n$	$n \times 1$ zero vector
$\mathbf{O}_n$	$n \times n$ zero matrix
$\mathrm{diag}(\mathbf{v})$	diagonal matrix whose diagonals are the entries of $\mathbf{v}$
$\mathrm{blkdiag}([\mathbf{Y_1}, \mathbf{Y_2}, \ldots])$	block diagonal matrix having the matrices $\mathbf{Y_1}, \mathbf{Y_2}, \ldots$ on its diagonal
$\mathrm{vec}\{\mathbf{A}\}$	vector which has the columns of the matrix $\mathbf{A}$ stacked one over another
$\mathbf{1}_n$	$n \times 1$ vector with all entries equal to one
$\mathbf{e}_j$	identity vector: a vector whose jth entry is one and the rest are zero

$\mathbf{E}_j = \text{diag}\{\mathbf{e}_n\}$	
$\check{\mathbf{E}}_j = \mathbf{I} - \mathbf{E}_j$	
$\mathbf{A} \otimes \mathbf{B}$	Kronecker matrix product
$(\cdot)^T$	transpose
$(\cdot)^*$	complex conjugate
$(\cdot)^H$	transpose complex conjugate (Hermitian) operation
$\approx$	approximately equal
$\doteq$	equal up to the first order
$\Re(\cdot)$	real part
$\Im(\cdot)$	imaginary part
$\in$	membership
ω	normalized frequency
κ	iteration index
t	time
M	number of destinations
K	number of sources
R	number of relays
η	relay noise
$\boldsymbol{\eta}$	relay noise vector
ν	receiver noise
s	information-bearing symbol
x	signal received at a relay
$\mathbf{x}$	vector of signals received at the relay(s)
$\mathbf{t}$	vector of signals received at the relay(s)
y	signal received at a destination
f	source-to-relay channel coefficient
g	relay-to-destination channel coefficient
w	relay weight coefficient
$\mathbf{w}$	relay weight vector

$\mathbf{W}$	relay weight matrix
$\mathcal{D}_m$	mth destination
$\mathcal{S}_k$	kth source
$\mathcal{R}_r$	rth relay
$\mathcal{T}_m$	mth transceiver
L	FIR filter length of source-to-relay and relay-to-destination channels
L_w	relay filter length
L_u	destination filter length
N_R	number of relay antennas
N_S	number of source antennas
P_{R}	relay sum power
$P_{\mathrm{R,max}}$	maximum relay sum power
p_r	transmit power of relay $\mathcal{R}_r$
$p_{r,\mathrm{max}}$	maximum transmit power of relay $\mathcal{R}_r$
P_k	transmit power of the kth source/transceiver
P_{S}	transmit power of the source (single source case)
$P_{\mathrm{S,max}}$	maximum transmit power of the source (single source case)
P_{T}	total network transmit power
$P_{\mathrm{T,max}}$	maximum total network transmit power
σ^2	noise power
γ	minimum QoS in terms of SNR/SINR
γ_m	minimum QoS in terms of SNR/SINR at the mth transceiver/destination

Acronyms

AF	amplify-and-forward
AFMS	amplify-and-forward multicasting system
BER	bit error rate
BPSK	binary phase-shift keying
CSI	channel state information
DBF	differential beamforming
DD	distributed differential
FF	filter-and-forward
FIR	finite-impulse-response
INR	interference-to-noise ratio
ISI	inter-symbol-interference
LTE	long term evolution
MIMO	multiple-input multiple-output
MISO	multiple-input-single-output
MUI	multi-user interference
OFDM	orthogonal frequency-division multiplexing
QCQP	quadratically constrained quadratic program
QoS	quality-of-service
RF	radio frequency
SDP	semidefinite program
SDR	semidefinite relaxation
SI	self-interference

SINR	signal-to-interference-plus-noise ratio
SISO	single-input-single-output
SNR	signal-to-noise ratio
STBC	space-time block coding
STC	space-time coding
TDMA	time division multiple access
UMTS	universal mobile telecommunications system

Chapter 1

Introduction

Radio broadcasting and mobile telephony are examples of services enabled by wireless communication. In wireless communication, electromagnetic radio waves carry the information signal sent by a source to a destination. Due to the open nature of the radio connection, the received signal suffers from attenuation due to path loss effects and signal shadowing when obstacles are located between the source and the destination. Moreover, multipath propagation due to reflections leads to the constructive and non-constructive superposition of multiple copies of the transmitted signal. If the direct radio connection between the source to the destination is too weak to be used for communication because of the mentioned signal fading effects, a relay station can forward signals from the source to the destination.

In the last decade novel applications have pushed the academic and industrial research on wireless communication via relays that has already been started in the 1970's with early works on relay channels. In this chapter, we introduce cellular networks and ad hoc networks that are typical applications of the novel relaying techniques developed in this thesis. Then, we present an overview of the existing relaying techniques and define the scope and the motivation of this work. Finally, an outline of the thesis and its contributions will be given.

1.1 Applications of relays

Wireless networks aim to meet user and service demands such as a data rate services under restrictions on the transmit power due to spectrum regulations and hardware constraints. Moreover, transmit power is usually strictly limited to avoid interference of radio signals and to save energy. Therefore, the fading effects cannot be simply compensated by increasing the signal strength and the radio connections in the wireless network may be too weak to be used. Consequently, one major

challenge of wireless networks is to guarantee the coverage.

In the following we review network types for which relaying is a prominent candidate to extend the coverage.

1.1.1 Relays in modern cellular networks

The information exchange between two mobile terminals in a cellular network is organized as follows: Each mobile terminal exchanges data with its assigned base station which is connected to a wire-line backbone network. In this network topology the bottleneck of the data exchange is the wireless connection of the terminals to the base station as this connection suffers from signal fading and crosstalk.

The complexity of providing coverage in cellular networks is mainly determined by the mobile terminals located at the cell edges [1]. These terminals have the longest physical distance to the base station and, consequently, suffer the most from signal attenuation due to path loss. Moreover, the cell edge users also suffer the most from inter-cell interference as their distance to the neighboring base stations is short compared with that of the users inside the cell. It is in particular challenging to establish the coverage of a cellular network that works at high frequencies as the signal attenuation increases at shorter wavelengths. However, wireless services such as video streaming and file transfer demand high data rates that can only be fulfilled by using large bandwidths which require communication at high carrier frequencies.

Note that nowadays, most of the traffic of the mobile terminals is no longer dominated by the classical voice calls but by mobile broadband data, i.e., internet applications via portable modems. To provide high data rate services, releases of the long term evolution (LTE) and LTE-Advanced standard for mobile communication support bandwidths up to 100 MHz at carrier frequencies above 2 GHz [2].

To establishing high data rate communication at high carrier frequencies by simply increasing the transmit power in cellular networks is usually not a feasible option due to interference limitations. To increase the coverage nevertheless, one approach is to decrease the size of the cell by reducing the signal attenuation caused by path loss. This, in turn, leads to a higher number of base stations. The latter approach has been made with heterogeneous networks including pico- and femtocells. However, for these cell types a costly wired *backhaul link* link (i.e., the link from the base station to the relay station) is required. As a cheap alternative to use more base stations, relay stations are integrated into the LTE-Advanced release to reduce the path loss and attenuation of the signal from the mobile terminals to the base station. Relays forward messages from the base station to the

mobile terminals and vice versa. From the mobile terminal point of view, the relay appears to be a base station whereas from the base station point of view, the relay is considered to be a mobile terminal. Hence, relays can be integrated into existing cellular networks using wide range macro cells.

Reducing the path loss, relays are also a prominent candidate to extend the outdoor macro coverage of cellular networks to coverage inside buildings, where the radio signal is severely attenuated during the building penetration [3] - [5].

1.1.2 Cooperative relaying in ad hoc networks

An ad hoc network is formed by a set of nodes which organize communication among each others themselves. Since a particular infrastructure is not provided, the terminals communicate peer-to-peer (p2p) in the sense that there exist no central nodes which direct the data traffic. This is in contrast to cellular networks, where the communication is realized through base stations. One example of an ad hoc networks is the wireless local area network, where relays increase both the coverage and the throughput [6], [7]. Another example is the wireless sensor network, where a large number of sensor nodes intend to communicate measurement data within the network [8], [9]. The most important resource of each sensor node is the energy of its battery which is not rechargeable within a short time or is not rechargeable at all [7], [10]. To save power, transmitting at high power may therefore not be permitted. However, due to the fading effects in the wireless communication, the direct radio connection between sensor nodes can be weak. To enable low power transmissions, some terminals can operate as relays and provide their resources to set up the communication between other terminals via two or multiple hops.

We remark that each relay creates additional signal paths resulting in additional spatial diversity. Diversity is desirable, as it increases the reliability of the wireless communication. As the spatial diversity in a relay network is created by cooperation among terminals, it is referred to as *cooperative diversity* [13]–[15].

Cooperative diversity is established by distributed systems whereas centralized systems benefit from multiple antennas which create multi-antenna diversity. In a distributed relay system each relay processes its signals independently of other relays. On the contrary, a single centralized multi-antenna system benefits from jointly processing the signals but is usually limited very in its size whereas the relays can widely distributed in space.

Many cooperative relaying schemes can be viewed as distributed versions of existing centralized

multi-antenna schemes. For instance, beamforming and space-time-coding (STC) schemes have originally been developed for centralized antenna arrays. These techniques have been adapted for virtual antenna arrays consisting of a group of distributed and non-connected relays [16]–[24]. Distributed relaying systems are especially attractive if side-conditions on the complexity, the size, and the price do not allow to equip the wireless terminals with more than one antenna. Due to the cheapness and flexibility of relays, employing them in mobile ad hoc networks is a promising technology path.

1.2 Relaying modes and protocols

Let us review basic concepts which define how relays receive, process, and send radio signals.

1.2.1 Relaying modes

In-band and out-band relaying

To avoid interference between the received and the transmitted signals, the relay transmission and reception have to be orthogonal to each other [11]. Orthogonality can be achieved in frequency, in time or in space. Relays can either operate in out-band or in in-band mode. For out-band relays, the spectrum of the received and transmitted signals do not overlap and, therefore, the receive and transmitted signals do not interfere. Consequently, out-band relays can work in full duplex mode, i.e., they are able to receive and transmit simultaneously. The advantage of out-band relays is that integrating them in an LTE-Advanced network does not require changes in the lower layers of the protocol stack [25]. A drawback of out-band relaying is however that two different carriers for transmission and reception are required. For in-band relays, the receiving and transmitting of radio signals takes place in the same frequency spectrum. To avoid self-interference (SI), that is interference of received signal with the transmitted signal, in-band relays operate in half duplex mode. In other words, they either transmit or receive but not simultaneously. In-band full duplex relaying is difficult as the power of the transmitted signal is orders of magnitude higher than the received signal power. Consequently, even a small error in the SI cancellation has a tremendous negative impact on the signal quality [12]. For in-band relays in cellular networks, during transmissions to the base station, it is therefore not possible to receive data from the users. Moreover, relays cannot transmit to users when they are supposed to receive signals from the base station. Therefore, the users must not expect to be served by the relays during relay-to-base station transmissions. To integrate relay-to-base station transmissions in the LTE-Advanced framework, the multimedia broadcast multicast service frame can be used [44].

One-directional and bi-directional relaying

In half-duplex in-band relaying, the communication of one information-bearing symbol from the source to the relay and from the relay to the destination requires at least two time slots. Extending this two time slot scheme to the bi-directional exchange of information between a pair of transceivers leads to a four time slot scheme, see Figure 1.1 (a). To overcome the loss in spectral efficiency, the bi-directional relay schemes of Figures 1.1 (b) and (c) communicate two information-bearing symbols in less than four time slots. In the scheme (b), for example, the complete exchange of two information-bearing symbols is performed in two time slots.

1.2.2 Relaying protocols in the LTE standard

In this thesis, relays are categorized based on their relaying protocols which specify how a relay processes its received signals before retransmitting them. Let us review two of the most popular relaying protocols.

A simple relay type is the amplify-and-forward (AF) relay. AF relays are referred to as repeaters, analog relays, or non-regenerative relays. In AF relaying, the signal received at the relay is weighted by a complex coefficient to adjust the amplitude and phase to establish a coherent re-transmission. Note that the whole received signal, which includes the useful signal part, the relay receiver noise, and interference that may be contained, is forwarded. Despite the drawback of noise and interference amplification, AF relaying has gained much interest in the current research due to its low complexity [16]–[24], [26]–[41]. Moreover, AF relaying can be integrated into existing cellular networks as AF relays are transparent to both the base station and the users [2]. In other words, both base station and users are unaware of the AF relay.

A second relaying protocol supported by the LTE standard is decode-and-forward (DF) relay type. DF relays are also known as digital relays or regenerative relays. The processing of the received signals in DF relaying is more complex compared with AF relaying as DF relays decode and re-encode the messages contained in the incoming signals [42], [43]. In contrast to an AF relay, it is possible to rebuild a noise- and interference-free signal at a DF relay if the decoding is successful. However, decoding and re-encoding implies a larger delay as compared with AF relaying [25]. In a study for the LTE-Advanced standard, two main types of DF relays were considered [44]. The “Type 1“ relay is non-transparent and appears as a regular base station to the users. Type 1 relays have their own physical cell identity, transmit their own reference symbols and provide the users with scheduling information and hybrid automatic repeat request feedback. A drawback of this approach

is the interference of signals of the "original" cell of the base station and the cell of the relay. Type 2 relays are transparent to the users and do not have an own physical cell identity.

1.3 Scope and vision of this work

The focus of this thesis lies on the physical layer aspects for two-hop relaying in cellular and cooperative ad hoc networks. In particular, we develop novel schemes using AF and filter-and-forward (FF) relays. In the FF scheme, the relays perform FIR filtering in the base-band domain to their received signals to equalize frequency selective channels. Note that FF relaying is a generalization of AF relaying and AF relays can be regarded as FF relays with an FIR filter of length one. For all the proposed schemes, the challenge is to find the optimum relay weights for AF relaying or the filter coefficients for FF relaying.

It is the author's belief that relays will play an important role in future mobile wireless networks with a growing number of devices and an increasing amount of data traffic.

Due to their simplicity, AF and FF relays are prominent candidates to be utilized in cost-efficient wireless networks. Especially FF relays are attractive for broadband wireless systems with a single-carrier. Single-carrier systems are a cheap alternative to orthogonal frequency-division multiplexing (OFDM) systems which employ multiple carriers to combat frequency selective fading channels. However, OFDM communication requires a highly efficient power amplifier to establish a high peak-to-average power and is sensitive to carrier frequency offset and phase noise. Also, OFDM transmission introduces a large delay if the utilized FFT block length is large. In this work, we regard the parallel communication of multiple users in single carrier networks with FF relays. Note that the interference of the signals of different users is in particular challenging in single carrier networks as an orthogonal transmission cannot be realized through the use of multiple carriers.

The herein developed FF relaying scheme is especially suitable for smart phone ad hoc networks (SPANs). SPANs enable the p2p communication if network infrastructure is not available. This is the case when natural disasters destroy the cellular towers or result in blackouts. Also events like festivals, where the number of subscribers is very large, the cellular network is overloaded. Then, relays are necessary to forward signals if the direct path between two users equipped with mobile phones is too week for communication. For SPANs, the single-carrier communication is particularly desirable as mobile phones are usually not equipped with expensive power amplifiers that can provide a high peak-to-average power. One important aspect in SPANs is the communication of user pairs. Therefore, we propose bi-directional schemes to enable a high rate parallel transmission of multiple

user pairs in this work.

Besides SPANs, another interesting example for mobile ad hoc networks are vehicular ad hoc network (VANET)s where cars exchange date for safety purposes and are provided with an internet connection. In contrast to networks, where the participants usually move slowly, VANETs can suffer from time selective fading due to multipath propagation and the rapid movement of cars. Time selective fading is challenging as information on the channel out-dates quickly when the channel is quickly evolving. In such a scenario, differential modulation enables a reliable transmission with knowledge of the channel state. Therefore, we introduce a bidirectional differential scheme that enables information exchange in environments with time-variant channels.

Apart from ad hoc networks, relays will enhance the efficient usage of the wireless medium of cellular networks. In cellular networks, multicast transmission of common data to many receivers at the same time exploits the broadcasting nature of the wireless channel and avoids exhaustive individual transmission. We believe that multicasting services will play an important role in future cellular networks and propose a novel and efficient scheme for multicasting relay networks.

Embedding relays in a cellular or ad hoc network is a complex task. For cellular network, this requires the specification of the air interface, including physical layer and data link layer aspects in the open systems interconnection (OSI) model of the communication system. The latter specification is beyond the scope of this work. Aspects of the relay communication that are out of the scope of this thesis are for instance the modulation and the coding scheme. Moreover, we do not consider control signaling and synchronization of the network. Other important aspects are data link layer aspects such as radio link control. Among other tasks, radio link control determines the transfer of data packets and organizes correction of erroneous data [2].

1.4 Background and contributions

The considered relaying schemes can be seen as extensions of the established schemes for direct communication, where relays are not involved. In particular, we consider the *single-user* communication of two terminals as depicted in Figure 1.2, where the communication is established by a network of relays. In single-user scenarios, the received signals are not corrupted by crosstalk but by noise. This is the case in networks where the various transmissions occur orthogonally in time or frequency and, therefore, do not overlap.

In the more general *multi-user* p2p scenario of Figure 1.3, there is interference from the different transmitted signals for non-orthogonal communication. In this scenario, the task is to create

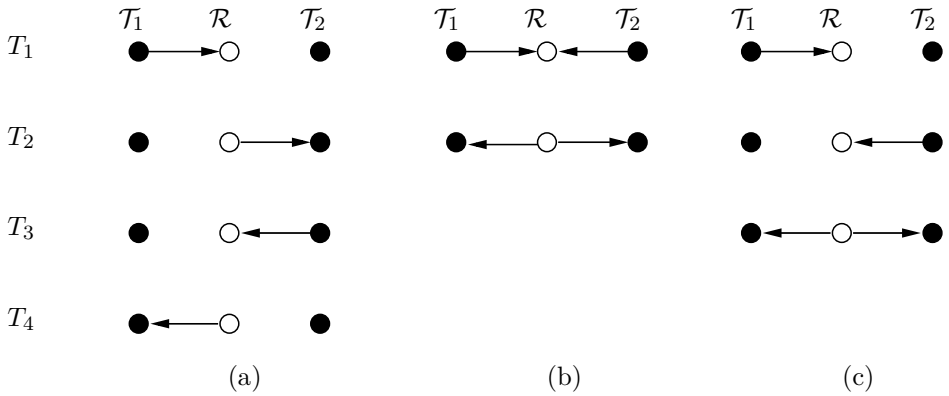

Figure 1.1: Bi-directional transmission schemes: (a) Four time slot transmission, (b) two time slot transmission, (c) three time slot transmission, •: Transceiver, ○: Relay.

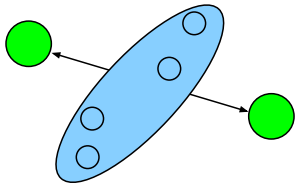

Figure 1.2: Single user pair communication. Blue: Relay network. Green: User pair.

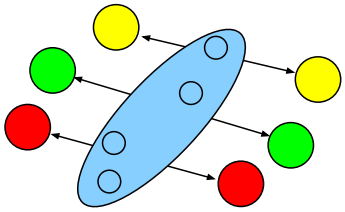

Figure 1.3: Multi-user p2p communication. Blue: Relay network. Else: User pairs.

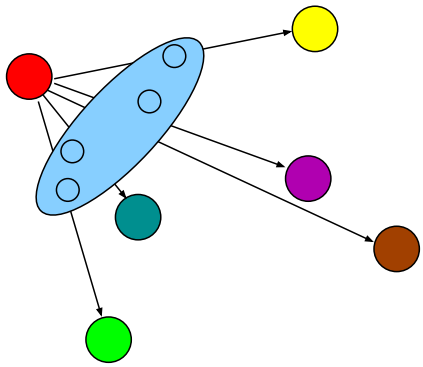

Figure 1.4: Multi-user downlink communication. Blue: Relay network. Red: Source. Else: Destinations.

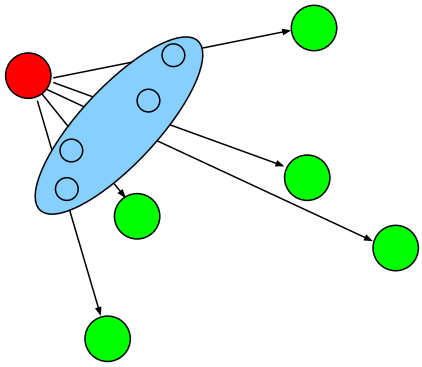

Figure 1.5: Single-group multicasting. Blue: Relay network. Red: Source. Green: Destinations.

communication links between the sources and the destinations and to mitigate interference between the different signals. Both the single- and the multi-user communication can be one-directional or bi-directional. Moreover, the multi-user downlink communication, as depicted in Figure 1.4, will be considered. In multi-user downlink communication, one terminal, e.g., the base station, transmits individual data to each destination terminal. The transmission is in general non-orthogonal and the multiple signals interfere with each other. The task of the relay network is to reduce the interference at the user terminals and to meet the service requirements.

Another useful transmission scheme that will be considered is the single-group multicasting scheme of Figure 1.5. In this scheme, common data is sent from one source terminal to multiple destination terminals in a single transmission. Multicasting schemes avoid exhaustive individual transmissions to serve many subscribers which demand the same data simultaneously. This is, for instance, the case in streaming applications.

The thesis can be divided in contributions in one-directional and bi-directional relaying. For one-directional relaying, the following schemes have been investigated:

In Chapter 3 FF relaying is applied to serve multiple users in frequency-selective environments. The frequency-selective channels and the multiple source-destination pairs cause inter-symbol- interference (ISI) and multi-user-interference (MUI), respectively. We investigate two scenarios where ISI and MUI occur. First, in Chapter 3.2, multi-user downlink beamforming according to Figure 1.4 for transmissions from a single multi-antenna source to multiple destinations in a frequency-selective environment is proposed. We consider that the source, the multi-antenna relays, and the destinations are equipped with linear filters to compensate for the frequency-selective channels and the MUI. Second, in Chapter 3.3, FF relaying is applied to the p2p scenario of Figure 1.3 in an ad hoc network. The p2p scenario turns out to be a special case of the multi-user downlink scenario.

In both chapters, we analyze the impact of the relay filter length and compare FF relaying to AF relaying.

In Chapter 4, a novel single-group multicasting scheme (see Figure 1.5) for AF relaying is proposed. As in single-group multicasting, there is only one data stream transmitted to all destinations, no MUI occurs. In contrast to Chapter 3, we assume frequency flat channels which lead to an ISI-free communication. Therefore, the only channel impairment is noise at the relays and destinations. In the proposed four time slot scheme, the relays use two different weights to increase the degrees of freedom in the relay beamformer design. To achieve simple decoding at the destinations, the received signals at the relays are encoded as in Alamouti's STC scheme [89]. To maximize the provided signal quality at destinations, we propose an optimization method that organizes the power allocation in the network and selects the relay weights.

To compare the performance of one-directional AF relaying schemes, we first consider single-user communication as illustrated in Figure 1.2 in Chapter 5. In this scenario the only channel impairment is noise at the relays and users. We derive analytical performance analysis for the three bi-directional relaying schemes of Figure 1.1 and the one-directional scheme and compare these schemes to each other in terms of their rate. For the single-user case, we show that the two time slot two-way scheme of Figure 1.1 (b) achieves almost two times the rate of the one-directional scheme. For the three time slot scheme of Figure 1.1 (c), we derive an upper bound on the maximum rate.

In Chapter 6, the two time slot two-way scheme for the communication of a single user pair via a cooperative relay network is extended to multiple user pairs and to multiple time slots. In this scenario, MUI occurs and the two time slot two-way scheme is generalized to multiple time slots to provide a trade-off between MUI and spectral efficiency.

In the Chapters 3–6, it has been assumed that the relay weights are computed based on the channel state information (CSI) that is accumulated at one processing node in the network. These assumptions are relaxed in Chapter 7, where a novel bi-directional scheme for the communication of a single user pair according Figure 1.1 (c) via a multi-antenna relay is proposed. This scheme utilizes differential beamforming (DBF) to bypass the acquisition of explicit CSI by using implicit CSI gained from the received signals at the relays. As the DBF scheme does not rely on (outdated) CSI, the DBF scheme is especially applicable to time-variant channels.

Table 1.1 gives an overview of the considered relaying scenarios in the rest of this thesis.

In the following chapter, we will review the basic concepts about the signal models used in the rest of the thesis. Furthermore, network optimization is briefly introduced.

Chapter	3	4	5	6	7
Single/Multi-user	MU	MU	SU	MU	SU
Channel impairment	MUI + ISI + noise	noise	noise	MUI + noise	noise
AF	√	√	√	√	√
FF	√	-	-	-	-
One-directional	√	√	√	-	-
Bi-directional	-	-	√	√	√
CSI available	√	√	√	√	-

Table 1.1: Overview of relaying scenarios.

Chapter 2

Signal models and network optimization

In this chapter, we first introduce models of the wireless multipath channel in point-to-point communication. The single-input-single-output (SISO) signal models are then generalized to the signal models of AF relaying and FF relaying. Finally, network optimization is introduced.

2.1 SISO channel models

Assuming a linear channel, the input-output relationship of the wireless channel can be described in a discrete-time baseband model as [45]

$$y(n) = \sum_{l=0}^{L-1} h_l s(n-l) + \eta(n), \tag{2.1}$$

where $y(n)$, $s(n)$, and $\eta(n)$ are the output signal, the input signal and the additive noise at time slot n, respectively. The wireless channel is modeled as a finite-impulse-response (FIR) filter of length L with the complex-valued filter taps $\{h_l\}_{l=0}^{L-1}$. The *time-invariant* model in (2.1) is justified if the *coherence time* of the channel is larger than the product of symbol duration and block length. The coherence time of the channel is defined as the duration after which the channel has significantly changed [45]. Note that the coherence time is proportional to the inverse of the *Doppler spread* which denotes the difference of the Doppler frequency shifts caused by motion of the communicators. In the remaining chapters, except for Chapter 7, it is assumed that the channels are time-invariant i.e., the model in (2.1) applies.

From (2.1), it can be seen that the output signal contains a mixture of multiple input symbols. This effect is referred to as ISI and is caused by multi-path propagation. A simplification of the

time-invariant model in (2.1) can be made if the *delay spread* is sufficiently small. The delay spread is the largest delay difference among the fading paths of the wireless radio link. If the delay spread is much smaller than the duration of one channel input symbol, only one input symbol is contained in each output signal and the channel is *frequency-flat*. Assuming a time-invariant channel, the input-output model in (2.1) results, by slight abuse of notation and for a frequency-flat channel response, in

$$y = hs + \eta, \tag{2.2}$$

where $y = y(n)$, $h = h(n)$, $s = s(n)$, $\eta = \eta(n)$. Note that in (2.2), the single channel coefficient h is sufficient for the representation of the channel. The application of the frequency-flat fading model in (2.2) applies can be verified based on the *coherence bandwidth*. Coherence bandwidth determines the width of the frequency band which can be considered to be flat. The coherence bandwidth is inversely proportional to the delay spread. If the coherence bandwidth is much larger than the bandwidth of the transmitted signal, then the model in (2.2) is an appropriate channel model.

2.2 AF relaying

In this section, we derive the signal model for networks with time-invariant frequency-flat channels using the channel model according to (2.2). We consider a network of single-antenna nodes that operate in a common frequency band. The network consists of R AF relays $\{\mathcal{R}_r\}_{r=1}^{R}$, K sources $\{\mathcal{S}_k\}_{k=1}^{K}$, and M destinations $\{\mathcal{D}_m\}_{m=1}^{M}$. The channels in the network are assumed to be flat-fading and perfectly known. Let $f_{k,r}$ denote the complex-valued coefficient of the channel in between source $\mathcal{S}_k$ and relay $\mathcal{R}_r$ and let $g_{r,m}$ denote the complex-valued coefficient of the channel in between relay $\mathcal{R}_r$ and destination $\mathcal{D}_m$. Let us assume that there is no direct link between the sources and the destinations and that the network is perfectly synchronized, which is a common assumption made in the literature [19], [20]-[24], [58], and [59].

In the rest of this section, we first derive the signal model for one-directional AF relaying and then extend this model to bi-directional AF relaying.

2.2.1 One-directional AF relaying

Transmissions from the sources to the destinations comprise two time slots. In the first time slot, source $\mathcal{S}_k$, $k = 1, \ldots, K$, transmits the signal $\sqrt{P_k}s_k$ to the relays, where s_k is the information-bearing symbol and P_k is the transmit power. Let η_r be the noise in the signal $x_r = \sum_{k=1}^{K} f_{k,r}s_k + \eta_r$

received at relay $\mathcal{R}_r$. Introducing

$$\begin{aligned}\mathbf{x} &\triangleq [x_1, x_2, \ldots, x_R]^T,\\ \mathbf{f}_k &\triangleq [f_{k,1}, f_{k,2}, \ldots, f_{k,R}]^T, \quad k = 1, \ldots, K,\\ \boldsymbol{\eta} &\triangleq [\eta_1, \eta_2, \ldots, \eta_R]^T,\end{aligned}$$

the vector of signals received at the relays is given by

$$\mathbf{x} = \sum_{k=1}^{K} \sqrt{P_k} s_k \mathbf{f}_k + \boldsymbol{\eta}. \tag{2.3}$$

Relay $\mathcal{R}_r$ weights its received signal x_r by a complex number w_r^* and sends $w_r^* x_r$ as a scaled and phase-adjusted copy of x_r to the destinations in the second time slot. We define

$$\mathbf{w} \triangleq [w_1, w_2, \ldots, w_R]^T, \tag{2.4}$$

$$\mathbf{W} \triangleq \mathrm{diag}(\mathbf{w}^*), \tag{2.5}$$

$$\mathbf{t} \triangleq [t_1, t_2, \ldots, t_R]^T, \tag{2.6}$$

where $\mathbf{w}$ is the relay weight vector and $\mathbf{W}$ is the relay weight matrix. Using these definitions, the complex vector of the transmitted signals $\mathbf{t}$ at the relays can be expressed as

$$\mathbf{t} = \mathbf{W}\mathbf{x}. \tag{2.7}$$

Let us introduce

$$\mathbf{g}_m \triangleq [g_{1,m}, g_{2,m}, \ldots, g_{R,m}]^T, \quad m = 1, \ldots, M, \tag{2.8}$$

such that the signal y_m received at destination $\mathcal{D}_m$ can be written as

$$y_m = \mathbf{g}_m^T \mathbf{t} + \nu_m, \tag{2.9}$$

where ν_m is the receiver noise at destination $\mathcal{D}_m$. In the rest of the thesis, it is assumed that the noise processes are zero mean Gaussian, spatially and temporally white so that $\mathrm{E}\{|\nu_m|^2\} = \sigma^2$ and $\mathrm{E}\{\boldsymbol{\eta}\boldsymbol{\eta}^H\} = \sigma^2\mathbf{I}$, where σ^2 denotes the noise power. Furthermore, it is assumed that the information-bearing symbols are uncorrelated with each other and with the noise.

2.2.2 Bi-directional AF relaying

In this section, bi-directional AF relaying is reviewed. As we have seen, in one-directional half-duplex relaying, the communication of one information-bearing symbol requires two time slots. Bi-directional AF networks have been extensively studied in the literature as they can reduce the number

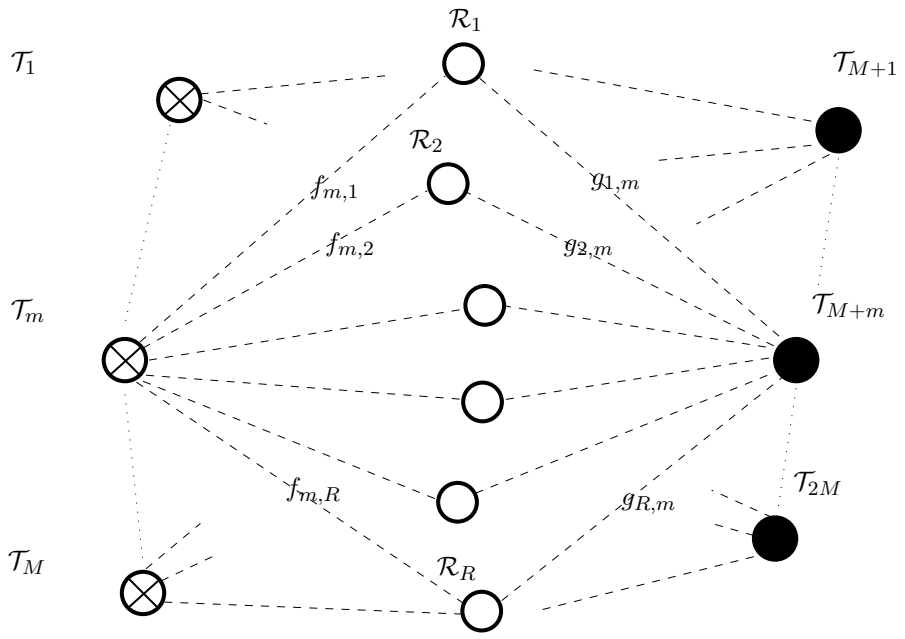

Figure 2.1: The relay network. $\otimes$: Source, $\circ$: Relay, $\bullet$: Destination.

of channel uses and improve the spectral efficiency [26], [27], [32]–[38], [46]–[56]. For instance, as illustrated in Figure 1.1 (b) and (c), the number of time slots to exchange two data symbols is reduced to two and three, respectively, whereas one-directional communication requires four time slots.

In our system model, we refer to the nodes which exchange messages as transceivers as they receive and transmit. This is in distinction to one-directional relaying, where sources only send messages to destinations which only receive messages. In our system, $K = M$ transceiver pairs exchange information. The total number of transceivers is then given by $2M$ and it is assumed that transceiver $\mathcal{T}_m$ and transceiver $\mathcal{T}_{M+m}$, $m = 1, \ldots, M$, form a pair. The system model for bi-directional AF relaying is a special case of the system model discussed in Section 2.2.1, where transceiver $\mathcal{T}_m$ corresponds to source $\mathcal{S}_m$ for $m \leq M$ and to destination $\mathcal{D}_{m-M}$ for $m > M$. Following Figure 2.1, $\mathbf{f}_m$ and $\mathbf{g}_m$ denote the vector of the channels between transceiver $\mathcal{T}_m$ and the relays and between transceiver $\mathcal{T}_{M+m}$ and the relays (for $m \leq M$), respectively. We will assume reciprocity so that the signals for transmissions from the transceivers to the relays and vice versa pass through the same channels. This assumption is realistic for narrowband time division duplex (TDD) systems [139].

Let us consider the two time slot scheme, where all transceivers send their information-bearing

symbols in the first time slot. The vector of signals received at the relays is then given by

$$\mathbf{x} = \sum_{m=1}^{M} \sqrt{P_m} s_m \mathbf{f}_m + \sum_{m=M+1}^{2M} \sqrt{P_m} s_m \mathbf{g}_{m-M} + \boldsymbol{\eta},$$

where $\sqrt{P_m}$ and s_m are respectively the transmit power and the information-bearing symbol at transceiver $\mathcal{T}_m$. In the second time slot, each relay sends a weighted version of its received signal to the transceivers. Using the notations of (2.4) - (2.6), the vector of transmitted signals at the relays is given by $\mathbf{t} = \mathbf{W}\mathbf{x}$. Then, the signal received at each transceiver is for $m \leq M$ can be expressed as

$$y_m = \mathbf{f}_m^T \mathbf{t} + \nu_m, \tag{2.10}$$

and for $m > M$

$$y_m = \mathbf{g}_m^T \mathbf{t} + \nu_m, \tag{2.11}$$

where ν_m is the noise at transceiver $\mathcal{T}_m$.

One fundamental difference of bi-directional relay compared with one-directional relaying is that the transceivers receive not only their desired signals, MUI and noise but also their own transmitted signals. The latter SI can be avoided by using zero-forcing methods at the relays [38], or by applying SI cancellation at each transceiver [26].

2.3 Network optimization using CSI

The goal of wireless networks is to provide service to the user terminals. In the LTE-standard three main service-related parameters are identified [2]:

- **Delay:** Mobile services such as video telephony require a very short delay, whereas for other services such as e-mail transfer, the delay requirements are relaxed.
- **Data rate:** The data rate is the amount of information quantified in bits communicated per unit of time. As pointed out before, there exists an increasing demand for high data rates in cellular networks.
- **Spectral efficiency:** For the mobile system operator, not only per-user data rates are important but also the total data rate that is on average provided in a cell per hertz of licensed spectrum.

The emphasis in this thesis lies on the *data rates* provided to the user terminals through the communication channels that are created by relays. The maximum rate C, i.e., the capacity, of an

interference-free point-to-point communication channel only impaired by additive white Gaussian noise, has been established by Shannon and is given by [57]

$$C = B_W \log_2 \left(1 + \frac{\mathrm{E}\{|y_\mathrm{S}|^2\}}{\mathrm{E}\{|y_\mathrm{N}|^2\}}\right), \tag{2.12}$$

where B_W is the bandwidth and $\mathrm{E}\{|y_\mathrm{S}|^2\}$ and $\mathrm{E}\{|y_\mathrm{N}|^2\}$ denote respectively the received signal and noise power. From equation (2.12), we observe that the data rate is fundamentally influenced by i) the bandwidth of the communication channel ii) the signal-to-noise ratio (SNR) given by

$$\mathrm{SNR}_m \triangleq \frac{\mathrm{E}\{|y_\mathrm{S}|^2\}}{\mathrm{E}\{|y_\mathrm{N}|^2\}}. \tag{2.13}$$

Note that the bit error rate (BER) of modulation schemes such as quadrature phase-shift keying is an analytical function of the SNR provided by the communication channel and high SNRs lead to low BERs.

In (2.12) and (2.13), it is assumed that the communication is only impaired by noise. However, if multiple terminals communicate in overlapping frequency bands, MUI is the dominant impairment in the communication. Moreover, due to multi-path propagation, the wireless communication can be impaired by ISI. In many aspects, the effect of interference on the wireless communication channel is similar to that of noise. In particular, the maximum data rate that can be achieved for a given bandwidth is limited by the available signal-to-interference-plus-noise ratio (SINR).

For communication which is corrupted by interference, we quantify the QoS of the mth receiver in terms of the received SINR given by

$$\mathrm{SINR}_m \triangleq \frac{\mathrm{E}\{|y_{m,\mathrm{S}}|^2\}}{\mathrm{E}\{|y_{m,\mathrm{I+N}}|^2\}}, \tag{2.14}$$

where $y_{m,\mathrm{S}}$ is the desired signal and $y_{m,\mathrm{I+N}} = y_{m,\mathrm{I}} + y_{m,\mathrm{N}}$ is the sum of the noise $y_{m,\mathrm{N}}$ and the interference $y_{m,\mathrm{I}}$ such that $y_m = y_{m,\mathrm{S}} + y_{m,\mathrm{I+N}}$.

In the considered relay communication scenario of this work, the signal, the noise, and the interference power are functions of the of network parameters, i.e., the relay weights and the transmit power of the source and the relays. To optimize the network, we aim to select these parameters according to the CSI such that a high QoS at the user terminals is achieved.

In the Chapters 3 - 6, it is assumed that the full instantaneous CSI is available at one processing node. This processing node computes the network variables such as the relay weight vector $\mathbf{w}$ and the power scaling factors and distribute them to the respective nodes in the network. Similar CSI assumptions are used, for example, in [19], [20], [41], [58], and [59].

In the DBF scheme of Chapter 7, the requirement on the CSI is relaxed and only implicit CSI contained in received signals is exploited. Moreover, no central processing is required for the DBF scheme.

The instantaneous CSI is exploited to solve the following two optimization problems.

Power minimization: One goal is to minimize a specific power P subject to constraints on the received QoS at the terminals as it was considered in [24], [30], [31], [39], [40], [41], [58], and [59]. Here, P can either be the relay sum power P_{R} or the total transmit power of the network P_{T}, including the power consumed by the relays and other terminals, e.g., the source power P_{S}.

Constraints on the minimum received QoS occur in many applications of cellular networks such as voice calls and video telephony. In the case that it is sufficient to satisfy a minimum QoS, it is desirable to transmit at small power. The reason is not only to save energy and consequently reduce the operating cost for the vendor of a cellular network but also to reduce the interference in the network and the interference to neighboring networks. Moreover, power minimization is essential for cooperative wireless networks that are composed of nodes which are powered by batteries. For such networks, minimizing the energy consumption for data transmission is one of the most important design considerations [60].

Using (2.14), the power minimization problem is formulated as

$$\begin{aligned} \min P \quad \text{s.t.} \quad & \mathrm{SINR}_m \geq \gamma_m, \quad m = 1, \ldots, M, \\ & p_r \leq p_{r,\max}, \quad r = 1, \ldots, R, \\ & P_{\mathrm{R}} \leq P_{\mathrm{R,max}}, \\ & P_{\mathrm{S}} \leq P_{\mathrm{S,max}}, \\ & P_{\mathrm{T}} \leq P_{\mathrm{T,max}}, \end{aligned} \tag{2.15}$$

where $p_{r,\max}$, $P_{\mathrm{R,max}}$, $P_{\mathrm{S,max}}$, and $P_{\mathrm{T,max}}$ denote the maximum allowable transmit powers p_r, $P_{\mathrm{R,max}}$, $P_{\mathrm{S,max}}$, and $P_{\mathrm{T,max}}$, respectively. γ_m is the threshold value of the minimum SINR at the mth receiver.

Note that the problem in (2.15) might not be feasible in general. The reason is that the SINR constraints cannot always be fulfilled. Especially in scenarios where one frequency band is used to serve multiple users at the same time, a high SINR requirement might be impossible to meet because of MUI.

Max-min fairness: The second optimization goal is to maximize the smallest QoS at the receivers, measured in SINR, subject to constraints on the power consumption in the network. The max-min fairness approach is well-established to define fairness in networks. To meet the max-min fairness

criterion, the goal is to improve the lowest received QoS and consequently increase the lowest possible data rate of all the users rather than maximizing the sum rate. The drawback of the latter approach is that the received QoS of some of the users might be very low.

Mathematically, the max-min fairness problem is formulated as

$$\begin{aligned} \max \min_{m=1,\ldots,M} \mathrm{SINR}_m \quad \text{s.t.} \quad & p_r \leq p_{r,\max}, \quad r = 1, \ldots, R, \\ & P_{\mathrm{R}} \leq P_{\mathrm{R,max}}, \\ & P_{\mathrm{S}} \leq P_{\mathrm{S,max}}, \\ & P_{\mathrm{T}} \leq P_{\mathrm{T,max}}. \end{aligned} \tag{2.16}$$

In contrast to the power minimization problem in (2.15) the max-min fairness problem has always a feasible solution since there is no fix threshold value for the minimum SINR at each receiver.

The max-min fairness approach is attractive if a certain amount of transmit power is available and the goal is to serve all the users in a network as well as possible. It is clear that the max-min fairness approach is therefore fundamentally different to the power minimization approach where minimum QoS requirements of the users must be met.

From the users' point of view, to obtain the largest possible SINR instead of a constant minimum SINR is desirable for packet-data traffic. There, the receivers demand the largest possible data rate rather than a certain constant data rate, as long as the average rate is satisfactory [2]. Optimization with the goal of max-min fairness has been considered in [29], [30], [33], [34], [108], and [95].

Introducing an auxiliary variable γ, the max-min fair problem in (2.16) can be equivalently rewritten as

$$\begin{aligned} \max \gamma \quad \text{s.t.} \quad & \mathrm{SINR}_m \geq \gamma, \\ & p_r \leq p_{r,\max}, \quad r = 1, \ldots, R, \\ & P_{\mathrm{R}} \leq P_{\mathrm{R,max}}, \\ & P_{\mathrm{S}} \leq P_{\mathrm{S,max}}, \\ & P_{\mathrm{T}} \leq P_{\mathrm{T,max}} \\ & \gamma > 0. \end{aligned} \tag{2.17}$$

Note that, in general, not all of the constraints in the problems (2.15) - (2.17) might be present.

Table 2.1 gives an overview of the optimization problems that are respectively solved in each chapter. Moreover, we indicate in Table 2.1, weather power allocation is considered in the respective

Chapter	3.2	3.3	4	5	6	7
Power minimization	√	-	√	-	-	-
Max-min fairness	√	√	√	-	√	√
Power allocation	-	-	√	√	-	√

Table 2.1: Power minimization and max-min fairness optimization in Chapters 3 - 7.

chapter. That is, in these chapters, besides the relay weight vector the power split between source and relay transmit power is subject of the mathematical optimization.

Note that in Chapter 5, the focus lies on maximizing the sum-rate of two users rather than achieving fairness.

2.4 Mathematical optimization methods

In the single user case, the problems (2.15) and (2.17) are relatively easy to solve and there exist closed form solutions to compute the optimum relay weight vector $\mathbf{w}$ or the relay weight matrix $\mathbf{W}$ [21], [132]. However, the problem is more complicated in the multi-user case. For instance, the task to select the optimum weights in centralized beamforming systems using a connected antenna array [94]–[103], or in distributed relay beamforming systems [39]–[41] for multicasting is highly non-trivial as it requires to form beams towards several destinations, each corresponding to a different spatial signature.

For the following review on optimization techniques, we consider a power minimization problem of the form (2.15), where a complex-valued weight vector $\mathbf{w}$ is the optimization variable. We assume that the SINR given in (2.14) can be expressed as

$$\mathrm{SINR}_m \triangleq \frac{\mathbf{w}^H \mathbf{Q}_{m,\mathrm{S}} \mathbf{w}}{\mathbf{w}^H \mathbf{Q}_{m,\mathrm{I+N}} \mathbf{w} + \sigma^2}, \tag{2.18}$$

where $\mathbf{Q}_{m,\mathrm{S}}$ is the positive semidefinite covariance matrix of the desired signal at destination $\mathcal{D}_m$ such that $\mathrm{E}\{|y_{m,\mathrm{S}}|^2\} = \mathbf{w}^H \mathbf{Q}_{m,\mathrm{S}} \mathbf{w}$ and where $\mathbf{Q}_{m,\mathrm{S}}$ is the positive semidefinite noise and interference covariance matrix of destination $\mathcal{D}_m$ such that $\mathrm{E}\{|y_{m,\mathrm{I+N}}|^2\} = \mathbf{w}^H \mathbf{Q}_{m,\mathrm{I+N}} \mathbf{w} + \sigma^2$. Here, σ^2 is receiver noise that is not a function of the weight vector $\mathbf{w}$.

Let us consider the problem

$$\min_{\mathbf{w}} \ \mathbf{w}^H \mathbf{D} \mathbf{w} \quad \text{s.t.} \quad \mathrm{SINR}_m \geq \gamma_m, \quad m = 1, \ldots, M, \tag{2.19}$$

where $\mathbf{D}$ is a positive definite matrix such that in (2.15) $P = \mathbf{w}^H\mathbf{D}\mathbf{w}$, and γ_m is the threshold value for the minimum received SINR at destination $\mathcal{D}_m$. Using (2.18), problem in (2.19) can be formulated as

$$\min_{\mathbf{w}} \ \mathbf{w}^H\mathbf{D}\mathbf{w} \quad \text{s.t.} \quad \mathbf{w}^H\mathbf{Q}_{m,\mathrm{S}}\mathbf{w} \geq \gamma_m\mathbf{w}^H\mathbf{Q}_{m,\mathrm{I+N}}\mathbf{w} + \gamma_m\sigma^2, \quad m = 1,\ldots,M. \tag{2.20}$$

The difficulty of the quadratically constrained quadratic problem (QCQP) (2.20) lies in the SINR constraints that are non-convex due to the positive semidefinite quadratic form $\mathbf{w}^H\mathbf{Q}_{m,\mathrm{S}}\mathbf{w}$ on the left-hand side of the inequality constraints. Non-convexity does not mean by default that an optimization problem is hard to solve. However, in [94], it has been shown that the problem of selecting the antenna weights for single-group multicasting is NP-hard. Note that the latter problem can be expressed in the problem formulation of (2.20).

To derive adequate solutions to beamforming problems which belong to the class of non-convex QCQPs, computationally efficient algorithms have been proposed which approximate the feasible set of the optimization problem [33], [39]–[41], [61]–[70], [94]–[103].

Outer approximation techniques

The approximation techniques used in this thesis to solve non-convex optimization problems can be divided in outer and inner approximation techniques. Outer approximation techniques replace the QCQPs by convex semidefinite programs (SDP) which can be solved efficiently [24], [71], [94]–[100], [108].

In the latter approach, the weight vector $\mathbf{w}$ is replaced by a positive semidefinite Hermitian matrix. Defining $\mathbf{X} \triangleq \mathbf{w}\mathbf{w}^H$, the problem in (2.20) can be reformulated as

$$\begin{aligned}\min_{\mathbf{X}} \ \mathrm{tr}(\mathbf{D}\mathbf{X}) \quad \text{s.t.} \quad & \mathrm{tr}\left((\mathbf{Q}_{m,\mathrm{S}} - \gamma_m\mathbf{Q}_{m,\mathrm{I+N}})\mathbf{X}\right) \geq \gamma_m\sigma^2, \quad m = 1,\ldots M, \\ & \mathfrak{R}(\mathbf{X}) = 1, \quad \mathbf{X} \succeq 0.\end{aligned} \tag{2.21}$$

The rank-one constraint is non-convex. However, the problem in (2.21) can be relaxed to a convex form by dropping this constraint, resulting in

$$\begin{aligned}\min_{\mathbf{X}} \mathrm{tr}(\mathbf{D}\mathbf{X}) \quad \text{s.t.} \quad & \mathrm{tr}\left((\mathbf{Q}_{m,\mathrm{S}} - \gamma_m\mathbf{Q}_{m,\mathrm{I+N}})\mathbf{X}\right) \geq \gamma_m\sigma^2, \quad m = 1,\ldots,M, \\ & \mathbf{X} \succeq 0.\end{aligned} \tag{2.22}$$

Note that a similar SDR approach has been used to efficiently solve non-convex problems in transmit beamforming, multi-user detection, and sensor array processing [78]-[80]. The problem in (2.22) is convex and can be solved efficiently using advanced interior point algorithms [74].

Since this so-called semidefinite relaxation (SDR) technique extends the feasible region, a solution matrix to the SDR problem lies not necessarily in the feasible set of the original problem. If the rank $\mathfrak{R}(\mathbf{X}^\star)$ of the solution matrix $\mathbf{X}^\star$ equals to one, the SDR solution is a global solution to the original problem. In practice, however, $\mathfrak{R}(\mathbf{X}^\star)$ might be greater than one and $\mathbf{X}^\star$ is not feasible for the original problem. For instance, in single-group multicasting scenarios where many destinations demand a minimum received quality-of-service (QoS), it is not likely that $\mathfrak{R}(\mathbf{X}^\star) = 1$. This is a consequence of the fact that existence of an SDR solution matrix with rank $\mathfrak{R}(\mathbf{X}^\star)$ is only guaranteed if $\mathfrak{R}(\mathbf{X}^\star) \geq \mathcal{O}(\sqrt{M})$, where M is the number of destinations [104]. If $\mathfrak{R}(\mathbf{X}^\star) > 1$, the objective value of the SDR solution is only a lower bound to the objective value of a QCQP. The accuracy of the lower bound decreases with a growing number M [96]. Therefore, for large M, the lower bound generated by SDR can lie quite far from the true minimum value.

In general, the rank of the optimal solution $\mathbf{X}^\star$ to (2.22) is greater than one. For $M = 2$, the problem in (2.22) becomes minimizing a quadratic form subject to only two quadratic inequality constraints. Strong duality holds for this type of problem and therefore, the existence of a rank-one solution to (2.22) is guaranteed [81]. If $\mathbf{X}^\star$ is of rank-one, its principal eigenvector is the optimal solution to the original problem in (2.20). Otherwise, *randomization techniques* [94] can be used to find a suboptimal solution to (3.62).

Inner approximation techniques

Inner approximation techniques aim to find convex approximations of the non-convex SINR constraint functions in (2.20). Starting from a feasible point, the iterative algorithms of [35], [39], [41], [61]–[70], and [103] solve a sequence of convex approximation problems, where the objective function of the respective optimization is improved in every iteration.

For instance, a convex approximation of (2.20) can be obtained by replacing the non-convex left hand side of the SINR constraints with its first order Taylor approximation around some feasible weight vector $\mathbf{w}^{(\kappa)}$, where κ is the iteration index. Introducing $\Delta\mathbf{w}$ as an update vector, we replace $\mathbf{w}$ by $\mathbf{w}^{(\kappa)} + \Delta\mathbf{w}$ and approximate (2.20) as

$$\begin{aligned}\min_{\Delta\mathbf{w}} \ (\mathbf{w}^{(\kappa)} + \Delta\mathbf{w})^H \mathbf{D} (\mathbf{w}^{(\kappa)} + \Delta\mathbf{w}) \quad \text{s.t.} \quad & \mathbf{w}^{(\kappa)H} \mathbf{Q}_{m,\mathrm{S}} \mathbf{w}^{(\kappa)} + 2\Re\{\Delta\mathbf{w}^H \mathbf{Q}_{m,\mathrm{S}} \mathbf{w}^{(\kappa)}\} \\ & \geq \gamma_m (\mathbf{w}^{(\kappa)} + \Delta\mathbf{w})^H \mathbf{Q}_{m,\mathrm{I+N}} (\mathbf{w}^{(\kappa)} + \Delta\mathbf{w}) + \gamma_m \sigma^2, \\ & \quad m = 1, \ldots, M \end{aligned} \tag{2.23}$$

where the non-convex term $\Delta\mathbf{w}^H \mathbf{Q}_{m,\mathrm{S}} \Delta\mathbf{w}$ of the left hand side of the inequality constraint is dropped. The above problem is indeed a convex problem since its goal is the minimization of a convex quadratic

Chapter	3.2	3.3	4	5	6	7
Outer approximation	√	-	√	-	-	-
Inner approximation	-	√	√	-	√	-

Table 2.2: Optimization methods in Chapters 3 - 7.

form subject to convex quadratic constraints. Note that the number of variables is not increased in the inner approximation problem in (2.23). This is an advantage to the SDR technique, where the number of variables is roughly squared.

After solving (2.23), the weight vector of the $(\kappa+1)$th iteration is given by

$$\mathbf{w}^{(\kappa+1)} = \mathbf{w}^{(\kappa)} + \Delta\mathbf{w}. \tag{2.24}$$

To solve (2.23), we have assumed that $\mathbf{w}^{(\kappa)}$ is feasible for (2.20). In practice, however, it is generally non-trivial to find a feasible solution that satisfies the SINR constraints. In [41], [39], and [73] feasibility search algorithms have been developed to find feasible points using slack variables.

In contrast to power minimization problems, the max-min fairness optimization according to (2.17) is always feasible. From the mathematical aspect, however, max-min fairness SINR maximization is harder than power minimization due to the additional variable γ. Therefore, we consider in the rest of this thesis mainly SINR maximization. It is straightforward to adapt the optimization methods to solve power minimization problems. Also feasibility search methods can easily be obtained, see [41], [39], and [73].

Table 2.2 gives an overview of the applied optimization methods in the rest of this thesis.

Chapter 3

Multi-user filter-and-forward relaying

3.1 Introduction

In the last years, a notable number of distributed AF beamforming techniques have been proposed [19]-[24]. All these techniques assume that the source-to-relay and relay-to-destination channels are frequency-flat. In practice frequency-selective fading is very likely to occur due to multipath propagation effects. Several approaches have been proposed to combat such type of fading and mitigate the resulting negative effects of ISI. For example, channel equalization techniques have been developed in [18] for distributed space-time codes. For distributed beamforming, an FF relaying protocol has been proposed as a natural extension of the AF scheme to the frequency-selective case [58], [59]. Even though OFDM combined with AF-relaying is also a popular candidate to cope with frequency selective channels, but suffers from large variations in the instantaneous power [2], [83]. Moreover, the resulting high peak-to-average power leads to high requirements on the linearity of power amplifier to prevent inter-carrier interference. Therefore, single-carrier transmission is preferred in applications where constraints on the cost and the power consumption of power amplifier exclude OFDM transmission. Such applications include sensor networks and the uplink transmission in cellular networks [2]

The essence of the FF strategy is to use an FIR filter at each relay node to compensate for the dispersive effects of the source-to-relay and relay-to-destination channels.

In this chapter, we develop an FF approach for a network with frequency-selective channels and multiple users. As a result, the problem formulation will include not only ISI (caused by the channel frequency selectivity), but also MUI caused by multiple peers. We consider two scenarios. First, we

consider the multi-user downlink case as depicted in Figure 1.4 and second, the multi-user p2p case as depicted in Figure 1.3.

In the multi-user downlink scenario, we assume a network comprising a single source with multiple antennas, multiple multi-antenna relays, and multiple single-antenna destinations. The source aims to serve each destination with individual data. To establish the multi-user downlink transmission the signals transmitted by the source are forwarded by the FF relays. It is assumed that no direct links from the source to the destinations exist. Multi-user downlink communication has also been treated in [111], where a single multi-antenna source sends individual messages to multiple destinations via a single multi-antenna relay. In [111], frequency-flat channels have been assumed. In this chapter, FF relaying is combined with channel equalization at the destinations to compensate for the frequency-selective channels as it has been proposed in the single-user scenarios of [83] and [84]. The FIR filter coefficients at the source, the relays and the destinations are chosen to solve the max-min fairness optimization problem of (2.16). As this problem turns out to be difficult to be solved directly, we propose an alternating algorithm which sequentially optimizes different subsets of variables by solving the respective subproblems. We propose to use convex inner approximations to solve the non-convex subproblems of computing the relay and source filter coefficients.

In the multi-user p2p scenario, we consider multiple source-destination pairs that aim to communicate via multiple FF relays. We assume that all nodes in the network have a single antenna only and we do not assume channel equalization at the destinations. The resulting system model is a special case of the system model for multi-user downlink communication. This multi-user p2p scenario can be seen as an extension of the works [58] and [59] on FF relaying, where only one source and one destination node have been assumed. From a somewhat different perspective, this contribution can be seen as a non-trivial extension of the p2p approach of [24] which considers the system model of 2.2.1 for $K = M$. Note that the problem formulation in [24] involves MUI (caused by multiple peers), but it does not include any ISI, as the channels are assumed to be frequency-flat. Here, two practically relevant beamforming problem formulations are developed. Our first formulation amounts to a problem of the form (2.15), as we aim to minimize the relay sum power subject to the destination QoS constraints. Our second problem is a max-min fairness problem of the form (2.16). The resulting problems are non-convex and, therefore, difficult to be solved exactly. We will use SDR to relax them to convex semi-definite programming (SDP) problems that can be solved efficiently using interior point methods.

Note that in the works of [85] and [86], FF relaying has been adapted to two-way relay networks.

Other works which consider FF multi-user relaying are [87] and [109]. Besides the works on FF relaying in frequency-selective environments, it has been proposed to use FF relays in OFDM networks with frequency-flat channels to reduce the number of relay coefficients [88].

The contributions of this chapter can be summarized as follows:

- In a frequency-selective environment, FF relaying has been combined with channel equalization at the destinations and precoding at the multi-antenna source for multi-user downlink communication.
- For the multi-user downlink communication, an iterative algorithm is proposed to solve the highly non-convex optimization problem of selecting the source filter coefficients, the relay filter coefficients and the destination filter coefficients.
- The single-user FF approach of the literature is generalized from a single source-destination scenario to a multi-user p2p scenario where MUI and ISI occur.
- The SDR method will be applied to solve the non-convex optimization problems of selecting the proper relay filter coefficients to minimize the relay transmit power or to maximize the smallest received QoS.

The content of this chapter has been partly published in
A. Schad, H. Chen, A.B. Gershman, and S. Shahbazpanahi, "Filter-and-forward peer-to-peer beamforming in relay networks with frequency selective channels,"*Proceedings of the International Conference on Acoustics, Speech, and Signal Processing (ICASSP'10),* Dallas, TX, USA, pp. 3246–3249 March 2010,
and
A. Schad, B. Khalaj, M. Pesavento, "Precoding in Relay Networks with Frequency Selective Channels," *Proceedings of the Asilomar Conference on Signals, Systems and Computers,* Pacific Grove, CA, Nov. 2012.

3.2 Multi-user downlink transmissions with precoding and channel equalization

3.2.1 Signal model

In this section, we generalize the signal model in Chapter 2.2.1 to one-directional relaying with frequency-selective channels, utilizing the channel model in (2.1). It is assumed that each relay is

equipped with N_R antennas and the FF relaying strategy is employed. That is, the signals received at each relay in the first stage are filtered by FIR filters. In the second transmission stage, each relay sends its filtered signals to the destinations. For all signals, the respective time slot is indicated in parentheses.

Let us consider a network comprising source $\mathcal{S}$ equipped with N_S antennas, R relays that are equipped with N_R antennas and M single-antenna destinations. The goal is to serve each destination with an individual data stream, see Figure 1.4. Since no direct source-to-destination paths exist, the communication from the source to the destinations is set up by the relays.

The downlink transmission from the source to the destinations is organized in two phases. In the first phase, source $\mathcal{S}$ transmits M data streams to the R relays. In the second phase, the relays forward linearly processed versions of their received signals to the destinations. The relays operate as out-band relays in full-duplex mode. Let $s_m(n)$ denote the information-bearing symbol assigned to destination $\mathcal{D}_m$ in time slot n. The information-bearing symbols are filtered by precoding FIR filters with length L_a. Here, precoding is introduced to mitigate both MUI and ISI and can be regarded as a combination of linear spatial filtering and pre-channel equalization.

The kth source antenna uses the filter coefficients $\{a^*_{m,k,l}\}_{l=0}^{L_a-1}$ for the mth data stream to transmit the signal $v_{m,k}(n) = \sum_{l=0}^{L_a-1} a^*_{m,k,l} s_m(n-l)$. Let us define

$$\mathbf{v}_m(n) \triangleq [v_{m,1}(n), v_{m,2}(n), \ldots, v_{m,N_S}(n)]^T, \quad m = 1, \ldots, M, \tag{3.1}$$

$$\mathbf{a}_{m,k} \triangleq [a^*_{m,k,0}, a^*_{m,k,1}, \ldots, a^*_{m,k,L_a-1}], \quad m = 1, \ldots, M, \quad k = 1, \ldots, N_S, \tag{3.2}$$

$$\mathbf{A}_m \triangleq [\mathbf{a}^T_{m,1}, \ldots, \mathbf{a}^T_{m,N_S}]^T, \quad m = 1, \ldots, M, \tag{3.3}$$

$$\mathbf{s}_{m,\mathfrak{A}}(n) \triangleq [s_m(n), \ldots, s_m(n-L_a+1)]^T, \quad m = 1, \ldots, M. \tag{3.4}$$

Using (3.1) - (3.4), the vector $\mathbf{v}(n)$ of the transmitted signals in the nth time slot is given by

$$\mathbf{v}(n) = \sum_{m=1}^{M} \mathbf{v}_m(n) = \sum_{m=1}^{M} \mathbf{A}_m \mathbf{s}_{m,\mathfrak{A}}(n). \tag{3.5}$$

The source-to-relay and relay-to-destination channels are modeled as linear FIR filters with the length L according to the channel model (2.1). Let $f_{k,q,l}$ be the lth filter tap of the channel from the kth source antenna to the qth relay antenna, $q = 1, \ldots, N_R R$. Note that the qth relay antenna belongs to relay $\mathcal{R}_r$ if $r = \lfloor q/N_R \rfloor$. Let $x_q(n)$ be the signal received at the qth relay antenna in the nth time slot which contains the additive noise $\eta_q(n)$ that is assumed to be spatially and temporally

white noise with power $\mathrm{E}\{|\eta_q(n)|^2\} = \sigma^2$ for all q, n. We further introduce

$$\mathbf{f}_{k,l} \triangleq [f_{k,1,l}, f_{k,2,l}, \ldots, f_{k,N_R R,l}]^T, \quad k = 1, \ldots, K, \quad l = 0, \ldots, L-1, \tag{3.6}$$

$$\mathbf{F}_l \triangleq [\mathbf{f}_{1,l}, \mathbf{f}_{2,l}, \ldots, \mathbf{f}_{K,l}], \quad l = 0, \ldots, L-1, \tag{3.7}$$

$$\mathbf{F} \triangleq [\mathbf{F}_0, \mathbf{F}_1, \cdots, \mathbf{F}_{L-1}], \tag{3.8}$$

$$\mathbf{x}(n) \triangleq [\mathbf{x}_1^T(n), \mathbf{x}_2^T(n), \ldots, \mathbf{x}_R^T(n)]^T, \tag{3.9}$$

$$\mathbf{x}_r(n) \triangleq [x_{N_R(r-1)+1}(n), x_{N_R(r-1)+2}(n), \ldots, x_{N_R r}(n)]^T, \tag{3.10}$$

$$\boldsymbol{\eta}(n) \triangleq [\eta_1(n), \eta_2(n), \ldots, \eta_{N_R R}(n)]^T, \tag{3.11}$$

$$\mathbf{v}_{\mathfrak{F}}(n) \triangleq [\mathbf{v}^T(n), \mathbf{v}^T(n-1), \ldots, \mathbf{v}^T(n-L+1)]^T. \tag{3.12}$$

Making use of (3.6) - (3.12), the vector $\mathbf{x}(n)$ of the signals received by the relays at the nth time slot can be written as

$$\mathbf{x}(n) = \sum_{l=0}^{L-1} \mathbf{F}_l \mathbf{v}(n-l) + \boldsymbol{\eta}(n) = \mathbf{F}\mathbf{v}_{\mathfrak{F}}(n) + \boldsymbol{\eta}(n). \tag{3.13}$$

To compensate for the frequency-selective source-to-relay and relay-to-destination channels, we will use the FF relaying scheme in which the relay received signals go through FIR filters with filter lengths L_w [58], [59]. The goal of the relay filters is to equalize the frequency selective channels, i.e., to reduce ISI. Moreover, the relay filter are operating as spatial filters to separate the various data streams and direct them to their respective destination. Compared with the AF relaying scheme, the number of degrees of freedom is increased by the factor L_w which improves the system performance in terms of the achieved SINR. The drawback of long relay filter lengths is however an increased signaling overhead that results from communicating the respective filter coefficients.

Let $\mathbf{t}_r(n) \triangleq [t_{N_R(r-1)+1}(n), t_{N_R(r-1)+2}(n), \cdots, t_{N_R r}(n)]^T$ denote the vector of transmitted signals in the nth time slot at the rth relay. The $N_R \times N_R$ FF beamforming matrices of relay $\mathcal{R}_r$ are denoted as $\{\mathbf{W}_{r,l}^H\}_{l=0}^{L_w-1}$ where $\mathbf{W}_{r,l}^H$ is the lth filter matrix of the rth relay such that transmit signal vector is given by

$$\mathbf{t}_r(n) = \sum_{l=0}^{L_w-1} \mathbf{W}_{l,r} \mathbf{x}_r(n-l). \tag{3.14}$$

Note that using multi-antenna FF relays has been proposed in [84]. In the latter work, it has been demonstrated that it is desirable to have the antennas concentrated in few relays rather than having many relays with few antennas.

Let us define the overall transmit vector of all relays as $\mathbf{t}(n) \triangleq [\mathbf{t}_1^T(n), \mathbf{t}_2^T(n), \cdots, \mathbf{t}_R^T(n)]^T$ and

let us introduce

$$\mathbf{W}_l \triangleq \text{blkdiag}([\mathbf{W}_{1,l}^H, \mathbf{W}_{2,l}^H, \ldots, \mathbf{W}_{R,l}^H]), \quad l = 0, \ldots, L_w - 1, \tag{3.15}$$

$$\mathbf{W} \triangleq [\mathbf{W}_0, \mathbf{W}_1, \ldots, \mathbf{W}_{L_w-1}], \tag{3.16}$$

$$\mathbf{F}_{\mathfrak{W}} \triangleq \underline{\mathbf{F}}_{(L_w,K)}, \tag{3.17}$$

$$\mathbf{v}_{\mathfrak{W}}(n) \triangleq [\mathbf{v}^T(n), \mathbf{v}^T(n-1), \ldots, \mathbf{v}^T(n-L-L_w+2)]^T, \tag{3.18}$$

$$\boldsymbol{\eta}_{\mathfrak{W}}(n) \triangleq [\boldsymbol{\eta}^T(n), \boldsymbol{\eta}^T(n-1), \ldots, \boldsymbol{\eta}(n-L_w+1)]^T, \tag{3.19}$$

where have used (B.1) to define the cyclic matrix $\underline{\mathbf{F}}_{(L_w,K)}$ that has a block Toepliz structure. Making use of (3.13) - (3.19), $\mathbf{t}(n)$ can be expressed as

$$\mathbf{t}(n) = \sum_{l=0}^{L_w-1} \mathbf{W}_l \mathbf{x}(n-l) = \mathbf{W}\left(\mathbf{F}_{\mathfrak{W}} \mathbf{v}_{\mathfrak{W}}(n) + \boldsymbol{\eta}^T(n)\right). \tag{3.20}$$

The signals transmitted by the relays pass through the relay-to-destination channels where $g_{q,m,l}$ denotes the lth filter tap of the channel from the qth relay antenna to destination $\mathcal{D}_m$. Introducing

$$\mathbf{g}_{m,l} \triangleq [g_{1,m,l}, g_{2,m,l}, \ldots, g_{N_R R,m,l}]^T, \quad m = 1, \ldots, M, \quad l = 0, \ldots, L-1, \tag{3.21}$$

$$\mathbf{g}_m \triangleq [\mathbf{g}_{m,0}^T, \mathbf{g}_{m,1}^T, \ldots, \mathbf{g}_{m,L-1}^T]^T, \tag{3.22}$$

$$\mathbf{t}_{\mathfrak{W}}(n) \triangleq [\mathbf{t}^T(n), \mathbf{t}^T(n-1), \ldots, \mathbf{t}^T(n-L+1)]^T, \tag{3.23}$$

the signal received at destination $\mathcal{D}_m$ can be written as

$$y_m(n) = \sum_{l=0}^{L-1} \mathbf{g}_{m,l}^T \mathbf{t}(n-l) + \upsilon_m(n) = \mathbf{g}_m^T \mathbf{t}_{\mathfrak{W}}(n) + \upsilon_m(n) \tag{3.24}$$

where $\upsilon_m(n)$ is the white receiver noise at destination $\mathcal{D}_m$ with power $\mathrm{E}\{|\upsilon_m(n)|^2\} = \sigma^2$ for all m, n.

It is assumed that the sequence of signals $y_m(n)$ received at destination $\mathcal{D}_m$ is passed through an FIR filter of length L_u with coefficients $\{u_{m,l}^*\}_{l=0}^{L_u-1}$ to obtain the signal $z_m(n)$ given by

$$\begin{aligned} z_m(n) &= \sum_{l=0}^{L_u-1} u_{m,l}^* y_m(n-l) \\ &= \mathbf{u}_m^H \mathbf{G}_{m,\mathfrak{U}} \mathbf{W}_{\mathfrak{U}} \mathbf{F}_{\mathfrak{U}} \sum_{m=1}^{M} \mathbf{A}_{m,\mathfrak{U}} \mathbf{s}_{m,\mathfrak{U}}(n) + \mathbf{u}_m^H \mathbf{G}_{m,\mathfrak{U}} \mathbf{W}_{\mathfrak{U}} \boldsymbol{\eta}_{\mathfrak{U}}(n) + \mathbf{u}_m^H \boldsymbol{\nu}_m(n), \end{aligned} \tag{3.25}$$

following (3.1) - (3.24) and using the definitions

$$\mathbf{u}_m \triangleq [u^*_{m,0}, \ldots, u^*_{m,L_u-1}]^T, \quad m = 1, \ldots, M, \tag{3.26}$$

$$\mathbf{G}_{m,\mathfrak{U}} \triangleq \underline{(\mathbf{g}_m)^T}_{(L_u,N_R R)}, \quad m = 1, \ldots, M, \tag{3.27}$$

$$\mathbf{g}_m \triangleq [\mathbf{g}^T_{m,0}, \ldots, \mathbf{g}^T_{m,L-1}]^T, \quad m = 1, \ldots, M, \tag{3.28}$$

$$\mathbf{W}_{\mathfrak{U}} \triangleq \underline{\mathbf{W}}_{(L_u+L-1,N_R R)}, \quad m = 1, \ldots, M, \tag{3.29}$$

$$\mathbf{F}_{\mathfrak{U}} \triangleq \underline{\mathbf{F}}_{(L_u+L_w+L-2,N_S)}, \tag{3.30}$$

$$\mathbf{A}_{m,\mathfrak{U}} = \underline{\mathbf{A}_m}_{(L_u+L_w+2L-3,1)}, \quad m = 1, \ldots, M, \tag{3.31}$$

$$\mathbf{s}_{m,\mathfrak{U}}(n) \triangleq [s_m(n), \ldots, s_m(n - L_a - L_w - L_u - 2L + 5)]^T, \quad m = 1, \ldots, M, \tag{3.32}$$

$$\boldsymbol{\eta}_{\mathfrak{U}}(n) \triangleq [\boldsymbol{\eta}^T(n), \ldots, \boldsymbol{\eta}(n - L_w - L_u - L + 3)]^T, \tag{3.33}$$

$$\boldsymbol{\nu}_m(n) \triangleq [\nu_m(n), \nu_m(n-1), \ldots, \nu_m(n - L_u + 1)]^T, \quad m = 1, \ldots, M. \tag{3.34}$$

In (3.27), (3.29), and (3.31), we have used (B.1) to define the block Toepliz matrices $\underline{(\mathbf{g}_m)^T}_{(L_u,N_R R)}$, $\underline{\mathbf{W}}_{(L_u+L-1,N_R R)}$ and $\underline{\mathbf{A}_m}_{(L_u+L_w+2L-3,1)}$ respectively. Let us select the symbol $s_m(n - n')$, $n' = L_u - 1$, for the detection at destination $\mathcal{D}_m$. Then, making use of the definitions (3.26) - (3.34), and further introducing the $(L_a + L_w + L_u + 2L - 4) \times 1$ identity vector $\mathbf{e}_{n'}$, $\mathbf{E}_{n'} = \mathrm{diag}(\mathbf{e}_{n'})$, and $\breve{\mathbf{E}}_{n'} = \mathbf{I} - \mathbf{E}_{n'}$, we can express (3.25) as $z_m(n) = z_{m,\mathrm{S}} + z_{m,\mathrm{ISI}} + z_{m,\mathrm{MUI}} + z_{\mathrm{N},m}$, where

$$z_{m,\mathrm{S}} \triangleq \mathbf{u}_m^H \mathbf{G}_{m,\mathfrak{U}} \mathbf{W}_{\mathfrak{U}} \mathbf{F}_{\mathfrak{U}} \mathbf{A}_{m,\mathfrak{U}} \mathbf{E}_{L_u} \mathbf{s}_{m,\mathfrak{U}}(n), \tag{3.35}$$

$$z_{m,\mathrm{ISI}} \triangleq \mathbf{u}_m^H \mathbf{G}_{m,\mathfrak{U}} \mathbf{W}_{\mathfrak{U}} \mathbf{F}_{\mathfrak{U}} \mathbf{A}_{m,\mathfrak{U}} \breve{\mathbf{E}}_{L_u} \mathbf{s}_{m,\mathfrak{U}}(n), \tag{3.36}$$

$$z_{m,\mathrm{MUI}} \triangleq \mathbf{u}_m^H \mathbf{G}_{m,\mathfrak{U}} \mathbf{W}_{\mathfrak{U}} \mathbf{F}_{\mathfrak{U}} \sum_{k=1,k\neq m}^{M} \mathbf{A}_{k,\mathfrak{U}} \mathbf{s}_{k,\mathfrak{U}}(n), \tag{3.37}$$

$$z_{m,\mathrm{N}} \triangleq \mathbf{u}_m^H \mathbf{G}_{m,\mathfrak{U}} \mathbf{W}_{\mathfrak{U}} \boldsymbol{\eta}_{\mathfrak{U}}(n) + \mathbf{u}_m^H \boldsymbol{\nu}_m(n), \tag{3.38}$$

and $z_{m,\mathrm{S}}$, $z_{m,\mathrm{ISI}}$, $z_{m,\mathrm{MUI}}$, and $z_{\mathrm{N},m}$ denote the desired signal, the ISI, the MUI and the noise, respectively.

3.2.2 SINR maximization

In this section, we aim to select the filter coefficients of the source, the relays, and the destinations to maximize the smallest QoS at the destinations. According to Chapter 2.3, we quantify the QoS in terms of the received SINR. The corresponding max-min fairness optimization problem can be

formulated according to (2.17) as

$$\begin{aligned}\max_{\substack{\{a^*_{m,k,l}\}_{l=0,m=1}^{La-1,M},\{\mathbf{W}_{r,l}^H\}_{l=0}^{Lw-1},\\ \{\mathbf{u}_m\}_{m=1}^M}} \gamma \quad \text{s.t.} \quad & \mathrm{SINR}_m \geq \gamma, \\ & p_r \leq p_{r,\max}, \quad r = 1,\ldots,R, \\ & P_{\mathrm{R}} \leq P_{\mathrm{R,max}}, \\ & P_{\mathrm{S}} \leq P_{\mathrm{S,max}}, \\ & P_{\mathrm{T}} \leq P_{\mathrm{T,max}} \\ & \gamma > 0. \end{aligned} \tag{3.39}$$

Note that a total power constraint as in (2.17) is not present and we do not consider power allocation between the source and the relays in the above problem. To make the optimization problem mathematically treatable, let us derive the SINR and the transmit powers in (3.39) as functions of the optimization variables. The SINR at destination $\mathcal{D}_m$ is given by

$$\mathrm{SINR}_m = \frac{\mathrm{E}\{|z_{m,\mathrm{S}}|^2\}}{\mathrm{E}\{|z_{m,\mathrm{ISI}}|^2\} + \mathrm{E}\{|z_{m,\mathrm{MUI}}|^2\} + \mathrm{E}\{|z_{m,\mathrm{N}}|^2\}}. \tag{3.40}$$

Defining

$$\mathbf{q}_{m,k}^H \triangleq \mathbf{u}_m^H \mathbf{G}_{m,\mathfrak{U}} \mathbf{W}_{\mathfrak{U}} \mathbf{F}_{\mathfrak{U}} \mathbf{A}_{k,\mathfrak{U}}, \quad m = 1,\ldots,M, \quad k = 1,\ldots,M, \tag{3.41}$$

and using (3.35) - (3.38) the terms in (3.40) can be identified as

$$\mathrm{E}\{|z_{m,\mathrm{S}}|^2\} \triangleq |\,[\mathbf{q}_{m,m}]_{L_u}\,|^2, \tag{3.42}$$

$$\mathrm{E}\{|z_{m,\mathrm{ISI}}|^2\} \triangleq \mathbf{q}_{m,m}^H \check{\mathbf{E}}_{L_u} \mathbf{q}_{m,m}, \tag{3.43}$$

$$\mathrm{E}\{|z_{m,\mathrm{MUI}}|^2\} \triangleq \sum_{k=1,k\neq m}^{M} \mathbf{q}_{m,k}^H \mathbf{q}_{m,k}, \tag{3.44}$$

$$\mathrm{E}\{|z_{m,\mathrm{N}}|^2\} \triangleq \sigma^2 \left(\mathbf{u}_m^H \mathbf{G}_{m,\mathfrak{U}} \mathbf{W}_{\mathfrak{U}}\right) \left(\mathbf{u}_m^H \mathbf{G}_{m,\mathfrak{U}} \mathbf{W}_{\mathfrak{U}}\right)^H + \sigma^2 \mathbf{u}_m^H \mathbf{u}_m. \tag{3.45}$$

Let us consider the power constraints in (3.39), where P_{S} is the power consumed at source $\mathcal{S}$ for transmitting $\mathbf{v}(n)$. P_{S} is given as the sum of the powers consumed at each antenna. Assuming uncorrelated symbols, hence, $\mathrm{E}\{s_{m_1}(n_1)s_{m_2}^*(n_2)\} = 1$ if $m_1 = m_2$ and $n_1 = n_2$, and $\mathrm{E}\{s_{m_1}(n_1)s_{m_2}^*(n_2)\} = 0$ otherwise, we obtain

$$P_{\mathrm{S}} = \sum_{k=1}^{N_S} \mathrm{E}\left\{\left|\sum_{m=1}^{M}\sum_{l=0}^{L_a-1} a_{m,k,l}^* s_m(n-l)\right|^2\right\} = \sum_{k=1}^{N_S}\sum_{m=1}^{M}\sum_{l=0}^{L_a-1} |a_{m,k,l}|^2 = \sum_{m=1}^{M} \mathbf{a}_m^H \mathbf{a}_m = \mathbf{a}^H \mathbf{a}, \tag{3.46}$$

where

$$\mathbf{a}_m \triangleq \mathrm{vec}\{\mathbf{A}_m\}, \quad m = 1, \ldots, M, \tag{3.47}$$

$$\mathbf{a} \triangleq [\mathbf{a}_1^T, \ldots, \mathbf{a}_M^T]^T, \tag{3.48}$$

and $\mathbf{a}$ is the $L_a N_S M \times 1$ vector that contains all the precoding filter coefficients.

The individual relay power $p_r = \mathrm{E}\{\|\mathbf{t}_r(n)\|^2\}$ in (3.39) is calculated in Appendix C.1.1 and can be expressed as the quadratic form

$$p_r = \mathbf{w}^H \mathbf{D}_r \mathbf{w}. \tag{3.49}$$

where $\mathbf{w}$ is $RN_R^2 L_w \times 1$ vector that contains all the relay filter coefficients and is defined by

$$\mathbf{w} \triangleq [\mathbf{w}_0^T, \ldots, \mathbf{w}_{L-1}^T]^T, \tag{3.50}$$

$$\mathbf{w}_l \triangleq [\mathrm{vec}\{\mathbf{W}_{1,l}^T\}^T, \ldots, \mathrm{vec}\{\mathbf{W}_{R,l}^T\}^T]^T. \tag{3.51}$$

The matrix $\mathbf{D}_r$ is defined according to (C.7). The individual relay power p_r can alternatively to (3.49) be formulated as a function of the precoding vector $\mathbf{a}$ according to Appendix C.1.2 such that

$$p_r = p_{r,\eta} + \mathbf{a}^H \mathbf{D}_{r,\mathfrak{A}} \mathbf{a}, \tag{3.52}$$

where $\mathbf{D}_{r,\mathfrak{A}}$ is defined in (C.10). In (3.52), $p_{r,\eta}$ denotes the power that is wasted to amplify the noise received at relay $\mathcal{R}_r$ and which cannot be influenced by the choice of $\mathbf{a}$.

Expressing the relay power in (3.49) and (3.52) as quadratic forms is convenient for the development of the iterative algorithm in the rest of this chapter. With the individual relay powers given by (3.49) and (3.52), the relay sum power in (3.39) is given according to (C.6) by

$$P_{\mathrm{R}} = \sum_{r=1}^{R} p_r = \mathbf{w}^H \left(\sum_{r=1}^{R} \mathbf{D}_r \right) \mathbf{w} = \mathbf{w}^H \mathbf{D} \mathbf{w}, \tag{3.53}$$

where $\mathbf{D} \triangleq \sum_{r=1}^{R} \mathbf{D}_r$.

The joint optimization of the variables $\mathbf{a}$, $\mathbf{w}$ and $\{\mathbf{u}_m\}_{m=1}^M$ leads to a highly nonlinear optimization problem which is difficult to be solved directly. We propose an alternating algorithm that sequentially optimizes one subset of variables while fixing the remaining variables. The proposed iterative algorithm enjoys the desirable property that the achieved SINR either improves or remains at the same level in each iteration.

We first consider the optimization of $\{\mathbf{u}_m\}_{m=1}^M$, then the optimization of $\mathbf{a}$ in Section 3.2.2 and finally the optimization of $\mathbf{w}$.

Destination filter optimization

In this section, the destination filter coefficients contained in the $L_u \times 1$ vectors $\{\mathbf{u}_m\}_{m=1}^{M}$ are optimized and it is assumed that $\mathbf{a}$ and $\mathbf{w}$ are constant. As the filter coefficients at the destination $\mathcal{D}_m$ do not affect the SINR at the other destinations, the max-min fairness optimization problem can be solved at each destination independently of the other destinations. Consequently, the max-min fairness problem reduces to

$$\max_{\mathbf{u}_m} \quad \text{SINR}_m \text{ for } m = 1, \ldots, M. \tag{3.54}$$

It is clear that the relay power and the source power are not functions of the destination filter coefficients. Therefore, the power constraints of (3.39) are not present in (3.54).

Using the definitions (C.13) - (C.17) of Appendix C.1.3, we have $\mathrm{E}\{|z_{m,\mathrm{S}}|^2\} = |\mathbf{u}_m^H \mathbf{h}_{m,\mathfrak{U}}|^2$, $\mathrm{E}\{|z_{m,\mathrm{ISI}}|^2\} = \mathbf{u}_m^H \mathbf{Q}_{m,\mathrm{ISI},\mathfrak{U}} \mathbf{u}_m$, $\mathrm{E}\{|z_{m,\mathrm{MUI}}|^2\} = \mathbf{u}_m^H\ \mathbf{Q}_{m,\mathrm{MUI},\mathfrak{U}} \mathbf{u}_m$, and $\mathrm{E}\{|z_{m,\mathrm{N}}|^2\} = \mathbf{u}_m^H\ \mathbf{Q}_{m,\mathrm{MUI},\mathfrak{N}} \mathbf{u}_m$. Then, we can rewrite (3.54) as

$$\max_{\mathbf{u}_m} \frac{|\mathbf{u}_m^H \mathbf{h}_{m,\mathfrak{U}}|^2}{\mathbf{u}_m^H \mathbf{Q}_{m,\mathfrak{U}} \mathbf{u}_m}, \tag{3.55}$$

where $\mathbf{Q}_{m,\mathfrak{U}} = \mathbf{Q}_{m,\mathrm{ISI},\mathfrak{U}} + \mathbf{Q}_{m,\mathrm{MUI},\mathfrak{U}} + \mathbf{Q}_{m,\mathrm{N},\mathfrak{U}}$.

For the problem in (3.55), the Wiener filtering solution $\mathbf{u}_m^\star = (\mathbf{Q}_{m,\mathfrak{U}})^{-1} \mathbf{h}_{m,\mathfrak{U}}$ is optimal and yields the value $\text{SINR}_m^\star = \mathbf{h}_{m,\mathfrak{U}}^H (\mathbf{Q}_{m,\mathfrak{U}})^{-1} \mathbf{h}_{m,\mathfrak{U}}$ [137].

Precoder optimization

In this section, we assume that $\{\mathbf{u}_m\}_{m=1}^{M}$ and $\mathbf{w}$ are constant and optimize with respect to the precoder filter coefficients $\mathbf{a}$. Using the definitions (C.18) - (C.24) of Appendix C.1.4, we find that

$$\text{SINR}_m = \frac{|\mathbf{a}^H \mathbf{h}_{m,\mathfrak{A}}|^2}{\mathbf{a}^H \mathbf{Q}_{m,\mathfrak{A}} \mathbf{a} + \sigma_{m,\mathfrak{A}}^2}, \tag{3.56}$$

where $\mathbf{Q}_{m,\mathfrak{A}}$ is the covariance matrix of ISI, MUI, and noise, $\mathbf{h}_{m,\mathfrak{A}}$ is the relay created channel vector from source $\mathcal{S}$ to destination $\mathcal{D}_m$, and $\sigma_{m,\mathfrak{A}}^2$ is the power of the noise at the destination which comprises noise forwarded by the relays as well as its own receiver noise.

Using (3.52) and (3.56), and introducing an auxiliary variable $\tau = 1/\gamma$ such that $\text{SINR}_m \geq 1/\tau$,

we can rewrite the max-min fairness problem in (3.39) as

$$\min_{\mathbf{a},\tau>0} \tau \quad \text{s.t.} \quad 0 \geq \frac{\mathbf{a}^H \mathbf{Q}_{m,\mathfrak{A}} \mathbf{a} + \sigma_{m,\mathfrak{A}}^2}{\tau} - |\mathbf{a}^H \mathbf{h}_{m,\mathfrak{A}}|^2, \quad m = 1, \ldots, M, \tag{3.57a}$$

$$\mathbf{a}^H \mathbf{a} \leq P_{\mathrm{S,max}}, \tag{3.57b}$$

$$\mathbf{a}^H \mathbf{D}_{r,\mathfrak{A}} \mathbf{a} + p_{r,\eta} \leq p_{r,\mathrm{max}}, \quad r = 1, \ldots, R, \tag{3.57c}$$

$$\sum_{r=1}^{R} \mathbf{a}^H \mathbf{D}_{r,\mathfrak{A}} \mathbf{a} + p_{r,\eta} \leq P_{\mathrm{R,max}}. \tag{3.57d}$$

Note that the problem in (3.57) has the same structure as the max-min fair multi-user downlink beamforming problem of conventional beamforming which has been treated in [110]. The constraint (3.57a) of the problem in (3.57) is non-convex due to the left hand side of the inequality. Note that the right-hand side of the constraint is convex as the fraction of a convex quadratic form divided by a linear form is a convex function [73]. We follow the inner approximation approach of Chapter 2.4 and propose to replace this constraint by a convex approximation. Note that SDR approach of Chapter 2.4 cannot be easily integrated in alternating algorithms. The reason is that the SDR-solution may not always lead to a feasible solution that improves the objective function of 3.39. Therefore, convergence and monotonicity cannot be guaranteed.

Let us introduce a linearization of the non-convex left-hand side of the inequality in (3.57a) around the fixed variables $\mathbf{a}^{(\kappa)}$ and $\tau^{(\kappa)}$, where the superscript κ denotes the iteration index. Let $\Delta\mathbf{a}$ and $\Delta\tau$ denote the update variables. We replace the original optimization variables $\mathbf{a}$ and τ in (3.57) by $\mathbf{a}^{(\kappa)} + \Delta\mathbf{a}$ and by $\tau^{(\kappa)} + \Delta\tau$, respectively. It is assumed that the set $(\mathbf{a}^{(\kappa)}, \tau^{(\kappa)})$ is feasible for (3.57). Thus $1/\tau^{(\kappa)} = \min_m \mathrm{SINR}_m^{(\kappa)}$ is achieved with $\mathbf{a}^{(\kappa)}$ in the kth iteration. Then, the non-convex term $|\mathbf{a}^H \mathbf{h}_{m,\mathfrak{A}}|^2$ in (3.57a) is replaced by its linearization $|\mathbf{a}^{(\kappa)H} \mathbf{h}_{m,\mathfrak{A}}|^2 + 2\Re\{\Delta\mathbf{a}^H \mathbf{h}_{m,\mathfrak{A}} \mathbf{h}_{m,\mathfrak{A}}^H \mathbf{a}^{(\kappa)}\}$ where the quadratic term $\Delta\mathbf{a}^H \mathbf{h}_{m,\mathfrak{A}} \mathbf{h}_{m,\mathfrak{A}}^H \Delta\mathbf{a}$ is neglected. The feasible set of the resulting convex optimization problem

$$\begin{aligned}
\min_{\Delta\mathbf{a},\Delta\tau} \tau^{(\kappa)} + \Delta\tau > 0 \quad \text{s.t.} \quad & 0 \geq \frac{(\Delta\mathbf{a} + \mathbf{a}^{(\kappa)})^H \mathbf{Q}_{m,\mathfrak{A}} (\Delta\mathbf{a} + \mathbf{a}^{(\kappa)}) + \sigma_{m,\mathfrak{A}}^2}{\tau^{(\kappa)} + \Delta\tau} \\
& - (|\mathbf{a}^{(\kappa)H} \mathbf{h}_{m,\mathfrak{A}}|^2 + 2\Re\{(\Delta\mathbf{a})^H \mathbf{h}_{m,\mathfrak{A}} \mathbf{h}_{m,\mathfrak{A}}^H \mathbf{a}^{(\kappa)}\}), \quad m = 1, \ldots, M, \\
& (\Delta\mathbf{a} + \mathbf{a}^{(\kappa)})^H (\Delta\mathbf{a} + \mathbf{a}^{(\kappa)}) \leq P_{\mathrm{S,max}}, \\
& (\Delta\mathbf{a} + \mathbf{a}^{(\kappa)})^H \mathbf{D}_{r,\mathfrak{A}} (\Delta\mathbf{a} + \mathbf{a}^{(\kappa)}) + p_{r,\eta} \leq p_{r,\mathrm{max}}, \quad r = 1, \ldots, R, \\
& \sum_{r=1}^{R} (\Delta\mathbf{a} + \mathbf{a}^{(\kappa)})^H \mathbf{D}_{r,\mathfrak{A}} (\Delta\mathbf{a} + \mathbf{a}^{(\kappa)}) + p_{r,\eta} \leq P_{\mathrm{R,max}},
\end{aligned} \tag{3.58}$$

is a subset of the feasible set of the problem in (3.57). Note that this method is referred to as

the concave-convex procedure (CCCP) and results in a convex inner approximation of the original optimization problem. CCCP-based algorithms are versatile approaches for non-convex optimization [140], [141], and have been recently applied to the optimization of multi-user p2p relay networks [31]. In the CCCP-based algorithm, the constraint and objective functions are decomposed into differences of two convex (DC) functions. The concave (negative convex) functions are then linearized, which leads to a convex (approximated) problem.

Let $(\Delta\mathbf{a}^\star, \Delta\tau^\star)$ be a solution to (3.58) and the updated variables are given by $\tau^{(\kappa+1)} = \tau^{(\kappa)} + \Delta\tau^\star$ and $\mathbf{a}^{(\kappa+1)} = \mathbf{a}^{(\kappa)} + \Delta\mathbf{a}^\star$. The linearization of the concave function yields a convex optimization problem. According to Theorem 5 of the Appendix A the following statements can be made

Corollary 1. *The updated variables* $(\mathbf{a}^{(\kappa+1)}, \tau^{(\kappa+1)})$*, obtained by a solution* $(\Delta\mathbf{a}^\star, \Delta\tau^\star)$ *to (3.58), are feasible and* $\tau^{(\kappa+1)} \leq \tau^{(\kappa)}$*.*

Therefore, $(\mathbf{a}^{(\kappa+1)}, \tau^{(\kappa+1)})$ satisfy the power constraints of (3.57) and $\Delta\tau^\star \leq 0$ and any non-trivial solution of (3.58) leads to a feasible update of $\mathbf{a}^{(\kappa)}$ which increases the smallest SINR since $1/\tau^{(\kappa+1)} \leq 1/\tau^{(\kappa)}$ holds true.

Relay beamformer optimization

The optimization of the relay filter coefficients is similar to the optimization of the precoding coefficients. However, even though the problem formulation of both problems is much the same, the relay beamformer optimization is not equivalent to the multi-user downlink beamforming problem in [110] as it was the case for the precoder optimization. The reason is that there is only one relay weight vector for all destinations, whereas for the precoder optimization, there is a particular precoding weight vector for each destination, see definition (3.47).

Let us utilize the definitions of Appendix C.1.4 to obtain

$$\mathrm{SINR}_m = \frac{|\mathbf{w}^H \mathbf{h}_{m,\mathfrak{W}}|^2}{\mathbf{w}^H \mathbf{Q}_{m,\mathfrak{W}} \mathbf{w} + \sigma^2}, , \tag{3.59}$$

where $\mathbf{Q}_{m,\mathfrak{W}}\mathbf{w}$ is the covariance matrix of ISI, MUI, and noise defined according to (C.27) and $\mathbf{h}_{m,\mathfrak{W}}$ is an $RN_R^2 L_w \times 1$ vector defined according to (C.26).

We formulate the approximated max-min fairness beamforming problem as

$$\begin{aligned}\min_{\Delta\mathbf{w},\Delta\tau} \tau^{(\kappa)}+\Delta\tau \quad \text{s.t.} \quad & \tau^{(\kappa)}+\Delta\tau>0,\\ & |\mathbf{w}^{(\kappa)H}\mathbf{h}_{m,\mathfrak{W}}|^2+2\Re\{(\Delta\mathbf{w})^H\mathbf{h}_{m,\mathfrak{W}}\mathbf{h}_{m,\mathfrak{W}}^H\mathbf{w}^{(\kappa)}\}\geq\\ & \quad\frac{(\Delta\mathbf{w}+\mathbf{w}^{(\kappa)})^H\mathbf{Q}_{m,\mathfrak{W}}(\Delta\mathbf{w}+\mathbf{w}^{(\kappa)})+\sigma^2\|\mathbf{u}_m\|^2}{\tau^{(\kappa)}+\Delta\tau}, \quad m=1,\ldots,M,\\ & (\Delta\mathbf{w}+\mathbf{w}^{(\kappa)})^H\mathbf{D}_r(\Delta\mathbf{w}+\mathbf{w}^{(\kappa)})\leq p_{r,\max}, \quad r=1,\ldots,R,\\ & (\Delta\mathbf{w}+\mathbf{w}^{(\kappa)})^H\mathbf{D}(\Delta\mathbf{w}+\mathbf{w}^{(\kappa)})\leq P_{\mathrm{R,max}},\end{aligned} \tag{3.60}$$

where we substituted the original optimization variables $\mathbf{w}$ and τ by $\mathbf{w}^{(\kappa)}+\Delta\mathbf{w}$ and $\tau^{(\kappa)}+\Delta\tau$, respectively, and $1/\tau^{(\kappa)}$ stands for the smallest SINR achieved with $\mathbf{w}^{(\kappa)}$. According to Corollary 1, a solution $(\Delta\mathbf{w}^\star,\Delta\tau^\star)$ of the convex optimization problem in (3.60) in the kth iteration leads to the feasible update $\tau^{(\kappa+1)}=\tau^{(\kappa)}+\Delta\tau^\star$ and $\mathbf{w}^{(\kappa+1)}=\mathbf{w}^{(\kappa)}+\Delta\mathbf{w}^\star$ and $1/\tau^{(\kappa+1)}\leq 1/\tau^{(\kappa)}$.

Alternating iterative algorithm

The proposed iterative algorithm consists of successively solving problems (3.54), (3.58), and (3.60). Note that (3.54) has a closed form solution and the convex optimization problems (3.58) and (3.60) can be efficiently solved using interior-point methods. We initialize $\mathbf{w}^{(0)}$ and $\mathbf{a}^{(0)}$ as complex circularly distributed Gaussian random variables, scaled to satisfy the power constraints in (3.39) and set $\mathbf{u}_m^{(0)}=[\mathbf{0}_{L_u-2}^T,1,0]^T$ for $m=1,\ldots,M$. For $\kappa=1,2,\ldots,$ $\mathbf{a}^{(\kappa)}$ is updated by solving (3.58) and $\mathbf{w}^{(\kappa)}$ is updated by solving (3.60). The iterative algorithm is terminated if the relative progress $(\min\mathrm{SINR}^{(\kappa+1)}-\min\mathrm{SINR}^{(\kappa)})/\min\mathrm{SINR}^{(\kappa)}$ is smaller than the threshold value 10^{-2}.

3.2.3 Simulation results

In the simulations, we consider a scenario of a source with $N_S=4$ antennas, $R=3$ relays with $N_R=2$ antennas and $M=4$ destinations. The relays and the destinations are placed on circles with radius r_1 =1 km, and r_2 =2 km around source $\mathcal{S}$, respectively, at equidistant angles as illustrated in Figure 3.1. A sampling frequency of 5 MHz and a path loss coefficient $\mu=3$ are assumed. The length L of the impulse responses of the source-to-relay and relay-to-destination channels is modeled as $L=6$. The filter taps of the channels are generated as zero mean circularly distributed Gaussian random variables with an exponential power delay profile. The variance of the lth tap, $l=0,\ldots,L-1$, is given by[82]

$$\frac{P_{\mathrm{MP}}}{\sigma_t}e^{-lT_s/\sigma_t}, \tag{3.61}$$

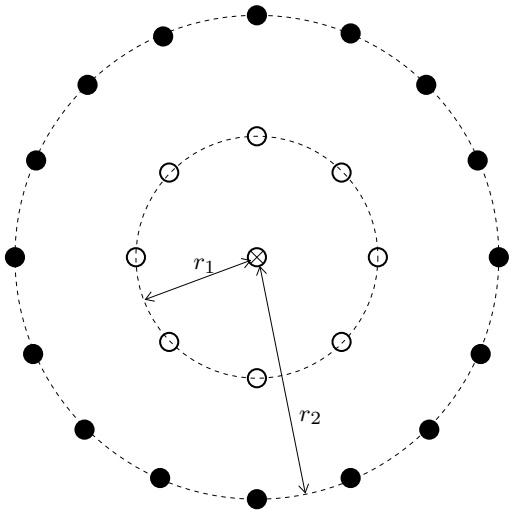

Figure 3.1: Setup of the network; ⊗: Source, ○: Relay, •: Destination.

where T_s is the symbol duration, P_{MP} is the average power of the multipath components, and σ_t characterizes the delay spread. Here, we choose $\sigma_{\mathrm{t}} = T_s(L-1)/\ln(0.01)$ and $P_{\mathrm{MP}} = (d/1\mathrm{km})^{-\mu}$ where d is the distance of the respective source-to-relay or relay-to-destination channel. The noise power is given by $\sigma^2 = 1$. The threshold values for the admitted powers are given by $P_{\mathrm{S,max}} = P_{\mathrm{R,max}} = 20\mathrm{dBm}$ above the noise level and $p_{r,\max} = P_{\mathrm{R,max}}/2$ for $r = 1, \ldots, R$. The results are averaged over 100 Monte Carlo runs. During the simulations, it is observed that updating $\mathbf{u}_m$ has minor impact on the progress compared with the updates of $\mathbf{a}$ and $\mathbf{w}$. To save computation time, $\mathbf{u}_m$ is updated only in every second iteration.

Figure 3.2 depicts the minimum SINR versus the destination filter length L_u, Figure 3.3 depicts the minimum SINR versus the relay filter length L_w and Figure 3.4 presents the minimum SINR versus the source filter length L_a. From Figure 3.2, we observe that the destination filter length has little impact on the performance. Figure 3.3 indicates that the relay filter length has impact if the source filter length is small. Figure 3.4 demonstrates that the source filter length has the most impact on the system performance. The figures indicate that the system performance saturates at approximately 15 dB that can be achieved via a long source filter length, regardless of the relay and destination filter lengths.

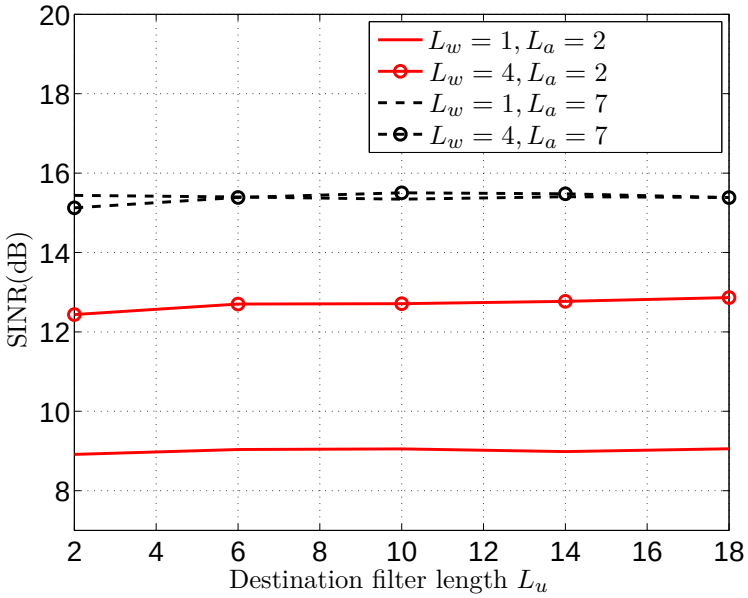

Figure 3.2: SINR versus the destination filter length L_u.

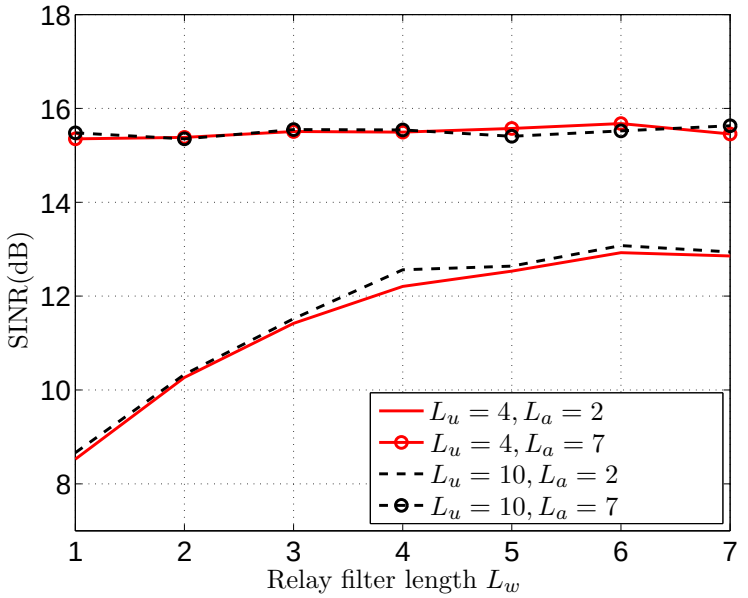

Figure 3.3: SINR versus the relay filter length L_w.

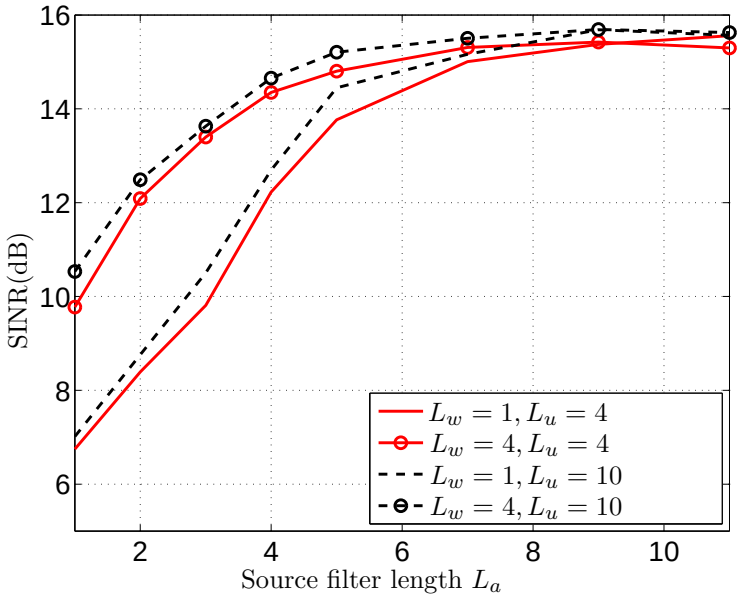

Figure 3.4: SINR versus the source filter length L_a.

3.3 Peer-To-Peer Relay Beamforming

In this section, we consider the p2p communication of $K = M$ source-destination pairs via R FF relays, see Figure 3.5. Each source, destination and relay node is equipped with a single antenna, $N_R = 1$. It is assumed without any loss of generality that source $\mathcal{S}_m$ transmits its message to destination $\mathcal{D}_m$. In this section, we do not consider precoding at the sources and channel equalization at the destinations. The signal model of this p2p scheme is a special case of the signal model developed in Section 3.2.1 with the parameters $N_S = M$, $N_r = 1$, $L_a = 1$, and $\mathbf{A}_m = \sqrt{P_m}\mathbf{e}_m$.

It is assumed that $s_m(n - n')$ is the desired information-bearing symbol, where $n' = \lfloor (2L + L_w - 3)/2 \rfloor$. Then, the signals $z_{m,\mathrm{S}}$, $z_{m,\mathrm{ISI}}$, $z_{m,\mathrm{MUI}}$, and $z_{\mathrm{N},m}$ are respectively given by (3.35) - (3.38) where $\mathbf{u}_m = [\mathbf{0}_{n'}^T, 1]^T$.

Here, we formulate the distributed p2p relay beamforming approaches using two different criteria. First, we develop an FF-based beamforming technique that minimizes the relay sum power subject to the QoS constraints. Our second approach is based on maximizing the worst destination QoS subject to the relay sum power and the individual relay power constraints.

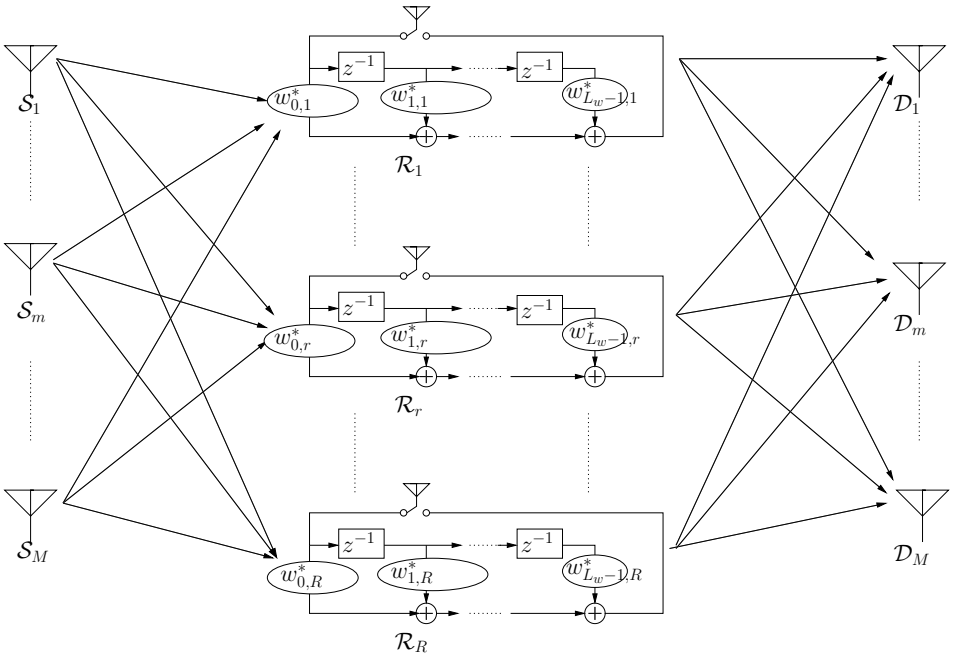

Figure 3.5: Filter-and-forward relay network.

3.3.1 Relay sum power minimization

We first consider the distributed FF beamforming problem that finds the weights by minimizing the relay sum power P_{R} subject to certain required QoS (SINR) constraints of the destinations. Mathematically, this problem is formulated as a power minimization problem according to (2.15). Let us use the definitions (C.26) - (C.31) of Appendix C.1.4 and define

$$\mathbf{Q}_{m,\mathrm{S}} \triangleq \mathbf{h}_{m,\mathfrak{W}}\mathbf{h}_{m,\mathfrak{W}}^H, \quad m = 1,\ldots,M.$$

To formulate the problem of minimizing the relay sum power as a function of the $RL_w \times 1$ relay filter vector $\mathbf{w}$ is then given by

$$\min_{\mathbf{w}} \ \mathbf{w}^H\mathbf{D}\mathbf{w} \quad \text{s.t.} \quad \mathbf{w}^H\left(\mathbf{Q}_{m,\mathrm{S}} - \gamma_m\mathbf{Q}_{m,\mathfrak{W}}\right)\mathbf{w} \geq \gamma_m\sigma^2, \quad m = 1,\ldots,M. \tag{3.62}$$

For any given values of $\{\gamma_m\}_{m=1}^M$, the feasibility of (3.62) can be checked. If one or more of the matrices $\left(\mathbf{Q}_{m,\mathrm{S}} - \gamma_m\mathbf{Q}_{m,\mathfrak{W}}\right)$ are *negative semi-definite* the problem in (3.62) is infeasible. However, in the multi-user case ($M > 1$), even if all the matrices $\left(\mathbf{Q}_{m,\mathrm{S}} - \gamma_m\mathbf{Q}_{m,\mathfrak{W}}\right)$ are not negative semi-definite, the optimization problem can be infeasible. The optimization problem is feasible if and only if a $\tilde{\mathbf{w}}$ exists such that $\tilde{\mathbf{w}}^H\left(\mathbf{Q}_{m,\mathrm{S}} - \gamma_m\mathbf{Q}_{m,\mathfrak{W}}\right)\tilde{\mathbf{w}} > 0$ for all $m = 1,\ldots,M$. Hence, a feasible solution can be obtained by re-scaling $\tilde{\mathbf{w}}$ to satisfy the constraints in (3.62).

In general, the problem in (3.62) is not convex and may not be solvable in polynomial time. Let us develop a way to relax the problem to a convex form and to solve it approximately via SDR.

Following the reformulation from (2.19) to (2.22), the SDR version of the problem in (3.62) is given by

$$\begin{aligned} \min_{\mathbf{X}} \operatorname{tr}(\mathbf{D}\mathbf{X}) \quad \text{s.t.} \quad & \operatorname{tr}\left((\mathbf{Q}_{m,\mathrm{S}} - \gamma_m \mathbf{Q}_{m,\mathfrak{W}})\mathbf{X}\right) \geq \gamma_m \sigma^2, \quad m = 1, \ldots, M, \\ & \mathbf{X} \succeq 0, \end{aligned} \tag{3.63}$$

where $\mathbf{X}$ is an $R \times R$ positive semidefinite Hermitian matrix.

3.3.2 SINR maximization

Let us consider another relevant distributed beamforming problem. Let us maximize the worst receiver SINR subject to both the sum and individual relay transmit power constraints. This problem can mathematically be formulated according to (2.17). Let $P_{\mathrm{R,max}}$ be the maximum relay sum power and let $p_{r,\max}$ be the maximum transmit power of relay $\mathcal{R}_r$. Using (3.53), the max-min fairness beamforming problem can be expressed as

$$\begin{aligned} \max_{\gamma,\mathbf{w}} \quad \gamma \quad \text{s.t.} \quad & \mathbf{w}^H \left(\mathbf{Q}_{m,\mathfrak{S}} - \gamma \mathbf{Q}_{m,\mathfrak{W}}\right) \mathbf{w} \geq \gamma \sigma^2, \quad m = 1, \ldots, M, \\ & \mathbf{w}^H \mathbf{D} \mathbf{w} \leq P_{\max}, \\ & \mathbf{w}^H \mathbf{D}_r \mathbf{w} \leq p_{r,\max}, \qquad r = 1, \ldots, R, \\ & \gamma > 0. \end{aligned} \tag{3.64}$$

This problem is non-convex and, therefore, cannot be solved efficiently. However, using the SDR approach (i.e., dropping the rank-one constraint $\mathfrak{R}(\mathbf{X}) = 1$), one can relax (3.64) to the following form

$$\begin{aligned} \max_{\gamma,\mathbf{X}} \quad \gamma \quad \text{s.t.} \quad & \operatorname{tr}\left(\left(\mathbf{Q}_{m,\mathrm{S}} - \gamma \mathbf{Q}_{m,\mathfrak{W}}\right)\right) \mathbf{X}\right) \geq \gamma \sigma^2, \quad m = 1, \ldots, M, \\ & \operatorname{tr}(\mathbf{D}\mathbf{X}) \leq P_{\max}, \\ & \operatorname{tr}(\mathbf{D}_r \mathbf{X}) \leq p_{r,\max}, \qquad r = 1, \ldots, R, \\ & \mathbf{X} \succeq 0, \quad \gamma > 0. \end{aligned} \tag{3.65}$$

In contrast to the problem in (3.63), the problem in (3.65) is always feasible, since the feasibility set is always non-empty as $(\gamma = 0, \mathbf{X} = \mathbf{O}_R)$ is always feasible.

The problem in (3.65) is *quasi-convex*, because for any value of γ, its related *feasibility problem*

$$\begin{aligned} \underset{\mathbf{X}}{\text{Find}}\ \mathbf{X} \quad \text{s.t.} \quad & \operatorname{tr}\left(\left(\mathbf{Q}_{m,\mathrm{S}} - \gamma \mathbf{Q}_{m,\mathfrak{W}}\right)\right) \mathbf{X}\right) \geq \gamma\sigma^2, \quad m = 1, \ldots, M, \\ & \operatorname{tr}(\mathbf{D}\mathbf{X}) \leq P_{\max}, \\ & \operatorname{tr}(\mathbf{D}_r\mathbf{X}) \leq p_{r,\max}, \qquad r = 1, \ldots, R, \\ & \mathbf{X} \succeq 0 \end{aligned} \tag{3.66}$$

belongs to the class of convex semi-definite programming problems. The problem in (3.66) can be solved by modern optimization software.

Let $\gamma^\star$ be the maximum objective value of (3.65) with solution matrix $\mathbf{X}^\star$. Then, for any $\gamma > \gamma^\star$, the problem in (3.66) is infeasible. If $\gamma \leq \gamma^\star$, then (3.66) is always feasible as $(\gamma, \mathbf{X}^\star)$ is feasible. Hence, $\gamma^\star$ and the corresponding optimum matrix $\mathbf{X}^\star$ can be found by using the bisection search. Introducing a search interval $[\gamma_l, \gamma_u]$ that involves $\gamma^\star$, we have that (3.66) is feasible for $\gamma = \gamma_l$ and is infeasible for $\gamma = \gamma_u$. For this interval, the bisection search technique can be formulated as the Algorithm 1. Here, ε denotes the accuracy value for determining $\gamma^\star$. It should be chosen small

Algorithm 1: SINR Maximization via SDR.

```
begin
    while (γ_u − γ_l)/γ_l > ε do
        Set γ := (γ_l + γ_u)/2.
        Solve the feasibility problem in (3.66).
        if (3.66) feasible then
            γ_l := γ
        else
            γ_u := γ
        end
    end
end
return τ*, X_1*, a*
```

enough to obtain a good final approximation of this parameter.

3.3.3 Simulation results

In the simulations, a relay network with $R = 10$ relays and quasi-static frequency-selective source-to-relay and relay-to-destination channels with the lengths $L = 5$ is considered. The channel impulse

response taps are modeled as zero mean complex Gaussian random variables with exponential power delay profile, according to (3.61). In the simulations, $P_{\mathrm{MP}} = 1$ and $\sigma_t = 2T_s$ are used. The relay and destination noise processes are assumed to have the same power $\sigma^2 = 1$, and for the sources the transmit power is 10 dB higher than σ^2. Throughout our examples, we consider the cases of $M = 2$ and $M = 3$ source-destination pairs. Our results are averaged over 500 simulation runs.

In the first example, we test the approach of Section 3.3.1 which is based on minimizing the relay sum power subject to the QoS constraints. Figure 3.6 depicts the relay sum power versus the minimum SINR $\gamma = \gamma_m, m = 1, \ldots, M$, for different filter lengths L_w. It is important to stress that the problem in (3.63) may be infeasible for some simulation runs due to the SINR constraints which may not be satisfiable. The reason is that MUI and relay noise can be the dominant factors in the SINR (and not the destination noise). Then, the SINR cannot be improved by simply increasing the relay power. If the problem is infeasible in less than 50% of the simulation runs, we drop the corresponding point from the figures. Otherwise, we display the corresponding point in the figures using the average of the feasible runs.

Figure 3.6 shows that the FF approach substantially reduces the relay sum power as compared with the AF approach ($L_w = 1$) and also significantly improves the SINR feasibility range of the distributed beamforming problem.

Figure 3.7 depicts the relay sum power versus the relay filter length L_w for different values of the required SINR at the destination. Again, we can see from this figure that, as compared with the AF scheme, the FF approach improves the feasibility and reduces the necessary relay sum power to meet the SINR constraints. Note that the relay sum power decreases monotonically as the length of the relay filter increases. It is worth noting that, according to the extensive simulations with the given relay network parameter values, the computed solution to (3.63) is always rank-one and, therefore, no randomization is needed in this example. In the latter case, the principal eigenvector of the solution to (3.63) gives the exact solution to the original the problem in (3.62).

In the second example, the approach of Section 3.3.2 is tested which maximizes the worst destination SINR subject to power constraints. As the optimization problem in (3.65) is always feasible, the average over all simulation runs is displayed in each figure. It is assumed that the relays have the maximum individual transmit power $p_{\max} = p_{r,\max}, r = 1, \ldots, R$, and that the maximum relay sum power is two times higher than $p_{\max}$, i.e., $P_{rmR,\max} = 2p_{\max}$.

It can be observed that the solution $\mathbf{X}^\star$ to the semi-definite relaxed problem in (3.65) is not always rank-one in this example. To obtain a good solution to the original problem (3.64), we

have used the randomization technique described in [94]. In particular, we have computed the eigendecomposition of $\mathbf{X}^\star = \mathbf{U}\mathbf{\Sigma}\mathbf{U}^H$ to generate a set of 1000 different random candidate vectors $\mathbf{w} = \mathbf{\Sigma}^{1/2}\mathbf{U}^H\mathbf{v}$, where $\mathbf{v}$ is a randomly generated vector whose entries are zero mean, unit-variance complex circular symmetric uncorrelated Gaussian random variables. Each candidate vector has been scaled to ensure the feasibility of (3.64) and the candidate vector with the highest worst receiver SINR has been selected as the final solution.

Figure 3.8 depicts the achieved SINR versus the individual relay transmit power $p_{\max}$ for different lengths of the relay filters. Figure 3.9 displays the SINR versus the relay filter length L_w for different values of the maximum individual relay transmit power $p_{\max}$. Both of these figures show that the SINR can be substantially improved by increasing the filter length L_w. These improvements are monotonic in L_w.

In the third example, the SINR is maximized subject to the constraint on the relay sum power only. The resulting problem is a special case of (3.64), since the constraints on the individual relay transmit powers are dropped.

Figure 3.10 depicts the achieved SINR versus the relay sum power $P_{\mathrm{R},\max}$ for different lengths of the relay filters and for $M = 2$ and $M = 3$. Figure 3.11 shows the SINR versus the relay filter length L_w for different values of the relay sum power $P_{\mathrm{R},\max}$. As in the previous examples, it can be seen from these figures that the FF approach substantially outperforms the AF approach and that increasing the filter length L_w monotonically improves the SINR. As in the first example, the optimal solution in this example is always rank-one.

In the fourth example, the goal is to maximize the QoS under individual relay power constraints only. It is assumed that the relays operate with the same maximum transmit power $p_{\max}$. This beamforming problem is also a special case of (3.64), where the constraint on the relay sum power is dropped. In this example, the solutions to the semi-definite relaxed problem were not always rank-one and we have used the randomization technique. Figure 3.12 shows the SINR versus the relay filter length L_w for different values of $p_{\max}$. Similar to Figure 3.9, it can be seen that the achieved SINR increases with the relay filter length and that increasing the number of source-destination pairs leads to higher individual relay powers to achieve the same QoS. Since there is no sum power constraint, the achieved SINRs are higher than in the second example. Compared with 3.12, the SINRs achieved in 3.11 are lower, because the individual power constraints are tighter than the constraint on the relay sum power.

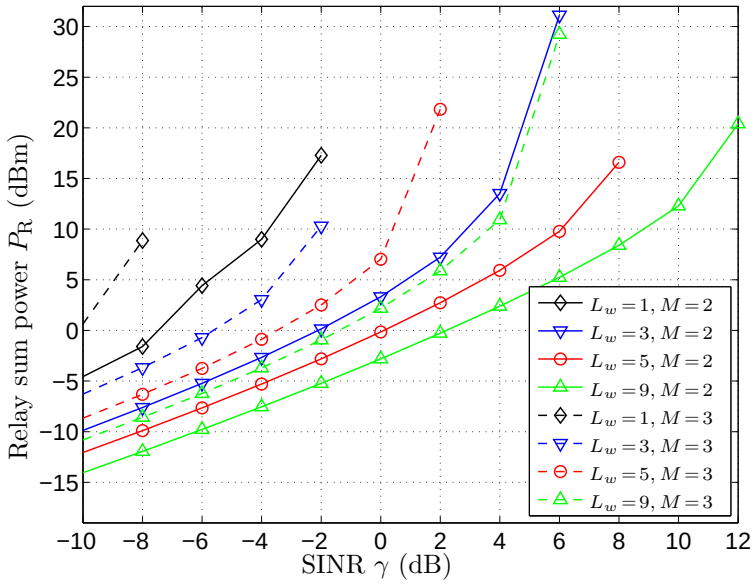

Figure 3.6: Relay sum power P_{R} versus required SINR; first example.

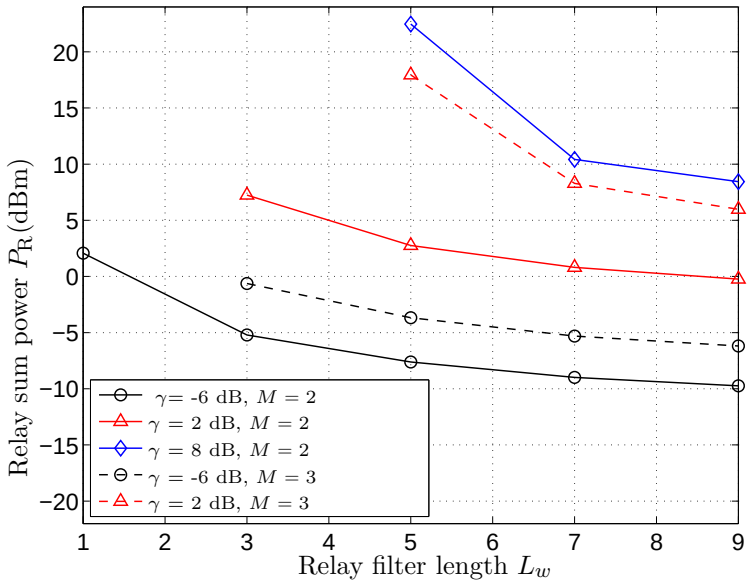

Figure 3.7: Relay sum power P_{R} versus relay filter length L_w; first example.

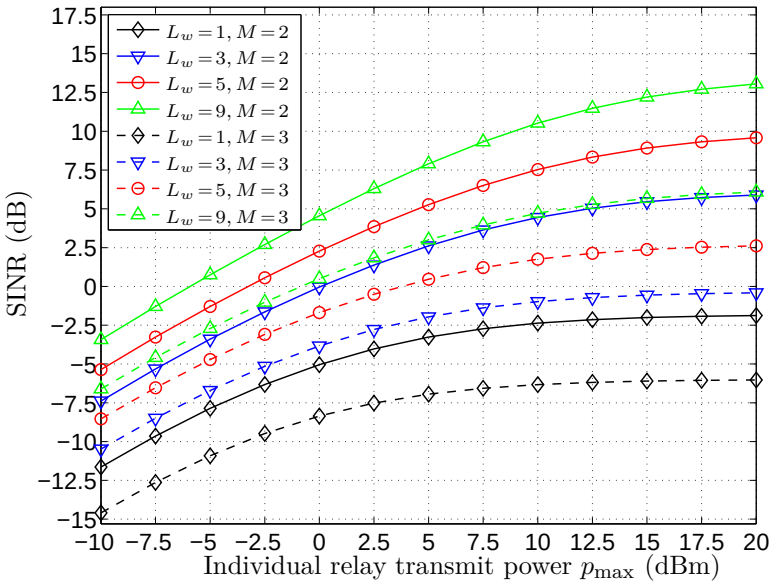

Figure 3.8: SINR versus the maximum individual relay transmit power $p_{\max}$; second example.

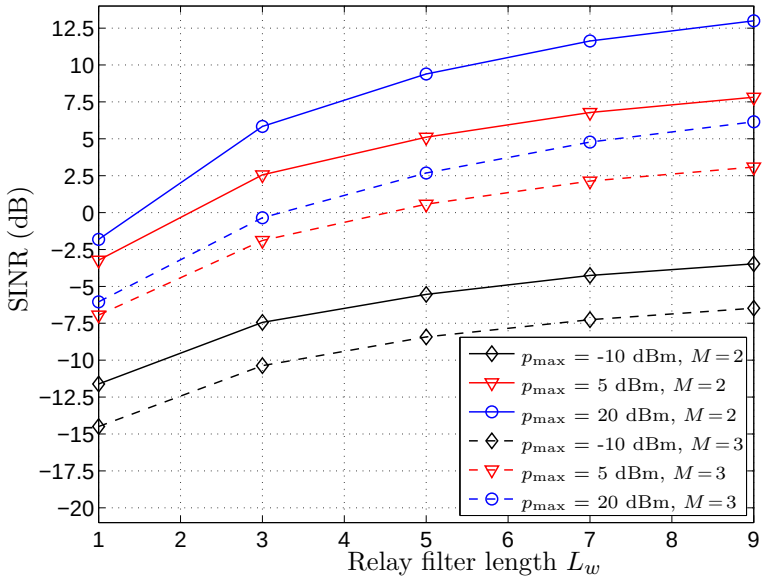

Figure 3.9: SINR versus relay filter length L_w; second example.

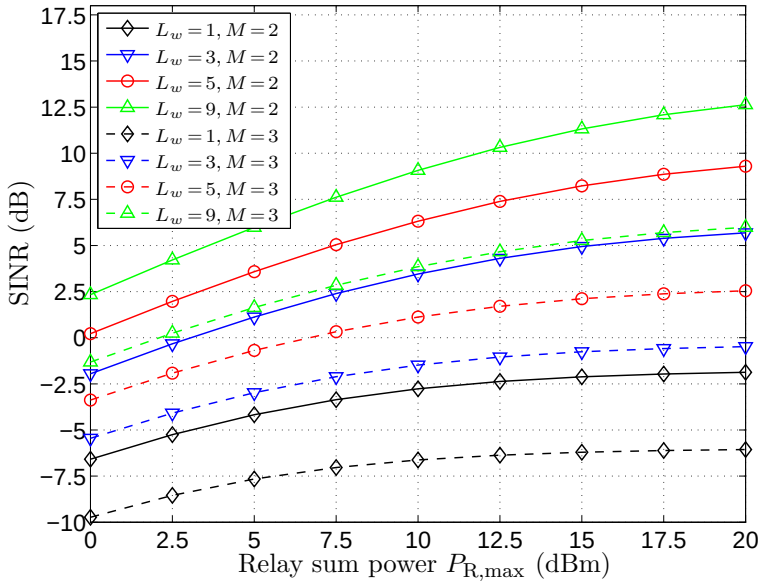

Figure 3.10: SINR versus the maximum relay sum power $P_{\mathrm{R,max}}$; third example.

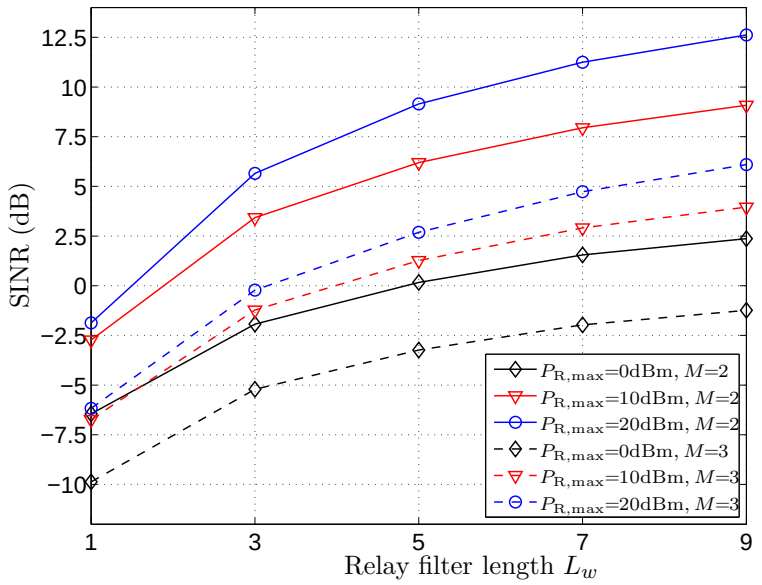

Figure 3.11: SINR versus relay filter length L_w; third example.

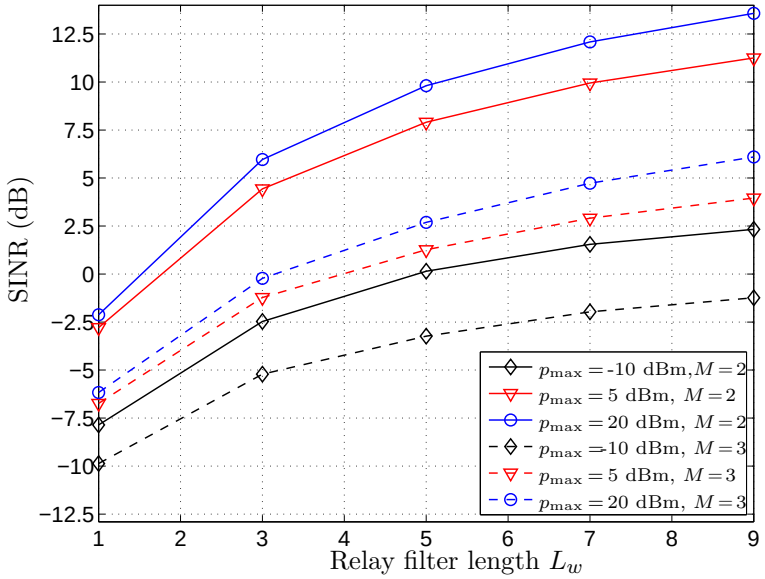

Figure 3.12: SINR versus the relay filter length L_w; fourth example.

3.4 Conclusion

In this chapter, we have considered FF relaying with frequency selective channels and multiple users.

First, we have proposed to use precoding at the multi-antenna source and channel equalization at the destinations to mitigate ISI and MUI in the multi-user downlink scheme. To compute the filter coefficients at the source, the relays, and the destinations, an iterative algorithm is proposed that is based on convex inner approximations. The simulation results demonstrate the performance gain due to precoding. Furthermore, at a large source filter length, the lengths of the relay and destination filters have little impact on the performance. To avoid exhaustive signaling of filter coefficients, it is attractive to reduce the lengths of the relays and destination filters by increasing the precoder length.

Second, we have considered multi-user p2p FF relaying, that can be regarded as a special case of the multi-user downlink scheme. In this scheme, we do not consider precoding or channel equalization at the destinations. Our simulation results have demonstrated that in frequency-selective scenarios, the proposed FF p2p methods provide substantial performance improvements as compared with the AF p2p beamforming approach, especially for high filter lengths. To solve the non-convex optimization problems to compute the relay filter weights, the SDR method was successfully applied and yielded in the majority of the simulation scenarios global optimum solutions. However, one

drawback of the SDR method for max-min fairness SINR maximization was the computational burden that is a consequence of the bisection search of Algorithm 1.

Chapter 4

Rank-two beamforming and power allocation in multicasting relay networks

4.1 Introduction

In the multi-user downlink scenario of Chapter 3.2, it is assumed that each destination requires individual data. However, in many applications multiple destinations demand common data. To avoid exhaustive individual transmissions, multimedia multicast and multimedia broadcast services are features of the LTE-Advanced standard [2].

In [94], it has been proposed to provide common data among multiple terminals using a multi-antenna source that performs beamforming. The authors of [94] have proposed to use the SDR method to reformulate the non-convex QCQPs into convex SDPs, as it has been done also in Chapter 3.3. As it was pointed out in Chapter 2.4, in the case of a high number of destinations M, the SDR solution matrix $\mathbf{X}^\star$ is likely to be infeasible for the original optimization problem, that is $\text{rank}(\mathbf{X}^\star) \geq 2$. Then, suboptimal solutions can be found by randomization techniques, however, the performance gap between these solutions and the theoretical bound (obtained by SDR as a by product) is known to be large for large number of destinations M.

Recently, in the two independent works [96] and [100], rank-two transmit beamforming techniques for multicasting have been proposed for which rank-one and rank-two SDR solution matrices are feasible. In these techniques, two weight vectors are used at the transmitter to process two data symbols jointly. Rank-two beamforming techniques have gained much interest in the current research as the system performance is enhanced due to the increased number of degrees of freedom resulting

from the additional weight vector [39], [96]–[100]. The gain in performance comes at virtually no additional cost of decoding at the receiver since symbol detection can be applied [89].

In this chapter, we propose a distributed rank-two beamforming scheme using a network of AF relays for single-group multicasting. Since we assume flat fading channels, no ISI occurs. In our AF multicasting scheme (AFMS), the relays forward common messages from a single source to multiple destinations. Note that no MUI occurs as all destinations demand the same data, and consequently, there is no interference of different transmitted data streams. The proposed AFMS is a non-trivial extension of the transmit beamforming technique of [96] and [100] to a distributed beamforming system. We will refer to our scheme as the Rank-2-AFMS in distinction to the conventional Rank-1-AFMS of [41]. As another generalization to the Rank-1-AFMS, we exploit direct link connections from the source to the destinations.

As the design criterion to select the power at the source and the relay weights, we aim to maximize the minimum QoS at the destinations according to (2.16) under constraints on the transmit power in the network. We consider constraints on the maximum transmit power of the source, on the individual power of every relay, on the sum power of the relays, and on the total power by both the relays and the source. To solve the non-convex max-min fairness optimization problem of jointly determining the relay weight vector and the power split between the relays and the source, we propose an iterative algorithm based on inner approximations according to Chapter 2.4. The proposed algorithm belongs to the class of CCCP algorithms. CCCP algorithms have been proposed for many optimization problems that arise in the context of wireless communication, including power allocation [30]–[31] and beamforming problems [64]–[68]. In contrast to the algorithms for max-min fair beamforming of [33], [108], [95], [68], [70] our algorithm derives both the relay weight vectors and distributes a power budget among the source and the relays. Note that the max-min fair beamforming approaches in [108] and [95] use algorithms similar to Algorithm 1 of Chapter 3.3.2 and combine the SDR technique with one-dimensional (1D) bisection search on the maximum QoS. To compare our CCCP algorithm (Max-Min-CCCP) with the latter SDR-based algorithms, we propose to combine the SDR method with 2D search (SDR2D) on both the maximum QoS and the best power split between the relays and the source. The SDR2D can be seen as a generalization of Algorithm 1.

To test the schemes under realistic conditions, we use the channel model of [138] to create the channel coefficients for our simulations. The results demonstrate the performance of the proposed rank-two scheme combined with the proposed algorithm compared with the rank-one scheme of the

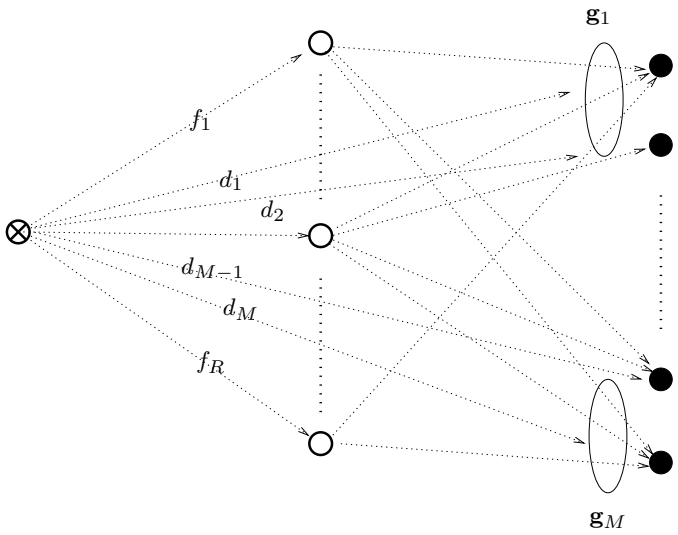

Figure 4.1: Multicasting via a relay network; ⊗: Source, ○: Relay, ●: Destination.

literature and the theoretical bound obtained by SDR2D. The Max-Min-CCCP algorithm outperforms the SDR2D algorithm for high destination numbers at a much lower run time. Moreover, the Max-Min-CCCP algorithm offers a good performance-run-time trade-off and achieves a minimum SNR which is less than 1 dB lower than the theoretical bound after three iterations.

The contribution of this chapter can be summarized as follows:

- The conventional Rank-1-AFMS of [41] has been generalized to the Rank-2-AFMS.
- The direct link connection from the source to the destinations is exploited.
- A CCCP algorithm has been successfully applied to the rank-two beamforming scheme. The weight vectors and the proper source power are jointly computed.
- The performance of the proposed system combined with the proposed Max-Min-CCCP algorithm is compared with the theoretical performance bound obtained by the SDR2D algorithm.
- The proposed algorithm offers an attractive trade-off between performance and run-time.

4.2 Signal model

Let us consider the wireless network of Chapter 2.2.1 comprising a single source ($K = 1$) $\mathcal{S}$ and M destinations, see Figure 4.1. As in Chapter 2.2.1 the channels in the network are frequency-flat and constant over the four considered time slots. In extension to the network model in Chapter 2.2.1,

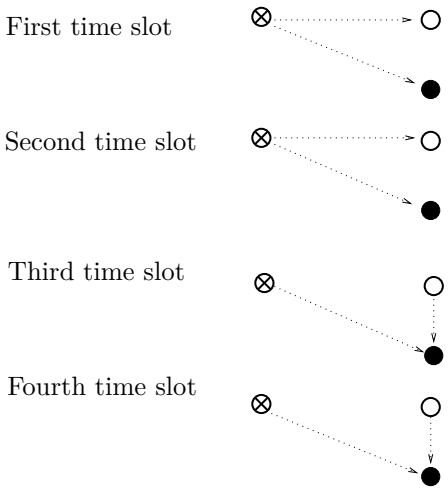

Figure 4.2: Proposed Alamouti Coded AFMS; ⊗: Source $\mathcal{S}$, ○: Relays, ●: Destinations.

it is assumed that there exist non-zero direct paths from the source to the destinations. The proposed Rank-2-AFMS is different to the conventional two time slots scheme of Chapter 2.2.1, as two information-bearing symbols are jointly processed in four time slots, see Figure 4.2.

In the first two time slots, the source S transmits the data symbols to the relays. In the third and the fourth time slot, the relays retransmit their received signals using the Alamouti STBC scheme. Here, the relays transmit their signals not over two different antennas as , e.g., the transmitter in a corresponding 2×1 MISO system, but over two different beams. In this fashion, our proposed Rank-2-AFMS enables the relays to create two different communication links from source S to the destinations. In the conventional Rank-1-AFMS of [41], the communication of one data symbol is performed in two time slots where one weight vector creates a single communication link.

In the first and the second time slot of the Rank-2-AFMS, source S transmits the data symbols s_1 and s_2^* which are drawn from a signal constellation $\mathcal{M}$, respectively. Both symbols are weighted by a real-valued power scaling factor α_1. Note that we have chosen the same scaling for both symbols to simplify the decoding at the destinations. The $R \times 1$ vectors $\mathbf{x}(1) \triangleq [x_1(1), \ldots, x_R(1)]^T$ and $\mathbf{x}(2) \triangleq [x_1(2), \ldots, x_R(2)]^T$ of the received signals at the relays in the first and in the second time slot are respectively given by

$$\mathbf{x}(1) = \mathbf{f}\alpha_1 s_1 + \boldsymbol{\eta}(1), \quad \mathbf{x}(2) = \mathbf{f}\alpha_1 s_2^* + \boldsymbol{\eta}(2), \tag{4.1}$$

where

$$\mathbf{f} \triangleq \mathbf{f}_1 = [f_{1,1}, \ldots, f_{1,R}]^T \tag{4.2}$$

is the $R \times 1$ vector, containing the complex coefficients of the frequency flat channels from source S to the relays and where $\boldsymbol{\eta}(1) \triangleq [\eta_1(1), \ldots, \eta_R(1)]^T$ and $\boldsymbol{\eta}(2) \triangleq [\eta_1(2), \ldots, \eta_R(2)]^T$ are the $R \times 1$ vectors of the relay noise of the first and the second time slot, respectively. The signals $y_m(1)$ and $y_m(2)$ received by destination $\mathcal{D}_m$ in the first and the second time slot, respectively, are given by

$$y_m(1) = d_m \alpha_1 s_1 + \nu_m(1), \qquad y_m(2) = d_m \alpha_1 s_2^* + \nu_m(2), \tag{4.3}$$

where d_m is the coefficient of the channel from source S to destination $\mathcal{D}_m$ and $\nu_m(1)$ and $\nu_m(2)$ are the destination noises in the first and the second time slot, respectively.

We make the practical assumptions that the noise processes in the network are spatially and temporally uncorrelated and complex Gaussian distributed. The noise power at the destinations is given by

$$\mathrm{E}\{|\nu_m(q)|^2\} = \sigma_\nu^2 \quad q \in \{1, 2, 3, 4\}, \tag{4.4}$$

and the noise at the relays is distributed according to

$$\boldsymbol{\eta}(1) \sim \mathcal{N}(\mathbf{0}_R, \sigma_\eta^2 \mathbf{I}_R), \quad \boldsymbol{\eta}(2) \sim \mathcal{N}(\mathbf{0}_R, \sigma_\eta^2 \mathbf{I}_R), \tag{4.5}$$

where σ_η^2 is the power of the noise at the relays.

The $R \times 1$ vectors $\mathbf{t}(3) \triangleq [t_1(3), \ldots, t_R(3)]^T$ and $\mathbf{t}(4) \triangleq [t_1(4), \ldots, t_R(4)]^T$ of the signals transmitted by the relays in the third and fourth time slot, respectively, can be expressed as

$$\mathbf{t}(3) = \mathbf{W}_1 \mathbf{x}(1) + \mathbf{W}_2 \mathbf{x}^*(2), \qquad \mathbf{t}(4) = -\mathbf{W}_2 \mathbf{x}^*(1) + \mathbf{W}_1 \mathbf{x}(2), \tag{4.6}$$

where $\mathbf{W}_1 \triangleq \mathrm{diag}(\mathbf{w}_1^H)$, $\mathbf{W}_2 \triangleq \mathrm{diag}(\mathbf{w}_2^H)$, and $\mathbf{w}_1 = [w_{1,1}, \ldots, w_{R,1}]^T$ and $\mathbf{w}_2 = [w_{1,2}, \ldots, w_{R,2}]^T$ are the complex $R \times 1$ weight vectors. In (4.6), the relays transmit their receive signal vectors $\mathbf{x}_1$ and $\mathbf{x}_2$ over the two weight vectors $\mathbf{w}_1$ and $\mathbf{w}_2$. Using two weight vectors in (4.6) increases the degrees of freedom in the distributed beamformer design. In general, due to superposition of the two symbols that are simultaneously transmitted over different beams leads to difficulties in the decoding at the destinations. In the Rank-2-AFMS however, symbol-by-symbol decoding is possible which follows from the particular encoding in (4.6). The latter encoding is similar to the encoding in Alamouti's STC scheme where two data symbols are transmitted over two channels [89]. In contrast to Alamouti's scheme which assumes no CSI at the transmitter, the Rank-2-AFMS creates two "artificial" channels which are shaped by choosing two beams with corresponding beamforming vectors designed based on the CSI knowledge at the relays. Note that according to (4.6), the signals transmitted at the relays consist of linear combinations of the received signals and their conjugates. This is also the case in distributed OSTBC schemes which, however, do not use CSI [105], [107].

To exploit the direct links from source S to the destinations, the source S transmits the signals $\alpha_3 s_1 + \alpha_4 s_2$ and $-\alpha_4 s_1^* + \alpha_3 s_2^*$ in the third and the fourth time slot, respectively, where α_3 and α_4 are complex-valued scaling factors.

The received signals of the third and fourth time slot at destination $\mathcal{D}_m$ can be written as

$$\begin{aligned} y_m(3) &= \mathbf{g}_m^T \mathbf{t}(3) + d_m \alpha_3 s_1 + d_m \alpha_4 s_2 + \nu_m(3), \\ y_m(4) &= \mathbf{g}_m^T \mathbf{t}(4) - d_m \alpha_4 s_1^* + d_m \alpha_3 s_2^* + \nu_m(4), \end{aligned} \tag{4.7}$$

where $\mathbf{g}_m$ is the $R \times 1$ complex vector of the frequency flat channels in between the relays and destination $\mathcal{D}_m$ and $\nu_m(3)$ and $\nu_m(4)$ are the received noise at destination $\mathcal{D}_m$ in the third and fourth time slot, respectively.

Introducing $\mathbf{y}_m$ as the vector of the received signals at destination $\mathcal{D}_m$, $\mathbf{n}_m$ as the vector of the noises at destination $\mathcal{D}_m$, and $\mathbf{H}_m$ as the equivalent channel matrix and making use of equations (4.1) and (4.6), the received signals in the four time slots in (4.3) and (4.7) can be compactly written as

$$\mathbf{y}_m = \mathbf{H}_m \mathbf{s} + \mathbf{n}_m, \tag{4.8}$$

where

$$\mathbf{y}_m \triangleq [y_m(1), y_m^*(2), y_m(3), y_m^*(4)]^T, \tag{4.9}$$

$$\mathbf{s} \triangleq [s_1, s_2]^T, \tag{4.10}$$

$$\mathbf{n}_m \triangleq \begin{bmatrix} \nu_m(1) \\ \nu_m(2)^* \\ \mathbf{w}_1^H \mathbf{G}_m \boldsymbol{\eta}(1) + \mathbf{w}_2^H \mathbf{G}_m \boldsymbol{\eta}^*(2) + \nu_m(3) \\ -\mathbf{w}_2^T \mathbf{G}_m^H \boldsymbol{\eta}(1) + \mathbf{w}_1^T \mathbf{G}_m^H \boldsymbol{\eta}^*(2) + \nu_m^*(4) \end{bmatrix}, \tag{4.11}$$

$$\mathbf{H}_m \triangleq \begin{bmatrix} \alpha_1 d_m & 0 \\ 0 & (\alpha_1 d_m)^* \\ h_{m,1} & h_{m,2} \\ -h_{m,2}^* & h_{m,1}^* \end{bmatrix}, \tag{4.12}$$

$$h_{m,1} \triangleq \alpha_1 \mathbf{w}_1^H \mathbf{G}_m \mathbf{f} + \alpha_3 d_m, \tag{4.13}$$

$$h_{m,2} \triangleq \alpha_1 \mathbf{w}_2^H \mathbf{G}_m \mathbf{f}^* + \alpha_4 d_m, \tag{4.14}$$

$$\mathbf{G}_m \triangleq \mathrm{diag}(\mathbf{g}_m). \tag{4.15}$$

Considering that the noise processes in the network are spatially uncorrelated and using (4.4), (4.5),

and (4.11) the covariance matrix of $\mathbf{n}_m$ in (4.8) is given by

$$\mathrm{E}\left\{\mathbf{n}_m\mathbf{n}_m^H\right\} = \mathrm{blkdiag}\left([\sigma_\nu^2\mathbf{I}_2, \sigma_{m,34}^2\mathbf{I}_2]\right) \tag{4.16}$$

where

$$\sigma_{m,34}^2 \triangleq \sigma_\eta^2(\mathbf{w}_1^H\mathcal{G}_m\mathbf{w}_1 + \mathbf{w}_2^H\mathcal{G}_m\mathbf{w}_2) + \sigma_\nu^2, \tag{4.17}$$

$$\mathcal{G}_m \triangleq \mathbf{G}_m\mathbf{G}_m^H = \mathrm{diag}([|g_{m,1}|^2, \ldots, |g_{m,R}|^2]). \tag{4.18}$$

To achieve equal noise power in all time slots, we transform both sides of equation (4.8) using the diagonal scaling matrix

$$\mathbf{U} \triangleq \mathrm{blkdiag}\left([\sigma_{m,34}/\sigma_\nu\mathbf{I}_2, \mathbf{I}_2]\right). \tag{4.19}$$

resulting in

$$\mathbf{U}\mathbf{y}_m = \mathbf{U}\mathbf{H}_m\mathbf{s} + \mathbf{U}\mathbf{n}_m. \tag{4.20}$$

According to (4.16), the noise covariance matrix of $\mathbf{U}\mathbf{n}_m$ is given by $\mathrm{E}\left\{\left(\mathbf{U}\mathbf{n}_m\right)\left(\mathbf{U}\mathbf{n}_m\right)^H\right\} = \sigma_{m,34}^2\mathbf{I}_2$. Then, using (4.20), the Maximum Likelihood (ML) detection problem of finding $\mathbf{s}$ can be equivalently reformulated as the Least Squares problem

$$\min_{\mathbf{s}\in\mathcal{M}\times\mathcal{M}} \|\mathbf{U}\mathbf{y}_m - \mathbf{U}\mathbf{H}_m\mathbf{s}\|^2. \tag{4.21}$$

From (4.12) and (4.19), we observe that the matrix $\mathbf{U}\mathbf{H}_m$ consists of the two column vectors that are orthogonal with norm

$$c = \sqrt{\alpha_1^2|d_m|^2\sigma_{m,34}^2/\sigma_\nu^2 + |h_{m,1}|^2 + |h_{m,2}|^2}. \tag{4.22}$$

Let us define the matrix $\mathbf{\Pi} \triangleq (1/c)[\mathbf{\Gamma}\mathbf{H}_m, \mathbf{Z}]$, where the matrix $\mathbf{Z}$ is chosen such that $\mathbf{\Pi}^H\mathbf{\Pi} = \mathbf{I}_2$. Then, (4.21) can be equivalently written as

$$\begin{aligned}&\min_{\mathbf{s}\in\mathcal{S}\times\mathcal{S}} \left\|\mathbf{\Pi}^H\mathbf{\Gamma}\mathbf{y}_m - c\begin{bmatrix}\mathbf{I}_2\\ \mathbf{O}_2\end{bmatrix}\mathbf{s}\right\|^2\\ &= \min_{\mathbf{s}\in\mathcal{S}\times\mathcal{S}} c^2\|\hat{\mathbf{s}}_m - \mathbf{s}\|^2 + \text{constant}\end{aligned} \tag{4.23}$$

where

$$\hat{\mathbf{s}}_m \triangleq \mathbf{B}\mathbf{y}_m = \mathbf{s} + \mathbf{B}\mathbf{n}_m, \tag{4.24}$$

and

$$\mathbf{B} \triangleq (1/c)^2(\mathbf{\Gamma}\mathbf{H}_m)^H\mathbf{\Gamma}. \tag{4.25}$$

From (4.23), the detection of s_1 and s_2 decouples into two scalar detection problems since

$$\hat{\mathbf{s}}_m \sim \mathcal{N}\left(\mathbf{s}, \sigma_m^2 \mathbf{I}_2\right), \tag{4.26}$$

$$\sigma_m^2 \triangleq \frac{\sigma_{m,34}^2 \sigma_\nu^2}{\alpha_1^2 |d_m|^2 \sigma_{m,34}^2 + \sigma_\nu^2 (|h_{m,1}|^2 + |h_{m,2}|^2)}, \tag{4.27}$$

which follows directly from (4.16) and (4.25). In other words, in the proposed four phase scheme simple scalar detection at the receiver is sufficient to perform ML detection. We remark that the diagonal structure of the error covariance matrix follows from the orthogonality of the coding in (4.6).

From (4.26) we see that the SNR in $\hat{\mathbf{s}}_m$ is given by

$$\mathrm{SNR}_m = \frac{1}{\sigma_m^2} = \frac{\alpha_1^2 |d_m|^2}{\sigma_\nu^2} + \frac{|h_{m,1}|^2 + |h_{m,2}|^2}{\sigma_{m,34}^2}, . \tag{4.28}$$

for both data symbols. For the sake of convenience, let us introduce the following vector notation

$$\mathbf{w} \triangleq [\tilde{\mathbf{w}}_1^T, \tilde{\mathbf{w}}_2^T]^T, \tag{4.29}$$

$$\tilde{\mathbf{w}}_1 \triangleq [\mathbf{w}_1, (\alpha_3 \alpha_1)^*]^T, \quad \tilde{\mathbf{w}}_2 \triangleq [\mathbf{w}_2^T, (\alpha_4 \alpha_1)^*]^T, \tag{4.30}$$

$$\mathbf{Q}_{m,\mathrm{N}} \triangleq \mathrm{blkdiag}([\tilde{\mathbf{Q}}_{m,\mathrm{N}}, \tilde{\mathbf{Q}}_{m,\mathrm{N}}]), \tag{4.31}$$

$$\tilde{\mathbf{Q}}_{m,\mathrm{N}} \triangleq \mathrm{blkdiag}([\sigma_\eta^2 \mathcal{G}_m, 0]). \tag{4.32}$$

Using (4.17) and (4.29) - (4.32), we find

$$\sigma_{m,34}^2 = \tilde{\mathbf{w}}_1^H \tilde{\mathbf{Q}}_{m,\mathrm{N}} \tilde{\mathbf{w}}_1 + \tilde{\mathbf{w}}_2^H \tilde{\mathbf{Q}}_{m,\mathrm{N}} \tilde{\mathbf{w}}_2 + \sigma_\nu^2 \tag{4.33}$$

$$= \mathbf{w}^H \mathbf{Q}_{m,\mathrm{N}} \mathbf{w} + \sigma_\nu^2. \tag{4.34}$$

Let us furthermore introduce

$$\mathbf{Q}_{m,\mathrm{S}} \triangleq \mathrm{blkdiag}([\tilde{\mathbf{Q}}_{m,1,\mathrm{S}}, \tilde{\mathbf{Q}}_{m,2,\mathrm{S}}]), \tag{4.35}$$

$$\tilde{\mathbf{Q}}_{m,1,\mathrm{S}} \triangleq \mathbf{q}_{m,1} \mathbf{q}_{m,1}^H, \quad \tilde{\mathbf{Q}}_{m,2,\mathrm{S}} \triangleq \mathbf{q}_{m,2} \mathbf{q}_{m,2}^H, \tag{4.36}$$

$$\mathbf{q}_{m,1} \triangleq [(\mathbf{G}_m \mathbf{f})^T, d_m]^T, \quad \mathbf{q}_{m,2}[(\mathbf{G}_m \mathbf{f}^*)^T, d_m]^T, \tag{4.37}$$

$$a \triangleq 1/|\alpha_1|^2, \tag{4.38}$$

where a is a power scaling factor. With equations (4.13), (4.14), and (4.35) - (4.38), we have

$$|h_{m,1}|^2 + |h_{m,2}|^2 = \left(\tilde{\mathbf{w}}_1^H \tilde{\mathbf{Q}}_{m,1,\mathrm{S}} \tilde{\mathbf{w}}_1 + \tilde{\mathbf{w}}_2^H \tilde{\mathbf{Q}}_{m,2,\mathrm{S}} \tilde{\mathbf{w}}_2\right) / a$$

$$= \mathbf{w}^H \mathbf{Q}_{m,\mathrm{S}} \mathbf{w} / a.$$

Using the above identity together with (4.33) and (4.34), we reformulate the SNR given in (4.28) in vector notations as

$$\begin{aligned}&\mathrm{SNR}_m(\tilde{\mathbf{w}}_1, \tilde{\mathbf{w}}_2, a)\\ &= \frac{\tilde{\mathbf{w}}_1^H \tilde{\mathbf{Q}}_{m,1,\mathrm{S}} \tilde{\mathbf{w}}_1 + \tilde{\mathbf{w}}_2^H \tilde{\mathbf{Q}}_{m,2,\mathrm{S}} \tilde{\mathbf{w}}_2}{(\tilde{\mathbf{w}}_1^H \tilde{\mathbf{Q}}_{m,\mathrm{N}} \tilde{\mathbf{w}}_1 + \tilde{\mathbf{w}}_2^H \tilde{\mathbf{Q}}_{m,\mathrm{N}} \tilde{\mathbf{w}}_2 + \sigma_\nu^2) a} + \frac{|d_m|^2}{\sigma_\nu^2 a},\end{aligned} \tag{4.39}$$

or, equivalently, as

$$\mathrm{SNR}_m(\mathbf{w}, a) = \frac{\mathbf{w}^H \mathbf{Q}_{m,\mathrm{S}} \mathbf{w}}{(\mathbf{w}^H \mathbf{Q}_{m,\mathrm{N}} \mathbf{w} + \sigma_\nu^2) a} + \frac{|d_m|^2}{\sigma_\nu^2 a}. \tag{4.40}$$

4.3 Beamformer design and power allocation

In this section, we aim to design the weight vectors and to distribute the power between different time slots and between source $\mathcal{S}$ and the relays. We consider the problem of maximizing the minimum QoS measured in terms of the SNR at the destinations subject to power constraints. The power constraints include constraints on the individual power of each relay and source $\mathcal{S}$, the sum power of the relays and the total power of the whole network.

Let $1/\tau$ be the minimum received SNR at the destinations as introduced in Chapter 3.2.2. Then, the max-min fair optimization problem is formulated according to (2.17) as

$$\begin{aligned}\min_{\mathbf{w},a,\tau} \quad & \tau \\ \text{s.t.} \quad & \tau > 0 \\ & \mathrm{SNR}_m(\mathbf{w}, a) \geq 1/\tau \quad \forall m \in \{1, \ldots, M\} \\ & (\mathbf{w}, a) \in \Omega,\end{aligned} \tag{4.41}$$

where $\mathbf{w}$ and a belong to the set

$$\Omega \triangleq \big\{ \mathbf{w}, a \mid \mathbf{w}, a \text{ satisfy (4.42) - (4.46)} \big\}$$

defined by the different power constraints

$$a > 0 \tag{4.42}$$

$$p_r(\mathbf{w}, a) \leq p_{r,\max} \quad \forall r \in \{1, \ldots, R\} \tag{4.43}$$

$$\sum_{r=1}^{R} p_r(\mathbf{w}, a) \leq P_{\mathrm{R,max}} \tag{4.44}$$

$$P_{\mathrm{S}}(\mathbf{w}, a) \leq P_{\mathrm{S,max}} \tag{4.45}$$

$$P_{\mathrm{T}}(\mathbf{w}, a) \leq P_{\mathrm{T,max}}. \tag{4.46}$$

In equations (C.33) - (C.35) of Appendix C.2 we provide expressions for the transmit powers in vector notations as functions of the beamforming vector $\mathbf{w}$ and power scaling factor α. With these, the power constraints (4.42) - (4.46) can be reformulated as

$$a > 0 \tag{4.47}$$

$$\mathbf{w}^H \mathbf{D}_r \mathbf{w}/a + \mathbf{w}^H \mathbf{E}_r \mathbf{w} \leq p_{r,\max} \quad \forall r \in \{1, \ldots, R\} \tag{4.48}$$

$$\sum_{r=1}^{R} \left(\mathbf{w}^H \mathbf{D}_r \mathbf{w}/a + \mathbf{w}^H \mathbf{E}_r \mathbf{w} \right) \leq P_{\mathrm{R,max}} \tag{4.49}$$

$$2/a + \mathbf{w}^H \mathbf{S} \mathbf{w}/a \leq P_{\mathrm{S,max}} \tag{4.50}$$

$$2/a + \mathbf{w}^H \mathbf{S} \mathbf{w}/a + 2 \sum_{r=1}^{R} \left(\mathbf{w}^H \mathbf{D}_r \mathbf{w}/a + \mathbf{w}^H \mathbf{E}_r \mathbf{w} \right) \leq P_{\mathrm{T,max}}, \tag{4.51}$$

respectively.

The difficulty of the problem in (4.41) lies in the SNR constraints which can be formulated as

$$\frac{\mathbf{w}^H \mathbf{Q}_{m,\mathrm{N}} \mathbf{w} + \sigma_\nu^2}{\tau} - \frac{\mathbf{w}^H (\mathbf{Q}_{m,\mathrm{S}} + (|d_m|^2/\sigma_\nu^2) \mathbf{Q}_{m,\mathrm{N}}) \mathbf{w} + |d_m|^2}{a} \leq 0, \tag{4.52}$$

where we have used the SNR expression in (4.40). Due to the negative term on the left hand side of the above inequality, the SNR constraints are non-convex in general.

4.3.1 Rank-two property and relation of the Rank-2-AFMS to the Rank-1-AFMS

The Rank-1-AFMS can be regarded as a special case of the Rank-2-AFMS where symbols are transmitted sequentially from a single beamformer, i.e., $\mathbf{w}_2 = \mathbf{0}_{R+1}$. In the Rank-1-AFMS, each symbol is communicated in two time slots where in the first time slot source $\mathcal{S}$ sends the signal to the relays and in the second time slot the relays forward their received signals to the destinations. Note that the number of time slots per transmitted data symbol is two for the Rank-1-AFMS ($\mathbf{w}_2 = \mathbf{0}_{R+1}$) and the proposed Rank-2-AFMS ($\mathbf{w}_2 \neq \mathbf{0}_{R+1}$).

We will now compare the Rank-1-AFMS to the Rank-2-AFMS, applying SDR to the problem in (4.41). It will be shown that for both schemes, the SDR versions of (4.41) are equivalent.

Let us now consider an equivalent representation of the SNR at destination $\mathcal{D}_m$ given by (4.39). Defining the matrix $\mathbf{A} \triangleq \mathrm{diag}([e^{2j\varphi_1}, \ldots, e^{2j\varphi_R}, 1])$, where $\varphi_r \triangleq \arg(f_r)$, we see from the definitions (4.35) and (4.36) that $\tilde{\mathbf{Q}}_{m,1,\mathrm{S}} = \mathbf{A}^H \tilde{\mathbf{Q}}_{m,2,\mathrm{S}} \mathbf{A}$. The unitary transformation $\hat{\mathbf{w}}_2 \triangleq \mathbf{A}\tilde{\mathbf{w}}_2$ has the useful property that $\tilde{\mathbf{w}}_2^H \tilde{\mathbf{Q}}_{m,2,\mathrm{S}} \tilde{\mathbf{w}}_2 = \hat{\mathbf{w}}_2^H \tilde{\mathbf{Q}}_{m,1,\mathrm{S}} \hat{\mathbf{w}}_2$. Moreover, $\tilde{\mathbf{w}}_2^H \tilde{\mathbf{Q}}_{m,\mathrm{S}} \tilde{\mathbf{w}}_2 = \hat{\mathbf{w}}_2^H \tilde{\mathbf{Q}}_{m,\mathrm{S}} \hat{\mathbf{w}}_2$, which follows from the definition of $\mathbf{A}$ and from (4.18) and (4.32). Then, using (4.39), the SNR constraints of

(4.52) can be formulated as

$$\begin{aligned}&\tilde{\mathbf{w}}_1^H \tilde{\mathbf{Q}}_{m,1,\mathrm{S}} \tilde{\mathbf{w}}_1 + \hat{\mathbf{w}}_2^H \tilde{\mathbf{Q}}_{m,1,\mathrm{S}} \hat{\mathbf{w}}_2 \geq \\ &\left(\frac{a}{\tau} - \frac{|d_m|^2}{\sigma_\nu^2}\right) (\tilde{\mathbf{w}}_1^H \tilde{\mathbf{Q}}_{m,\mathrm{N}} \tilde{\mathbf{w}}_1 + \hat{\mathbf{w}}_2^H \tilde{\mathbf{Q}}_{m,\mathrm{N}} \hat{\mathbf{w}}_2 + \sigma_\nu^2). \end{aligned} \tag{4.53}$$

Due to the quadratic forms $\tilde{\mathbf{w}}_1^H \tilde{\mathbf{Q}}_{m,1,\mathrm{S}} \tilde{\mathbf{w}}_1$ and $\hat{\mathbf{w}}_2^H \tilde{\mathbf{Q}}_{m,1,\mathrm{S}} \hat{\mathbf{w}}_2$, the above inequality describes a non-convex set. Let us follow the SDR approach of Chapter 2.4 and replace $\mathbf{w}_1 \mathbf{w}_1^H$ by $\mathbf{X}_1$ and $\hat{\mathbf{w}}_2 \hat{\mathbf{w}}_2^H$ by $\mathbf{X}_2$ to approximate (4.41) as

$$\begin{aligned} \min_{\mathbf{X}_1, \mathbf{X}_2, \tau, a} \quad & \tau \\ \text{s.t.} \quad & \tau > 0 \\ & \mathrm{tr}\big((\mathbf{X}_1 + \mathbf{X}_2)\, \tilde{\mathbf{Q}}_{m,1,\mathrm{S}}\big) \geq \\ & \left(\frac{a}{\tau} - \frac{|d_m|^2}{\sigma_\nu^2}\right) \big(\mathrm{tr}((\mathbf{X}_1 + \mathbf{X}_2)\tilde{\mathbf{R}}_m) + \sigma_\nu^2\big) \\ & \forall m \in \{1, \ldots, M\} \\ & (\mathbf{X}_1 + \mathbf{X}_2, a) \in \mathrm{Y} \\ & \mathbf{X}_1 \succeq 0, \mathbf{X}_2 \succeq 0 \end{aligned} \tag{4.54}$$

where the constraints $\mathrm{rank}(\mathbf{X}_1) = 1$ and $\mathrm{rank}(\mathbf{X}_2) = 1$ are neglected and where the set

$$\mathrm{Y} \triangleq \big\{\mathbf{X}, a \mid \mathbf{X}, a \text{ satisfy (4.55) - (4.59)}\big\}$$

is defined by the power constraints

$$a > 0 \tag{4.55}$$

$$\mathrm{tr}\big(\mathbf{X}(\tilde{\mathbf{D}}_r/a + \tilde{\mathbf{E}}_r)\big) \leq p_{r,\max} \quad \forall r \in \{1, \ldots, R\} \tag{4.56}$$

$$\sum_{r=1}^{R} \mathrm{tr}\big(\mathbf{X}(\tilde{\mathbf{D}}_r/a + \tilde{\mathbf{E}}_r)\big) \leq P_{\mathrm{R,max}} \tag{4.57}$$

$$2/a + \mathrm{tr}\big(\mathbf{X}\tilde{\mathbf{S}}\big)/a \leq P_{\mathrm{S,max}} \tag{4.58}$$

$$2/a + \mathrm{tr}\big(\mathbf{X}\tilde{\mathbf{S}}\big)/a + 2\sum_{r=1}^{R} \mathrm{tr}\big(\mathbf{X}(\tilde{\mathbf{D}}_r/a + \tilde{\mathbf{E}}_r)\big) \leq P_{\mathrm{T,max}}. \tag{4.59}$$

Here (4.55) - (4.59) correspond to (4.47) - (4.51), respectively. Note that for the Rank-1-AFMS $\hat{\mathbf{w}}_2 = \mathbf{0}_{R+1}$ follows from $\mathbf{w}_2 = \mathbf{0}_{R+1}$ and $\mathbf{X}_2 = \mathbf{O}_{R+1}$ holds true. For the Rank-1-AFMS, the SDR

version of (4.54) is given by

$$\begin{aligned}
\min_{\mathbf{X}_1,\tau,a} \quad & \tau \\
\text{s.t.} \quad & \tau > 0 \\
& \mathrm{tr}\big(\mathbf{X}_1\tilde{\mathbf{Q}}_{m,1,\mathrm{S}}\big) \geq \\
& \left(\frac{a}{\tau} - \frac{|d_m|^2}{\sigma_\nu^2}\right)\big(\mathrm{tr}\big(\mathbf{X}_1\tilde{\mathbf{R}}_m\big)+\sigma_\nu^2\big) \;\; \forall m \in \{1,\ldots,M\} \\
& (\mathbf{X}_1, a) \in \Upsilon \\
& \mathbf{X}_1 \succeq 0.
\end{aligned} \tag{4.60}$$

Theorem 1. *The optimum value $\tau^\star$ of the problem in (4.54) corresponding to the Rank-2-AFMS is the same as for the problem in (4.60) corresponding to the Rank-1-AFMS.*

Proof. Let $(\mathbf{X}_1^\star, \tau^\star, a^\star)$ be a solution to (4.60), then $(\mathbf{X}_1^\star, \mathbf{X}_2 = \mathbf{O}_{R+1}, \tau^\star, a^\star)$ is a solution to (4.54) as the constraint functions in (4.54) only depend on the sum of $\mathbf{X}_1$ and $\mathbf{X}_2$. On the other hand, if $(\mathbf{X}_1^\star, \mathbf{X}_2^\star, \tau^\star, a^\star)$ is a solution to (4.54), then $(\mathbf{X}_1^\star + \mathbf{X}_2^\star, \tau^\star, a^\star)$ is a solution to (4.60) as the sum of positive semidefinite matrices results in a positive semidefinite matrix. □

As a consequence of the latter theorem, the SDR versions of (4.41) for the Rank-1-AFMS given by (4.60) and for the Rank-2-AFMS given by (4.54) are equivalent. For the Rank-2-AFMS, the following considerations will demonstrate that the SDR solution is feasible for (4.41) if $\Re(\mathbf{X_1}^\star) \leq 2$. The reverse statement is however not true.

Let now $\mathbf{X_1}^\star$ be a solution to (4.60) and let us assume $\Re(\mathbf{X_1}^\star) = 2$ such that $\mathbf{X}_1^\star = \lambda_1\mathbf{u}_1\mathbf{u}_1^H + \lambda_2\mathbf{u}_2\mathbf{u}_2^H$ with non-zero eigenvalues λ_1 and λ_2 and the respective eigenvectors $\mathbf{u}_1$ and $\mathbf{u}_2$. Then, the solution $\mathbf{X}_1^\star$ of the relaxed problem is a feasible global solution to (4.41). The decomposition of $\mathbf{X}_1^\star$ into two components is not unique and can be obtained from any vector pair $\tilde{\mathbf{w}}_1$ and $\hat{\mathbf{w}}_2$ satisfying $\mathbf{X}_1^\star = \tilde{\mathbf{w}}_1\tilde{\mathbf{w}}_1^H + \hat{\mathbf{w}}_2\hat{\mathbf{w}}_2^H$. This is however different for the Rank-1-AFMS approach where a single beamforming vector $\tilde{\mathbf{w}}_1$ needs to be computed. In the proposed Rank-2-AFMS, the number of degrees of freedom is increased due to the introduction of two linearly independent weight vectors.

We remark that the problem in (4.60) still represents a non-convex problem, as the fractions of two linear terms in (4.56), (4.57), and (4.59) are non-convex functions. Moreover, the multiplication of the two linear terms in the SNR-constraints of (4.60) results in a non-convex function.

However, for constant τ and a the *feasibility problem*

$$\begin{aligned} \text{Find} \quad & \mathbf{X}_1 \\ \text{s.t.} \quad & \mathrm{tr}\big(\mathbf{X}_1 \tilde{\mathbf{Q}}_{m,1,\mathrm{S}}\big) \geq \\ & \left(\frac{a}{\tau} - \frac{|d_m|^2}{\sigma_\nu^2}\right) \big(\mathrm{tr}\big(\mathbf{X}_1 \tilde{\mathbf{R}}_m\big) + \sigma_\nu^2\big) \;\; \forall m \in \{1, \ldots, M\} \\ & (\mathbf{X}_1, a) \in \mathrm{Y} \\ & \mathbf{X}_1 \succeq 0, \end{aligned} \tag{4.61}$$

to compute a feasible matrix $\mathbf{X}_1$ is convex. Remember that in Chapter 3.3.2, 1D bisection search was applied to find the optimum parameter γ (here $\gamma = 1/\tau$). In contrast to this, in order to solve (4.60), a 2D search is required since there is an additional power scaling factor a involved. Note that the optimum power allocation factor $a^\star$ cannot be found by bisection search as it is a-priori not possible to determine an appropriate search interval.

Therefore, we propose to perform grid search on a and define N as the number of grid search points. Let ε be the precision of the bisection search to find τ. A 2D search algorithm to determine the optimum solution to (4.60) (within the search precision given by N and ε) is the SDR2D algorithm, described in Algorithm 1. Note that we have initialized the bisection search algorithm with values τ_l, τ_u to guarantee that the interval $[\tau_l, \tau_u]$ is adequately large to contain $\tau^\star$. In line 5 of the SDR2D algorithm, to save run time, we avoid the bisection search on τ for values of a that are infeasible for the smallest feasible τ that has been found in previous iterations.

One drawback of the SDR2D algorithm is its computational burden to solve an SDP in each iteration of an exhaustive search. Another drawback is that $\Re(\mathbf{X}_1^\star) > 2$ in general. In this case, the computed $\tau^\star$ is only a lower bound for the problem in (4.60) (within the grid search precision) as $\mathbf{X}_1^\star$ is not feasible for the problem in (4.41) since there exists no decomposition $\mathbf{X}_1^\star = \tilde{\mathbf{w}}_1 \tilde{\mathbf{w}}_1^H + \hat{\mathbf{w}}_2 \hat{\mathbf{w}}_2^H$.

In the rest of this chapter we develop an iterative algorithm which computes the weight vector and adjusts the source power to maximize the minimum SNR at the destinations.

4.3.2 Convex inner approximation technique

In the max-min fair beamforming problem in (4.41), the left hand side of the constraints of (4.52) is the difference of $(\mathbf{w}^H \mathbf{Q}_{m,\mathrm{N}} \mathbf{w} + \sigma_\nu^2)/\tau$ and $(\mathbf{w}^H (\mathbf{Q}_{m,\mathrm{S}} + (|d_m|^2/\sigma_\nu^2)\mathbf{Q}_{m,\mathrm{N}})\mathbf{w} + |d_m|^2)/a$. As $\mathbf{Q}_{m,\mathrm{N}}$ and $\mathbf{Q}_{m,\mathrm{S}}$ are positive semidefinite matrices, these functions are both convex since they consist of a convex quadratic form divided by a linear term and a constant divided by a linear term [73].

Algorithm 2: SDR2D

```
begin
    Initialize τ* := 10^6
    for n = 0 : N do
        a := 2/ ((n/N)P_S,max),
        if τ*, a feasible for (4.61) then
            τ_l := 10^−6, τ_u = τ*
            while |τ_u − τ_l|/τ_u > ε do
                τ := (τ_u + τ_l)/2
                Solve (4.61) for given τ, a
                if (4.61) is feasible with solution X_1 then
                    τ_u = τ,
                    if τ < τ* then
                        τ* := τ
                        X_1* := X_1
                        a* := 2/ ((n/N)P_S,max)
                    end
                else
                    τ_l = t
                end
            end
        end
    end
end
return τ*, X_1*, a*
```

Therefore, the left hand side of (4.52) is a DC function and (4.41) belongs to the class of DC programs [140], [141].

To solve (4.41) approximately, we propose an iterative algorithm as discussed in Chapter 2.4 that uses inner approximations which are similar to that of Chapter 3.2.2. However, in this chapter we also consider power allocation. Note that both power allocation and beamforming have also been addressed in [31], where a CCCP algorithm has been proposed to minimize the transmit power in a cooperative relay network.

Let $\mathbf{w}^{(\kappa)}$, $a^{(\kappa)}$, and $\tau^{(\kappa)}$ be the optimization variables a and τ at the kth iteration, respectively. They are updated according to

$$\mathbf{w}^{(\kappa+1)} = \mathbf{w}^{(\kappa)} + \Delta\mathbf{w}, \quad a^{(\kappa+1)} \triangleq \Delta a + a^{(\kappa)}, \quad \tau^{(\kappa+1)} \triangleq \Delta\tau + \tau^{(\kappa)},$$

where $\Delta\mathbf{w}$, Δa, and $\Delta\tau$ are the update variables. To derive a convex approximation of the constraints (4.52) let us replace the concave part by its first order Taylor approximation around $(\mathbf{w}^{(\kappa)}, a^{(\kappa)}, \tau^{(\kappa)})$ resulting in the convex constraint

$$\begin{aligned}\lambda_m^{(\kappa)}(\Delta\mathbf{w}, \Delta a, \Delta\tau) \triangleq\ & \frac{\mathbf{w}^{(\kappa)H}(\mathbf{Q}_{m,\mathrm{S}}+(|d_m|^2/\sigma_\nu^2)\mathbf{Q}_{m,\mathrm{N}})\mathbf{w}^{(\kappa)}+|d_m|^2}{a^{(\kappa)}}\cdot\left(\frac{\Delta a}{a^{(\kappa)}}-1\right)\\ &+\frac{(\Delta\mathbf{w}+\mathbf{w}^{(\kappa)})^H\mathbf{Q}_{m,\mathrm{N}}(\Delta\mathbf{w}+\mathbf{w}^{(\kappa)})+\sigma_\nu^2}{\tau^{(\kappa)}+\Delta\tau}\\ &-\frac{2\Re\{\Delta\mathbf{w}^H(\mathbf{Q}_{m,\mathrm{S}}+(|d_m|^2/\sigma_\nu^2)\mathbf{Q}_{m,\mathrm{N}})\mathbf{w}^{(\kappa)}\}}{a^{(\kappa)}} \le 0. \end{aligned} \tag{4.62}$$

The problem

$$\begin{aligned}\min_{\Delta\mathbf{w},\Delta a,\Delta\tau}\ & \tau^{(\kappa)}+\Delta\tau\\ \text{s.t.}\quad & \lambda_m^{(\kappa)}(\Delta\mathbf{w},\Delta a,\Delta\tau)\le 0\ \ \forall m\in\{1,\dots,M\}\\ & \tau^{(\kappa)}+\Delta\tau>0\\ & (\Delta\mathbf{w}+\mathbf{w}^{(\kappa)},\Delta a+a^{(\kappa)})\in\Omega\end{aligned} \tag{4.63}$$

is convex and can be regarded as an inner approximation of (4.41). The constraint functions of (4.41) are DC functions. As their concave part has been linearized in (4.63), the *DC Programming Theorem* of the Appendix is valid. From the latter theorem follows

Corollary 2. *The updated variables* $(\mathbf{w}^{(\kappa+1)}, a^{(\kappa+1)}, \tau^{(\kappa+1)})$*, obtained by a solution* $(\Delta\mathbf{w}^\star, \Delta a^\star, \Delta\tau^\star)$ *to (4.63), are feasible for (4.41) and* $\tau^{(\kappa+1)} \le \tau^{(\kappa)}$*.*

The property $1/\tau^{(\kappa+1)} \ge 1/\tau^{(\kappa)}$ ensures that the minimum SNR increases or remains unchanged in each iteration. Repeatedly solving (4.63) for $\kappa = 0, 1, 2, \dots$ creates a monotonically non-decreasing

sequence of minimum SNR values $1/\tau^{(0)} \leq 1/\tau^{(1)} \leq 1/\tau^{(2)} \ldots$ with feasible weight vectors and a feasible transmission power. Interestingly, we can show that the latter iterative procedure does not exhibit divergence or oscillation. Moreover, the sequence $(\mathbf{w}^{(\kappa)}, a^{(\kappa)}, \tau^{(\kappa)})$ converges to a point where necessary optimality conditions are satisfied.

Theorem 3. *Let us assume that the power factor a is bounded by $a_{\max} \geq a$. Then, for any feasible initial point $(\mathbf{w}^{(0)}, a^{(0)}, \tau^{(0)})$, the sequence $(\mathbf{w}^{(\kappa)}, a^{(\kappa)}, t^{(\kappa)})$ converges to a stationary point.*

Proof. According to Theorem 10 of [141], the sequence $(\mathbf{w}^{(\kappa)}, a^{(\kappa)}, \tau^{(\kappa)})$ *globally* converges if the mapping $(\mathbf{w}^{(\kappa)}, a^{(\kappa)}, \tau^{(\kappa)}) \rightarrow (\mathbf{w}^{(\kappa+1)}, a^{(\kappa+1)}, \tau^{(\kappa+1)})$ is uniformly compact. This is the case if the feasible set of $\mathcal{M}$ is compact [141]. We now demonstrate that the variables lie inside a compact set. Using our assumption and the constraint on the source power (C.34), a is bounded by $2/P_{\mathrm{S,max}} \leq a \leq a_{\max}$. Moreover, due to the power constraints (4.48) - (4.51) it is clear that the weight vector $\mathbf{w}$ is bounded. For τ we have $\tau_{\mathrm{opt}} \leq \tau \leq \tau^{(0)}$, where τ_{opt} is the (unknown) optimum value. □

For the latter proof, we have assumed that $a \leq a_{\max}$ which implies that the source power during the first two time slots does not vanish. Adding $a \leq a_{\max}$ as an additional constraint to $\mathcal{M}$ is therefore not critical if we choose a large $a_{\max}$. Then, the approximated problem (4.63) becomes

$$\begin{aligned} \min_{\Delta\mathbf{w},\Delta a,\Delta\tau} \quad & \tau^{(\kappa)} + \Delta\tau \\ \text{s.t.} \quad & \lambda_m^{(\kappa)}(\Delta\mathbf{w}, \Delta a, \Delta\tau) \leq 0 \quad \forall m \in \{1, \ldots, M\} \\ & a^{(\kappa)} + \Delta a \leq a_{\max} \\ & \tau^{(\kappa)} + \Delta\tau > 0 \\ & (\Delta\mathbf{w} + \mathbf{w}^{(\kappa)}, \Delta a + a^{(\kappa)}) \in \Omega. \end{aligned} \tag{4.64}$$

The Max-Min-CCCP algorithm outlined in Algorithm 2 starts at a random point and iterates until the relative progress $\rho \triangleq |\tau^k - \tau^{k+1}|/\tau^k$ falls below the threshold value ε.
(4.63) is solved exactly. To reduce the computational cost, it is possible to use an inaccurate solution [103]. A detailed description of an implementation is beyond the scope of this work. We consider here and in the rest of this chapter to solve the subproblems exactly that arise in every iteration of our proposed algorithm.

4.4 Simulation results

To test the proposed scheme under realistic conditions, we consider a relay network where the channel coefficients of the source-to-relay, relay-to-user, and source-to-user channels are created by using the urban micro scenario [138]. The system parameters are chosen according to the LTE standard for mobile communication [2]. The system is operated at a carrier frequency of 1800 MHz and we choose

Algorithm 3: Max-Min-CCCP

begin
  Set $\kappa := 0$. Create and scale random $\mathbf{w}^{(0)} \neq \mathbf{0}_{R+1}$ and $a^{(0)} \neq 0$ to satisfy the constraints of (4.41). Compute $\tau^{(0)} = 1/(\min \mathrm{SNR}_m)$. Set $\rho > \varepsilon$.
  while $\rho > \varepsilon$ **do**
    $\kappa := \kappa + 1$.
    Compute $(\Delta\mathbf{w}^\star, \Delta a^\star, \Delta\tau^\star)$ by solving (4.64), using $(\mathbf{w}^{(\kappa)}, a^{(\kappa)}, \tau^{(\kappa)})$, update $\mathbf{w}^{(\kappa+1)} = \mathbf{w}^{(\kappa)} + \Delta\mathbf{w}^\star$, $a^{(\kappa+1)} = a^{(\kappa)} + \Delta a^\star$ and $\tau^{(\kappa+1)} = \tau^{(\kappa)} + \Delta\tau^\star$.
    $\rho := |\tau^{(\kappa)} - \tau^{(\kappa+1)}|/\tau^{(\kappa)}$.
  end
end
return $\mathbf{w}^{(\kappa)}, a^{(\kappa)}, \tau^{(\kappa)}$

$T_S = 66.7\mu$sec as the symbol duration and the duration of one time slot. Then, the bandwidth is given by $1/T_S$ which corresponds to the bandwidth of a subcarrier in a multi-carrier LTE system. We assume frequency flat fading channels. We created the channel coefficients such that there is no shadow fading from the source to the relays, but from the source and the relays to the destinations. The noise power is set to $\sigma_\nu^2 = \sigma_\eta^2 = -132$ dBm. The maximum power values are given as $P_{T,\max}$, $P_{S,\max} = P_{T,\max}/2$, $P_{R,\max} = P_{T,\max}/3$ and $p_{r,\max} = P_{T,\max}/15$, respectively.

In the network, $R = 10$ relays are placed at a distance of 250 meters around source $\mathcal{S}$ at equidistant angles. The destinations are randomly distributed between 600 and 800 meters around source $\mathcal{S}$, see Fig. 4.3. The source, the relays, and the destinations are placed at a height of 10, 5, and 1.5 meters, respectively.

We investigate the performance of the following transmission schemes, scenarios and algorithms: The Rank-2-AFMS combined with the Max-Min-CCCP algorithm (R2-Max-Min-CCCP) and the SDR2D algorithm (R2-SDR2D). Furthermore, the Rank-1-AFMS combined with the CCCP algorithm (R1-Max-Min-CCCP) and the SDR2D algorithm (R1-SDR2D). Moreover, we consider for comparison also direct source-to-destination (DSD) communication where no relays are involved. All results are compared with the theoretical upper bound (SDR2D-UB) obtained by the SDR2D algorithm, see Subsection 4.3.1.

To solve the subproblems (4.61) of the SDR2D algorithm and subproblems (4.63) of the Max-Min-CCCP algorithm we have utilized the cvx interface for convex programming in a Matlab environment [75]. As the solver, we have chosen Mosek 7.0.0.103 working in default precision [76]. For the SDR2D algorithm, we search over $N = 200$ grid points and select $\varepsilon = 10^{-2}$ as the precision in the bisection search. $\varepsilon = 10^{-2}$ is also the threshold value for the relative progress of the Max-Min-CCCP

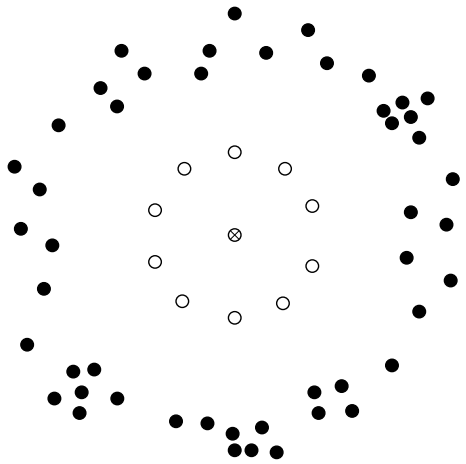

Figure 4.3: Setup of the network; ⊗: source, ○: relay, ●: destination.

algorithm.

In the case that the solution matrix to the optimization problem in (4.60) obtained by the SDR2D method is not feasible for (4.41), we will apply the Gaussian randomization procedure of [100]. For the Rank-1-AFMS, we select the best out of 200 random vectors where each vector is properly scaled to meet the power constraints. For the Rank-2-AFMS, we create 200 random vector pairs. Each pair is properly scaled by solving a linear program using the function `linprog.m` of the Matlab optimization toolbox [77].

In our first example, we examine the performance of all setups in terms of the average minimum achieved rate by solving (4.41). The minimum achieved rate is given by $1/2\log_2(1+\mathrm{SNR})$ (the prefactor $1/2$ takes into account the time slots per communicated symbol) for communication with relays and by $\log_2(1+\mathrm{SNR})$ for DSD, as one symbol per time slot can be communicated.

Fig. 4.4 depicts the average minimum rate versus $P_{T,\max}$ in the case that the direct source-to-destination paths are exploited for $M = 100$ destinations. In simulation results depicted in Fig. 4.5 it is assumed that no direct source-to-destination paths exist.

Both figures demonstrate that R2-Max-Min-CCCP achieves near-optimum performance close to the upper bound. The Rank-1-AFMS is clearly outperformed by the Rank-2-AFMS. Comparing Fig. 4.4 with Fig. 4.5, we see that the performance improves significantly if the source-to-destination paths are exploited.

Fig. 4.6 depicts the average minimum rate versus the number of destinations M in the case that the direct source-to-destination paths are exploited for $P_{T,\max}$ =5dBm. In Fig. 4.7 the same setups are considered, assuming that no direct source-to-destination paths exist.

M	10	40	70	100	130
Average $\mathfrak{R}(\mathbf{X}_1^\star)$	1.8	2.5	3.0	3.3	3.4

Table 4.1: Average $\mathfrak{R}(\mathbf{X}_1^\star)$ versus number of destinations M.

Algorithm	SDR2D	R1-Rand	R2-Rand	R1-CCCP	R2-CCCP
Run time	10^3	0.57	72	81	83

Table 4.2: Average run time in seconds. R1-Rand: Rank-one randomization, R2-Rand: Rank-two randomization, R1-CCCP: R1-Max-Min-CCCP, R2-CCCP: R2-Max-Min-CCCP.

Both Fig. 4.6 and Fig. 4.7 demonstrate that R2-Max-Min-CCCP achieves near-optimum performance close to the upper bound. For small M, the SDR2D algorithm performs slightly better than the Max-Min-CCCP algorithm due to the fact, that in most cases, the respective solution matrix has a rank smaller or equal to two. As illustrated in Table 4.1, the rank of the SDR solution matrix increases with increasing M. This leads to suboptimal solutions generated by the randomization technique.

In our second example, we examine the computational aspects of the considered algorithms for $M = 100$. Table 4.2 shows the average run time in seconds of the different algorithms. We see that the Max-Min-CCCP algorithm is more than ten times faster than the SDR2D algorithm. Fig. 4.8 depicts the number of iterations of the Max-Min-CCCP algorithm for the Rank-2-AFMS versus the minimum SNR. As a comparison, the performance of the SDR-based approaches is depicted. From this figure we observe that the main progress of the Max-Min-CCCP algorithm is achieved in the first three iterations. In the following iterations, the gain that can be obtained is less than 1dB. Since the Max-Min-CCCP algorithm exhibits excellent performance within a few iterations it is suitable for real time applications which require a short computational time.

4.5 Conclusion

In this chapter, a novel Rank-2-AFMS for single-group multicasting has been proposed. The proposed scheme generalizes the rank-one multicasting scheme of the literature to a rank-two multicasting scheme and considers a direct path from the source to the destinations. To select the proper source power and to adjust the relay weights we propose an iterative algorithm to maximize the lowest SNR at the destinations. The simulation results demonstrate that the proposed Rank-2-AFMS

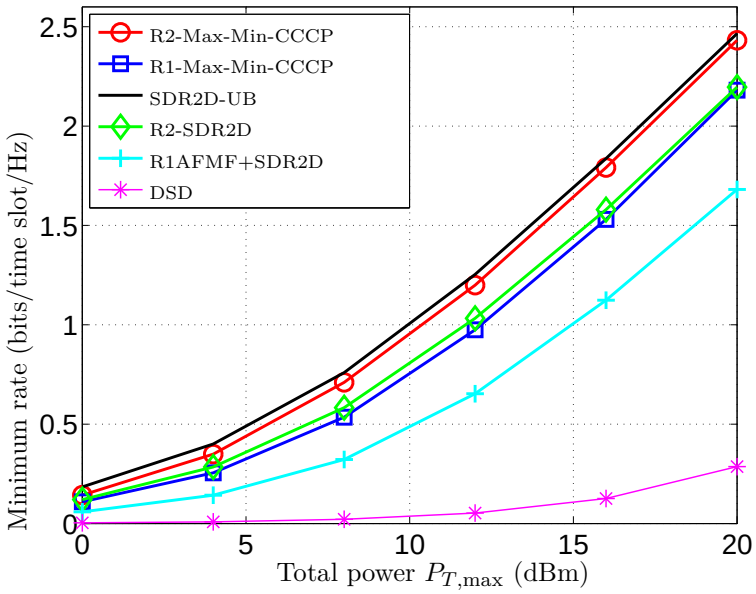

Figure 4.4: Minimum rate versus total power $P_{T,\max}$, first example.

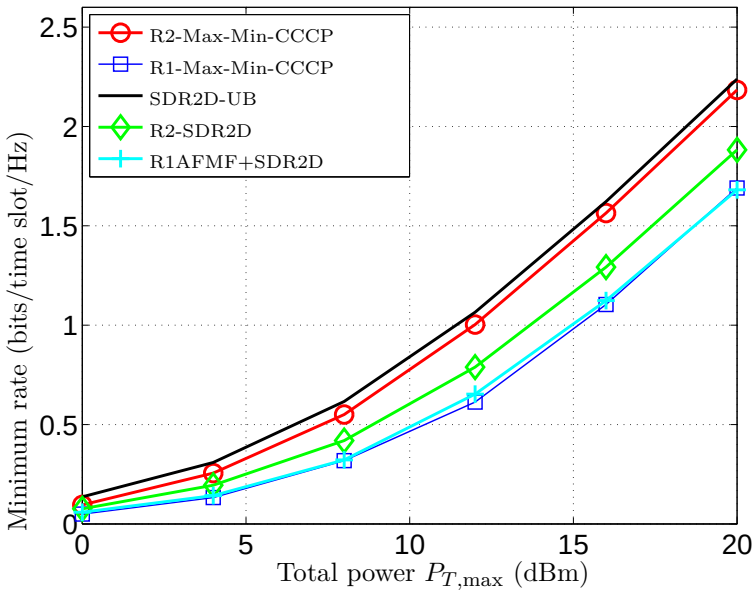

Figure 4.5: Minimum rate versus total power $P_{T,\max}$, first example.

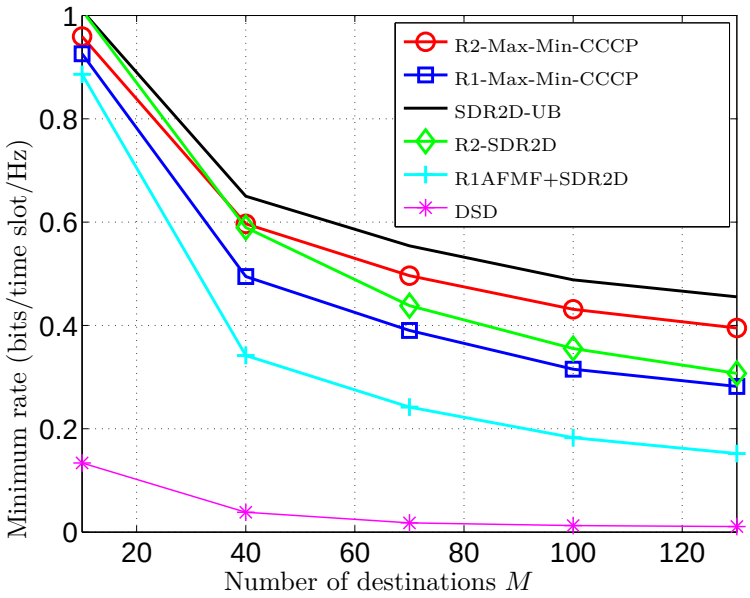

Figure 4.6: Minimum rate versus number of destinations M, first example.

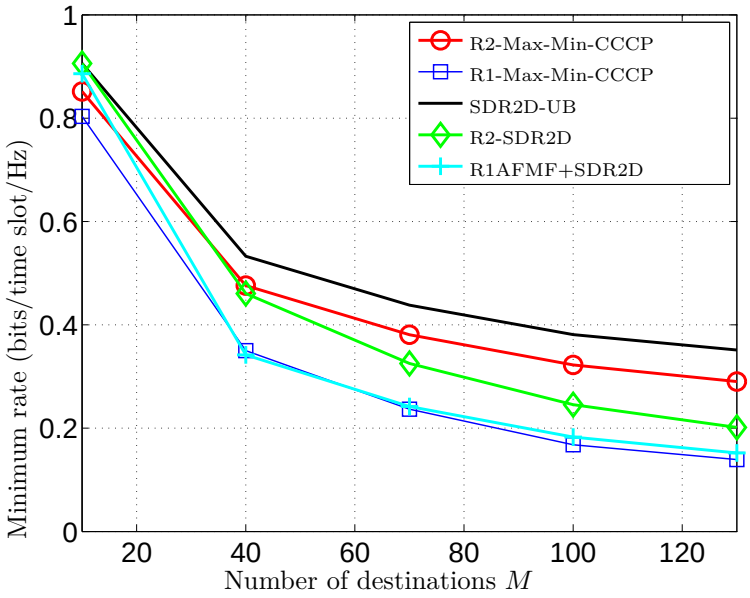

Figure 4.7: Minimum rate versus number of destinations M, first example.

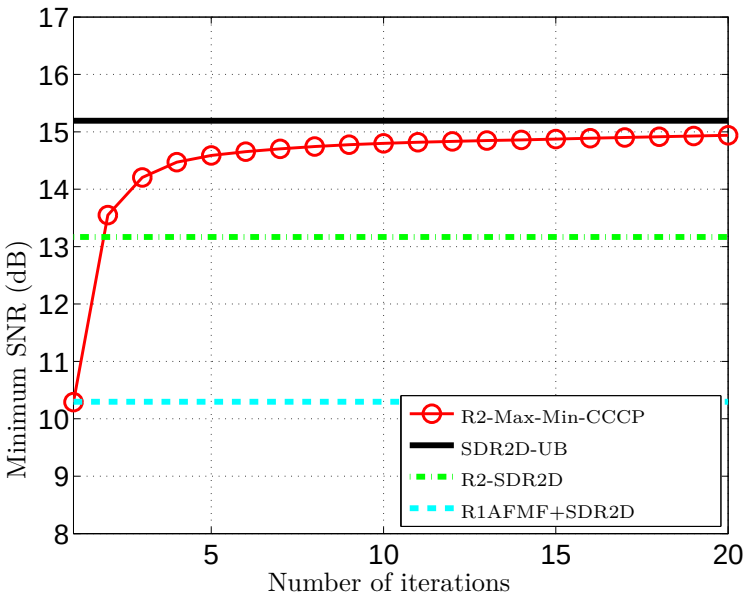

Figure 4.8: Minimum SNR versus number of iterations.

combined with the proposed iterative algorithm yields a performance close to the theoretical upper bound. The SDR-based optimization yields optimum performance for a small number of destinations, where the SDR solution matrices are of low rank. Moreover, we have seen that the SDR2D algorithm which is based on outer approximations is computationally expensive and requires on top of the SDR method a 2D search. The reason is that the SDR method is only directly applicable to QCQPs. In contrast, the inner approximation method is a more flexible approach since it considers the more general DC programming problems (QCQPs are a subset DC problems).

Chapter 5

Rate maximization in one- and bi-directional single-user networks

5.1 Introduction

In the previous Chapters 3–4, we have considered one-directional networks, in which one or more sources send data to multiple destinations. In this chapter, we analyze one-directional and bi-directional AF relaying for a single transceiver pair with a total transmit power constraint, including the transmit power of the relays and the transceivers. We assume no direct link between the two transceivers. We consider the network of Chapter 2.2.2 in the case $K = M = 1$. Based on the results on one-directional relaying, the three bi-directional schemes of Figure 1.1 are studied and compared in terms of their maximum rate. We consider rate maximization rather than SNR maximization to take number of time slots of the respective schemes into account. We show that the optimum relay weight vectors for the bi-directional two time slot scheme and the one-directional scheme are identical. Moreover, we prove that the one-directional scheme yields in both directions the same maximum performance. Then, we analytically compare the maximum rate of the one-directional scheme to the bi-directional two time slot scheme and propose a 1D search algorithm to compute the parameters of the bi-directional four time slot scheme that achieves the maximum sum rate. For the maximum sum rate of the bi-directional three time slot scheme, we provide an upper bound. All results are then verified by our numerical experiments.

The contribution and results of this chapter can be summarized as:

- For AF relaying, the three bi-directional relaying schemes of Figure 1.1 and the one-directional scheme are compared with each other in terms of their rate.
- We analytically show that the two time slot two-way scheme of Figure 1.1 (b) achieves almost

two times the rate of the one-directional scheme.

- For the four time slot scheme of Figure 1.1 (a), we propose a grid search to compute the optimum power allocation between the users and the relays which maximizes the rate.
- For the three time slot scheme of Figure 1.1 (c), we derive an upper bound on the maximum rate.

The content of this chapter has been published in
A. Schad, A.B. Gershman, and S. Shahbazpanahi, "Capacity maximization for distributed beamforming in one- and bi-directional relay networks," *Proceedings of the International Conference on Acoustics, Speech, and Signal Processing (ICASSP'11), Prague, Czech Republic,* pp. 2804–2807, May 2011.

Note that single-user one-directional AF relaying has been treated in [19], where individual relay power constraints have been considered, and in [21], where a constraint on the relay sum power has been assumed. Bi-directional AF relaying using the two time slot scheme has been treated in [26], [27], [28], where rate maximization has been studied in [27]. In [28], a comparison of the schemes of Figure 1.1 has been derived where a direct path between the transceivers has been assumed. In [33], the network model of a single transceiver pair is generalized for a model with multiple transceiver pairs.

5.2 The one-directional scheme

We first consider the one-directional AF relaying scheme of Chapter 2.2.1 for $K = M = 1$ and review already established results. It is outlined how the optimum power allocation and relay weight vector can be computed to achieve the maximum rate. Furthermore, it is shown that the maximum rate of the one-directional scheme is the same for transmissions from transceiver $\mathcal{T}_1$ to transceiver $\mathcal{T}_2$ and for transmissions from transceiver $\mathcal{T}_2$ to transceiver $\mathcal{T}_1$.

For the sake of brevity and as there is only one transceiver pair, we define $f_r \triangleq f_{1,r}$, $g_r \triangleq g_{r,1}$, $r = 1, \ldots, R$, and $\mathbf{f} \triangleq \mathbf{f}_1$, $\mathbf{g} \triangleq \mathbf{g}_1$. The rate of the one-directional two time slot scheme is given by $\mathcal{C} = 1/2 \log_2(1 + \mathrm{SNR}_2)$ where the factor $1/2$ takes into account the number time slots. To achieve the maximum rate, we consider the problem of maximizing the SNR at transceiver $\mathcal{T}_2$ by choosing an optimal relay weight vector under the constraint that the total power $P_\mathrm{T} = P_1 + P_\mathrm{R}$ is limited by $P_{\mathrm{T,max}}$. This problem is formulated as

$$\max_{P_1, P_\mathrm{R}, \mathbf{w}_1} \quad \mathrm{SNR}_2 \qquad \text{s.t.} \quad P_1 + P_\mathrm{R} \leq P_{\mathrm{T,max}}, \tag{5.1}$$

where SNR_2 is the SNR at transceiver $\mathcal{T}_2$ and $\mathbf{w}_1$ is the relay weight vector for transmissions from transceiver $\mathcal{T}_1$ to transceiver $\mathcal{T}_2$. Using (2.3) - (2.9), the objective function of (5.1) can be expressed as

$$\mathrm{SNR}_2 = \frac{\mathrm{E}\{|\sqrt{P_1}\mathbf{g}^T\mathbf{W}_1\mathbf{f}s_1|^2\}}{\mathrm{E}\{|\mathbf{g}^T\mathbf{W}_1\boldsymbol{\eta}+\nu_2|^2\}} = \frac{P_1\mathbf{w}_1^H\mathbf{h}\mathbf{h}^H\mathbf{w}_1}{\sigma^2+\sigma^2\mathbf{w}_1^H\mathbf{G}\mathbf{G}^H\mathbf{w}_1} \tag{5.2}$$

holds, where $\mathbf{G} \triangleq \mathrm{diag}(\mathbf{g})$, $\mathbf{h} \triangleq \mathbf{G}\mathbf{f}$ and $\mathbf{W}_1 = \mathrm{diag}(\mathbf{w}_1^*)$. The relay sum power is given by

$$P_{\mathrm{R}} = \mathrm{E}\{\mathbf{t}^H\mathbf{t}\} = P_1\mathbf{w}_1^H\mathbf{F}\mathbf{F}^H\mathbf{w}_1 + \sigma^2\mathbf{w}_1^H\mathbf{w}_1, \tag{5.3}$$

where $\mathbf{F} \triangleq \mathrm{diag}(\mathbf{f})$. To make the problem in (5.1) mathematically treatable, it is reformulated as

$$\max_{P_1,P_{\mathrm{R}}} \max_{\mathbf{w}_1} \frac{P_1\mathbf{w}_1^H\mathbf{h}\mathbf{h}^H\mathbf{w}_1}{\sigma^2+\sigma^2\mathbf{w}_1^H\mathbf{G}\mathbf{G}^H\mathbf{w}_1} \quad \text{s.t.} \quad P_1+P_{\mathrm{R}} \leq P_{\mathrm{T,max}}. \tag{5.4}$$

In (5.4), P_1 is a constant in the inner problem that is adjusted by solving the exterior problem. A closed form solution to the inner problem of (5.4) is given in [21] where the authors have shown that $\arg([\mathbf{w}_1]_r) = \arg(f_r g_r)$ maximizes SNR_2, as this choice yields the coherent summation of the desired signals at transceiver $\mathcal{T}_2$. Choosing

$$|[\mathbf{w}_1]_r| = \frac{\sqrt{P_{\mathrm{T,max}}-P_1}|f_r g_r|}{(P_{\mathrm{T,max}}-P_1)|g_r|^2+(P_1|f_r|^2+\sigma^2)\sigma^2} \cdot \frac{1}{\sqrt{\sum_{r=1}^{R}\frac{(P_1|f_r|^2+\sigma^2)|f_r g_r|^2}{\{(P_{\mathrm{T,max}}-P_1)|g_r|^2+(P_1|f_r|^2+\sigma^2)\sigma^2\}^2}}} \tag{5.5}$$

for all $r = 1, \ldots, R$, the maximum SNR at transceiver $\mathcal{T}_2$ results in

$$\mathrm{SNR}_2(P_1) = \sum_{r=1}^{R} \frac{P_1(P_{\mathrm{T,max}}-P_1)|f_r g_r|^2}{(P_{\mathrm{T,max}}-P_1)|g_r|^2+\sigma^2(P_1|f_r|^2+\sigma^2)}, \tag{5.6}$$

where $P_1 \in [0, P_{\mathrm{T,max}}]$. In [27], it has been proposed to find a zero of the first derivative of the function $\mathrm{SNR}_2(P_1)$ by bisection search to determine the solution of the exterior problem in (5.4). Note that $\mathrm{SNR}_2(P_1)$ is a strictly concave function in P_1. Consequently, the first derivative of function $\mathrm{SNR}_2(P_1)$ is a strictly monotonically increasing function and any zero is unique. Therefore, a bisection search on the first derivative of the function $\mathrm{SNR}_2(P_1)$ leads to together with (5.5) to the maximizer of the problem in (5.1).

Further note that the power constraint in (5.1) is met with equality at the optimum. To prove this, assume that there exists a feasible optimal solution. Then, increasing P_1 leads to a larger objective function, thus contradicting optimality. From (5.3), we obtain that $P_1 = (P_{\mathrm{T,max}} - \sigma^2\mathbf{w}_1^H\mathbf{w}_1)/(1+\mathbf{w}_1^H\mathbf{F}\mathbf{F}^H\mathbf{w}_1)$ holds true at an optimum of (5.1). Let us substitute P_1 in the objective function of the problem in (5.1) to reformulate it as

$$\max_{\mathbf{w}_1} \frac{(P_{\mathrm{T,max}}-\sigma^2\mathbf{w}_1^H\mathbf{w}_1)\mathbf{w}_1^H\mathbf{h}\mathbf{h}^H\mathbf{w}_1}{\sigma^2(1+\mathbf{w}_1^H\mathbf{G}\mathbf{G}^H\mathbf{w}_1)(1+\mathbf{w}_1^H\mathbf{F}\mathbf{F}^H\mathbf{w}_1)} \triangleq \varphi(P_{\mathrm{T,max}}). \tag{5.7}$$

As (5.7) is highly nonlinear, the evaluation of $\varphi(P_{\mathrm{T,max}})$ is achieved by solving the equivalent problem in (5.4) using a simple bisection search to determine P_1 rather than solving (5.7) directly. Inserting the optimum P_1 in (5.6), we obtain $\varphi(P_{\mathrm{T,max}})$ and the corresponding weight vector is given by (5.5).

As the problems (5.1) and (5.7) are equivalent, it is proven that the maximum SNR for transmissions from transceiver $\mathcal{T}_1$ to transceiver $\mathcal{T}_2$ is the same as for reverse transmissions. Moreover, the maximum SNR is achieved by the same optimum relay weight vector. Let us consider transmissions from transceiver $\mathcal{T}_2$ to transceiver $\mathcal{T}_1$ to prove the reciprocity result. Let P_2 be the transmit power of transceiver $\mathcal{T}_2$ and $\mathbf{w}_2$ be the relay weight vector for transmissions from transceiver $\mathcal{T}_2$ to transceiver $\mathcal{T}_1$. In this case, the SNR maximization problem is given by

$$\max_{P_2,P_{\mathrm{R}},\mathbf{w}_2} \mathrm{SNR}_1 \qquad \text{s.t.} \quad P_2 + P_{\mathrm{R}} \leq P_{\mathrm{T,max}}, \tag{5.8}$$

where the SNR at transceiver $\mathcal{T}_1$ and the relay power are given by

$$\mathrm{SNR}_1 = \frac{P_2 \mathbf{w}_2^H \mathbf{h}\mathbf{h}^H \mathbf{w}_2}{\sigma^2 + \sigma^2 \mathbf{w}_2^H \mathbf{F}\mathbf{F}^H \mathbf{w}_2}, \tag{5.9}$$

$$P_{\mathrm{R}} = P_2 \mathbf{w}_2^H \mathbf{G}\mathbf{G}^H \mathbf{w}_2 + \sigma^2 \mathbf{w}_2^H \mathbf{w}_2, \tag{5.10}$$

respectively. Similarly, as for the problem in (5.1), at an optimum point the inequality constraint of (5.8) is satisfied with equality leading to the equivalent problem

$$\max_{\mathbf{w}_2} \frac{(P_{\mathrm{T,max}} - \sigma^2 \mathbf{w}_2^H \mathbf{w}_2) \mathbf{w}_2^H \mathbf{h}\mathbf{h}^H \mathbf{w}_2}{\sigma^2 (1 + \mathbf{w}_2^H \mathbf{G}\mathbf{G}^H \mathbf{w}_2)(1 + \mathbf{w}_2^H \mathbf{F}\mathbf{F}^H \mathbf{w}_2)}. \tag{5.11}$$

Comparing (5.7) and (5.11), we see that the problems (5.1) and (5.8) are equivalent and the optimum relay weight vectors $\mathbf{w}_1$ and $\mathbf{w}_2$ are identical. Note that the corresponding power allocation may be different, i.e., P_1 and P_2 are not identical in general and the optimum relay sum powers (5.3) and (5.10) vary.

In the rest of this chapter, we regard rate maximization with respect to the weight vector and the power allocation in the network. For fixed beamformers, the rate $\mathcal{C}$ of the one-directional scheme is given by the formula $\mathcal{C} = \frac{1}{2}\log_2(1 + \mathrm{SNR})$, where the factor $1/2$ accounts for the number of time slots. Let $\mathcal{C}_1$ denote the maximum rate of transmissions from transceiver $\mathcal{T}_2$ to transceiver $\mathcal{T}_1$ and let $\mathcal{C}_2$ denote the maximum rate of transmissions from transceiver $\mathcal{T}_1$ to transceiver $\mathcal{T}_2$. According to the reciprocity result, we have

$$\max \mathcal{C}_1 = \max \mathcal{C}_2 = \frac{1}{2}\log_2(1 + \varphi(P_{\mathrm{T,max}})). \tag{5.12}$$

5.3 The bi-directional two time slot scheme

Let us consider the bi-directional two time slot scheme of Figure 1.1 (b). The challenge of the two time slot is to establish a reliable communication link between the two transceivers using a single weight vector. This is different to the three and the four time slot schemes which utilize two relay weight vectors and therefore have more degrees of freedom available.

In the first time slot, the transceivers $\mathcal{T}_1$ and $\mathcal{T}_2$ send their respective information-bearing symbols s_1 and s_2 to the relays that forward their received signals in the second time slot. Let $\mathbf{w}$ denote the relay weight vector and $\mathbf{W} = \mathrm{diag}(\mathbf{w}^*)$. According to Chapter 2.2.2 and to (2.10) and (2.11), the signals received at transceiver $\mathcal{T}_1$ and $\mathcal{T}_2$ in the second time slot are respectively given by

$$\begin{aligned} y_1 &= \mathbf{f}^T\mathbf{t} + \nu_1 = \mathbf{f}^T\mathbf{W}\mathbf{x} + \nu_1 = \sqrt{P_1}\mathbf{f}^T\mathbf{W}\mathbf{f}s_1 + \sqrt{P_2}\mathbf{f}^T\mathbf{W}\mathbf{g}s_2 + \mathbf{f}^T\mathbf{W}\boldsymbol{\eta} + \nu_1 \\ y_2 &= \mathbf{g}^T\mathbf{t} + \nu_2 = \mathbf{g}^T\mathbf{W}\mathbf{x} + \nu_2 = \sqrt{P_2}\mathbf{g}^T\mathbf{W}\mathbf{g}s_2 + \sqrt{P_1}\mathbf{g}^T\mathbf{W}\mathbf{f}s_1 + \mathbf{g}^T\mathbf{W}\boldsymbol{\eta} + \nu_2. \end{aligned} \tag{5.13}$$

The received signal y_1 contains the SI term $\sqrt{P_1}\mathbf{f}^T\mathbf{W}\mathbf{f}s_1$, originating from transceiver $\mathcal{T}_1$ itself and y_2 is corrupted with $\sqrt{P_2}\mathbf{g}^T\mathbf{W}\mathbf{g}s_2$, originating from transceiver $\mathcal{T}_2$. Since the channel coefficients, the relay weights, and the own transmitted signal are known at each transceiver, it is possible to remove the unwanted SI terms and we obtain

$$\begin{aligned} \hat{y}_1 &= y_1 - \sqrt{P_1}\mathbf{f}^T\mathbf{W}\mathbf{f}s_1 = \underbrace{\sqrt{P_2}\mathbf{w}^H\mathbf{F}\mathbf{g}s_2}_{\text{desired Signal}} + \underbrace{\mathbf{w}^H\mathbf{F}\boldsymbol{\eta} + \nu_1}_{\text{noise}} \\ \hat{y}_2 &= y_2 - \sqrt{P_2}\mathbf{g}^T\mathbf{W}\mathbf{g}s_2 = \underbrace{\sqrt{P_1}\mathbf{w}^H\mathbf{G}\mathbf{f}s_1}_{\text{desired Signal}} + \underbrace{\mathbf{w}^H\mathbf{G}\boldsymbol{\eta} + \nu_2}_{\text{noise}}. \end{aligned} \tag{5.14}$$

The problem of maximizing the sum rate $\mathcal{C}$ subject to a constraint on the total power can be formulated as

$$\max \mathcal{C} \quad \text{s.t.} \quad P_1 + P_2 + P_\mathrm{R} \leq P_{\mathrm{T,max}}. \tag{5.15}$$

In [27], it has been shown that solving (5.15) is equivalent to solving the problem in (5.7) and leads to the maximum sum rate

$$\max \mathcal{C} = \frac{1}{2}\log_2\left(1 + \varphi(P_{\mathrm{T,max}}) + \frac{\varphi(P_{\mathrm{T,max}})^2}{4}\right). \tag{5.16}$$

To compare the maximum rate of the one-directional scheme and the bi-directional two time slot scheme, let us analyze the two cases where $P_{\mathrm{T,max}}$ is very small and very large. For large power, the function $\varphi(P_{\mathrm{T,max}})$ can be arbitrarily large due to the fact that it increases at least linearly in $P_{\mathrm{T,max}}$. For a proof of this statement, let us introduce the real-valued scalar $\alpha > 1$ and let $\mathbf{w}^\star$ be

the optimal weight vector in (5.7) to obtain $\varphi(P_{\mathrm{T,max}})$. Then

$$\begin{aligned}\alpha\varphi(P_{\mathrm{T,max}}) &= \frac{\alpha(P_{\mathrm{T,max}} - \sigma^2(\mathbf{w}^\star)^H\mathbf{w}^\star)(\mathbf{w}^\star)^H\mathbf{h}\mathbf{h}^H\mathbf{w}^\star}{\sigma^2(1+(\mathbf{w}^\star)^H\mathbf{G}\mathbf{G}^H\mathbf{w}^\star)(1+(\mathbf{w}^\star)^H\mathbf{F}\mathbf{F}^H\mathbf{w}^\star)} \\ &< \max_{\mathbf{w}} \frac{(\alpha P_{\mathrm{T,max}} - \sigma^2\mathbf{w}^H\mathbf{w})\mathbf{w}^H\mathbf{h}\mathbf{h}^H\mathbf{w}}{\sigma^2(1+\mathbf{w}^H\mathbf{G}\mathbf{G}^H\mathbf{w})(1+\mathbf{w}^H\mathbf{F}\mathbf{F}^H\mathbf{w})} = \varphi(\alpha P_{\mathrm{T,max}}). \end{aligned} \tag{5.17}$$

If $P_{\mathrm{T,max}}$ is large, the maximum sum rate of the two time slot scheme of Figure 1.1 (b) can be approximated according to

$$\max\mathcal{C} \approx 2\cdot\max\mathcal{C}_1 - 1. \tag{5.18}$$

To prove (5.18), consider $P_{\mathrm{T,max}} \gg 1$. Then $\varphi(P_{\mathrm{T,max}}) \gg 1$ and $\varphi(P_{\mathrm{T,max}})^2 \gg \varphi(P_{\mathrm{T,max}})$ hold true due to (5.17). For large $P_{\mathrm{T,max}}$, it is found that

$$\begin{aligned}\max\mathcal{C} - \max\mathcal{C}_1 &= \frac{1}{2}\log_2\left(1+\varphi(P_{\mathrm{T,max}}) + \frac{\varphi(P_{\mathrm{T,max}})^2}{4}\right) - \frac{1}{2}\log_2(1+\varphi(P_{\mathrm{T,max}})) \\ &\approx \frac{1}{2}\log_2\left(\frac{\varphi(P_{\mathrm{T,max}})^2}{4}\right) - \frac{1}{2}\log_2(\varphi(P_{\mathrm{T,max}})) = \frac{1}{2}\log_2(\varphi(P_{\mathrm{T,max}})) - 1 \\ &\approx \max\mathcal{C}_1 - 1.\end{aligned}$$

If $P_{\mathrm{T,max}}$ is sufficiently small, $\varphi(P_{\mathrm{T,max}}) \ll 1$ and $\frac{\varphi(P_{\mathrm{T}})^2}{4} \ll \varphi(P_{\mathrm{T,max}})$. From equations (5.12) and (5.16), it can be seen that

$$\mathcal{C} \approx \max\mathcal{C}_1, \tag{5.19}$$

for small $P_{\mathrm{T,max}}$.

From (5.18), we see that the maximum rate for the bi-directional two time slot is roughly twice as large as the maximum rate for the one-directional scheme if the transmit power is high. For small transmit power, however, both schemes achieve approximately the same maximum rate according to (5.19).

5.4 The bi-directional four time slot scheme

The traditional four time slot scheme of Figure 1.1 (a) comprises sequential one-directional transmissions from transceiver $\mathcal{T}_1$ to transceiver $\mathcal{T}_2$ and vice versa. The sum rate of the four time slot scheme can be expressed as

$$\mathcal{C} = \frac{1}{4}(\log_2(1+\mathrm{SNR}_1) + \log_2(1+\mathrm{SNR}_2)) = \frac{1}{4}\log_2((1+\mathrm{SNR}_1)(1+\mathrm{SNR}_2)), \tag{5.20}$$

where the factor $1/4$ takes into account the number of time slots. As the logarithm is monotonic in its argument, maximizing the sum rate in (5.20) is accomplished by maximizing the function $(1+$

$\mathrm{SNR}_1)(1+\mathrm{SNR}_2)$. Let $P_{\mathrm{T,max}}$ denote the total amount of transmit power consumed in the network during the four time slots. Then, using (5.20) along with (5.2) and (5.9), sum rate maximization can be achieved by solving

$$\max_{\mathbf{w}_1,\mathbf{w}_2,P_2,P_1} \left(1+\frac{P_2\mathbf{w}_2^H\mathbf{h}\mathbf{h}^H\mathbf{w}_2}{\sigma^2+\sigma^2\mathbf{w}_2^H\mathbf{F}\mathbf{F}^H\mathbf{w}_2}\right)\left(1+\frac{P_1\mathbf{w}_1^H\mathbf{h}\mathbf{h}^H\mathbf{w}_1}{\sigma^2+\sigma^2\mathbf{w}_1^H\mathbf{F}\mathbf{F}^H\mathbf{w}_1}\right)$$
$$\text{s.t.} \quad P_1(1+\mathbf{w}_1^H\mathbf{F}\mathbf{F}^H\mathbf{w}_1)+P_2(1+\mathbf{w}_2^H\mathbf{G}\mathbf{G}^H\mathbf{w}_2)+\sigma^2(\mathbf{w}_1^H\mathbf{w}_1+\mathbf{w}_2^H\mathbf{w}_2)\leq P_{\mathrm{T,max}}, \quad (5.21)$$

where $\mathbf{w}_1$ and $\mathbf{w}_2$ denote respectively the relay weight vectors of the first and second relay transmissions. The power constraint in (5.21) is derived from equations (5.3) and (5.10).

The problem in (5.21) is highly nonlinear and multi-dimensional. It can however be replaced by a one-dimensional power allocation problem based on the following considerations. For any arbitrary power allocation between the first and second transmission, the optimal beamformers $\mathbf{w}_1$ and $\mathbf{w}_2$ and the powers P_1 and P_2 are given by the individual solutions of the decoupled problems (5.1) and (5.8). Let $0\leq\varepsilon\leq 1$ denote the fraction of available power $P_{\mathrm{T,max}}$ that is assigned to the first one-directional transmission. Then, $\varepsilon P_{\mathrm{T,max}}$ and $(1-\varepsilon)P_{\mathrm{T,max}}$ are the respective transmit powers of the first and second transmission. The maximum SNRs are given by $\varphi(\varepsilon P_{\mathrm{T,max}})$ and $\varphi((1-\varepsilon)P_{\mathrm{T,max}})$ due to (5.7). Therefore, the problem in (5.21) is equivalent to the following power allocation problem

$$\max\mathcal{C}=\max_{0\leq\varepsilon\leq 1}\frac{1}{4}\log_2(1+\varphi(\varepsilon P_{\mathrm{T}}))(1+\varphi((1-\varepsilon)P_{\mathrm{T,max}})). \quad (5.22)$$

As the problem in (5.22) is one-dimensional, it is easily solved by applying grid search.

Let us refer to the four time slot scheme with $\varepsilon=1/2$ as the *fair four time slot scheme* since the transmit power for both directions is equal. Note that the maximum sum rate of the fair four time slot scheme and the maximum rate of the one-directional scheme are the same in the case that the total available power of two time slots is half of the total available power of four time slots. In general, an unequal allocation of $P_{\mathrm{T,max}}$ can lead to a higher sum rate.

5.5 The bi-directional three time slot scheme

In this section, we derive an upper bound on the maximum rate achieved by the three time slot scheme depicted in Figure 1.1 (c). Similarly as the four time slot scheme, the three time slot scheme also utilizes two different relay weight vectors, however, with a reduced number of time slots.

Let $\mathbf{x}(1)$ and $\mathbf{x}(2)$ be the vectors of signal received in time slot one from transceiver $\mathcal{T}_1$ and in time slot two from transceiver $\mathcal{T}_2$, respectively. In vector notation, we have $\mathbf{x}(1)=\sqrt{P_1}\mathbf{f}s_1+\boldsymbol{\eta}(1)$ and $\mathbf{x}(2)=\sqrt{P_2}\mathbf{g}s_2+\boldsymbol{\eta}(2)$, where $\boldsymbol{\eta}(1)$ and $\boldsymbol{\eta}(2)$ are the relay noise vectors of the first and second

time slot, respectively. In the third time slot, the relays simultaneously forward their received signals to the transceivers. The transmit signal vector $\mathbf{t} = \mathbf{W}_1\mathbf{x}(1) + \mathbf{W}_2\mathbf{x}(2)$ is a weighted combination of $\mathbf{x}(1)$ and $\mathbf{x}(2)$, where $\mathbf{W}_1 \triangleq \mathrm{diag}(\mathbf{w}_1^*)$ and $\mathbf{W}_2 \triangleq \mathrm{diag}(\mathbf{w}_2^*)$, and $\mathbf{w}_1$ and $\mathbf{w}_2$ are the complex relay weights corresponding to the first and second time slot, respectively. The received signals y_1 of transceiver $\mathcal{T}_1$ and y_2 of transceiver $\mathcal{T}_2$ contain SI. The SI can be subtracted from the received signals. The resulting SI-free signals are given by

$$y_1 - \sqrt{P_1}\mathbf{f}^T\mathbf{W}_1\mathbf{f}s_1 = \underbrace{\sqrt{P_2}\mathbf{w}_2^H\mathbf{F}\mathbf{g}s_2}_{\text{desired signal}} + \underbrace{\mathbf{w}_1^H\mathbf{F}\boldsymbol{\eta}(1) + \mathbf{w}_2^H\mathbf{F}\boldsymbol{\eta}(2) + \nu_1}_{\text{noise}}, \tag{5.23}$$

$$y_2 - \sqrt{P_2}\mathbf{g}^T\mathbf{W}_2\mathbf{g}s_2 = \underbrace{\sqrt{P_1}\mathbf{w}_1^H\mathbf{G}\mathbf{f}s_1}_{\text{desired signal}} + \underbrace{\mathbf{w}_1^H\mathbf{G}\boldsymbol{\eta}(1) + \mathbf{w}_2^H\mathbf{G}\boldsymbol{\eta}(2) + \nu_2}_{\text{noise}}. \tag{5.24}$$

The relay sum power $P_{\mathrm{R}} = \mathrm{E}\{\mathbf{t}^H\mathbf{t}\}$ of the three time slot scheme is given by

$$P_{\mathrm{R}} = P_1\mathbf{w}_1^H\mathbf{F}\mathbf{F}^H\mathbf{w}_1 + P_2\mathbf{w}_2^H\mathbf{G}\mathbf{G}^H\mathbf{w}_2 + \sigma^2(\mathbf{w}_1^H\mathbf{w}_1 + \mathbf{w}_2^H\mathbf{w}_2), \tag{5.25}$$

where it is assumed that s_1 and s_2 are uncorrelated and independent of the noise. Note that P_{R} contains the sum power of two one-directional transmissions, one with the weight vector $\mathbf{w}_1$ from transceiver $\mathcal{T}_1$ to transceiver $\mathcal{T}_2$, given by (5.3), and another with the weight vector $\mathbf{w}_2$ from transceiver $\mathcal{T}_2$ to transceiver $\mathcal{T}_1$, given by (5.10). From (5.23) and (5.24), one can derive the SNRs at transceiver $\mathcal{T}_1$ and $\mathcal{T}_2$ as

$$\mathrm{SNR}_1 = \frac{P_2\mathbf{w}_2^H\mathbf{h}\mathbf{h}^H\mathbf{w}_2}{\sigma^2 + \sigma^2(\mathbf{w}_2^H\mathbf{F}\mathbf{F}^H\mathbf{w}_2 + \mathbf{w}_1^H\mathbf{F}\mathbf{F}^H\mathbf{w}_1)}, \tag{5.26}$$

$$\mathrm{SNR}_2 = \frac{P_1\mathbf{w}_1^H\mathbf{h}\mathbf{h}^H\mathbf{w}_1}{\sigma^2 + \sigma^2(\mathbf{w}_1^H\mathbf{G}\mathbf{G}^H\mathbf{w}_1 + \mathbf{w}_2^H\mathbf{G}\mathbf{G}^H\mathbf{w}_2)}. \tag{5.27}$$

We obtain the maximum sum rate of the three time slot by solving

$$\max \mathcal{C} = \max \frac{1}{3}(\log_2(1+\mathrm{SNR}_1) + \log_2(1+\mathrm{SNR}_2)) \quad \text{s.t.} \quad P_1 + P_2 + P_{\mathrm{R}} \le P_{\mathrm{T,max}}. \tag{5.28}$$

To find an upper bound on the value of the objective function of (5.28), let us consider the argument of the logarithm in the objective function. By neglecting the terms $\sigma^2\mathbf{w}_1^H\mathbf{F}\mathbf{F}^H\mathbf{w}_1$ and $\sigma^2\mathbf{w}_2^H\mathbf{G}\mathbf{G}^H\mathbf{w}_2$ in the denominators of (5.26) and (5.27), respectively, upper bound functions for SNR_1 and SNR_2 are given. Then solving the problem

$$\begin{aligned}\max_{\mathbf{w}_1,\mathbf{w}_2,P_2,P_1} & \left(1 + \frac{P_2\mathbf{w}_2^H\mathbf{h}\mathbf{h}^H\mathbf{w}_2}{\sigma^2 + \sigma^2\mathbf{w}_2^H\mathbf{F}\mathbf{F}^H\mathbf{w}_2}\right)\left(1 + \frac{P_1\mathbf{w}_1^H\mathbf{h}\mathbf{h}^H\mathbf{w}_1}{\sigma^2 + \sigma^2\mathbf{w}_1^H\mathbf{F}\mathbf{F}^H\mathbf{w}_1}\right) \\ \text{s.t.} \quad & P_1(1 + \mathbf{w}_1^H\mathbf{F}\mathbf{F}^H\mathbf{w}_1) + P_2(1 + \mathbf{w}_2^H\mathbf{G}\mathbf{G}^H\mathbf{w}_2) + \sigma^2(\mathbf{w}_1^H\mathbf{w}_1 + \mathbf{w}_2^H\mathbf{w}_2) \le P_{\mathrm{T,max}},\end{aligned} \tag{5.29}$$

we obtain an upper bound on the maximum rate in (5.28). Comparing (5.29) with (5.21), it is easy to see that these problems are equivalent. Thus, a bound on the maximum rate of the three time slot scheme is obtained by maximizing the rate of the traditional four time slot scheme.

5.6 Numerical results

In the simulations, a network with $R = 10$ relays is considered, where the channel vectors $\mathbf{f}$ and $\mathbf{g}$ are generated in each of the 100 simulation runs as complex zero mean circular Gaussian distributed random variables with variances σ_f^2 and σ_g^2, respectively. The noise power is $\sigma^2 = 1$.

Figure 5.1 depicts the maximum rate versus the available power per time slot for $\sigma_f^2 = \sigma_g^2 = 1$. The total available power $P_{\mathrm{T,max}}$ for each scheme is given by the number of time slots multiplied by the available power per time slot. It can be seen from Figure 5.1 that for the available power values greater than 0 dB, the two time slot scheme yields a substantially higher rate than the one-directional scheme and the traditional four time slot scheme, which perform similarly. The upper bound on rate achieved by the three time slot scheme is substantially lower than the rate of the two time slot scheme in the high total power region. For a high available total power, the maximum rate of the two time slot scheme is well approximated by (5.18).

Figure 5.2 depicts the maximum rate versus the number of relays R for $\sigma_f^2 = \sigma_g^2 = 1$. The available power per time slot is 10 dB over the noise power. For all schemes, an increased number of relays results in a higher rate. Again, the two time slot scheme yields a substantially higher rate than the one-directional scheme and the traditional four time slot scheme, which perform similarly. We observe that the approximation made in (5.18) is accurate for a high number of relays.

In Figure 5.3, we examine the influence of non-symmetric channel strengths. We set $\sigma_g^2 + \sigma_f^2 = 2$ and depict the maximum rate versus σ_f^2. From Figure 5.3, we see that the maximum rate for all schemes is achieved if $\sigma_g^2 = \sigma_f^2$.

5.7 Conclusion

In this chapter, we have compared the one-directional AF relaying scheme to the bi-directional relaying schemes of Figure 1.1. The two time slot-scheme achieves the largest rate, using one single relay weight vector. The three and four time slot schemes achieve lower rate due to the higher number of time slots. This loss in spectral efficiency cannot be compensated by an increased number of degrees of freedom offered by the two weight vectors of the three time slot and the four time slot scheme.

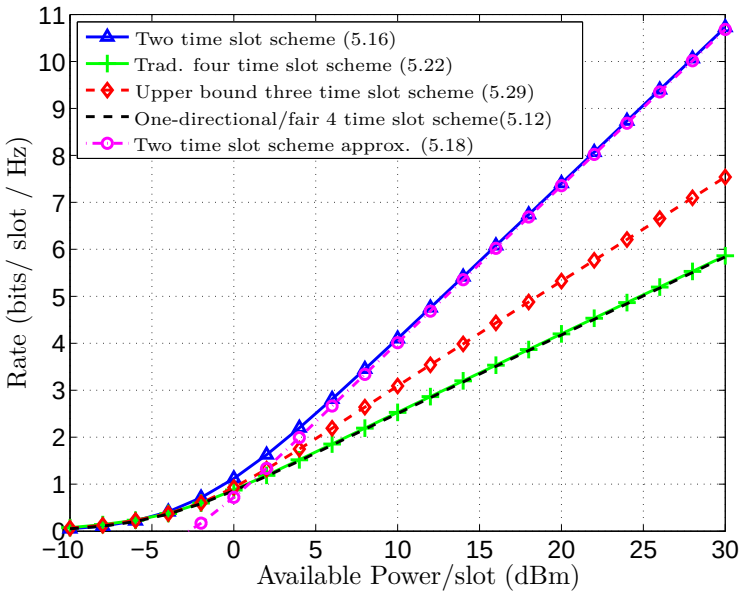

Figure 5.1: Rate versus the total available power.

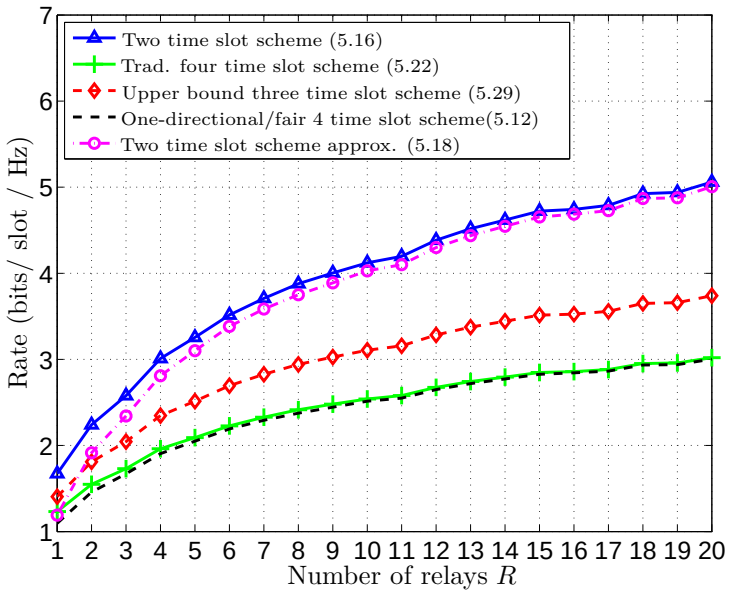

Figure 5.2: Rate versus the total number of relays.

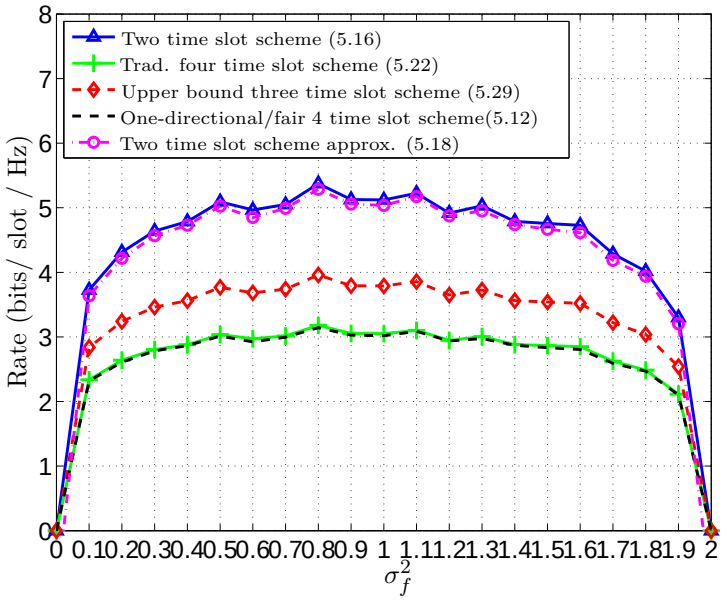

Figure 5.3: Rate versus σ_f^2.

Chapter 6

Multiuser bi-directional relay networks

6.1 Introduction

In Chapter 5, we have observed that the rate of the bi-directional two time slot scheme is roughly twice as large as that of the four time slot scheme for a single transceiver pair.

Here, we develop two-way multi-user p2p AF schemes that can be considered as an extension of the one-directional (one-way) multi-user p2p AF scheme of [23] and [24]. Moreover, it can be seen as a generalization of the two-way two time slot scheme for a single user pair of Figure 1.1 (b) that has been treated in Chapter 5.3 to multiple user pairs. In contrast to the bi-directional communication of a single user pair, in a multi-user environment, the signals received by each user are corrupted not only by noise but also by the interference of the other user pairs. To achieve a trade-off between spectral efficiency and the number of degrees of the freedom to mitigate MUI, we introduce a class of TDMA schemes for bi-directional AF networks with multiple user pairs.

In the proposed schemes, the transceiver pairs are partitioned into N groups and each group contains at least one transceiver pair. The transmissions from the transceivers to the relays take place in N consecutive multiple access (MAC) phases. In the nth MAC phase, the members of the nth group send their information-bearing symbols to the relays. After the N MAC phase, the relays broadcast weighted versions of their received signals to the respective destinations in a single broadcasting phase. Contrary to existing multi-user schemes in the literature for one-directional relay networks proposed in [24] and [41], and bi-directional relay networks proposed in [33], the up-link transmission from the transceivers to the relays comprises multiple phases in the proposed schemes.

To select the relay weights we aim to solve the max-min fairness problem in (2.16) subject to constraints on the individual transmit power of each relay and a constraint on the sum power transmitted by the relays. It is proposed to compute relay weights according to a iterative algorithm of low complexity that is based on convex inner approximations. In the special case that every single user pair forms a group, a second-order cone programming based algorithm obtains the global solution to the max-min fairness optimization problem.

The following contributions are made in this chapter:

- A class of time division multiple access (TDMA) schemes for distributed bi-directional multi-user communication is proposed. The two time slot two-way scheme is generalized to multiple time slots to provide a trade-off between MUI and spectral efficiency.
- An iterative algorithm of low computational complexity that attacks the non-convex max-min-fair relay beamforming problem is proposed.

The content of this chapter has been published in
A. Schad and M. Pesavento, "Multiuser bi-directional communications in cooperative relay networks," *Proc. IEEE CAMSAP'11*, pp. 217 – 220, San Juan, Puerto Rico, Dec. 2011,
and
A. Schad and M. Pesavento, "Time Division Multiple Access Methods in Bi-Directional Cooperative Relay Networks," *Proceedings of the IEEE Sensor Array and Multichannel Signal Processing Workshop,* pp. 89–92, Hoboken, USA, June 2012.

Interestingly, distributed bi-directional multi-user p2p relaying has been treated in [35] that has been published slightly earlier than the content of this chapter. In contrast to [35], here, zero-forcing methods are not applied and the proposed schemes comprise more than two time slots, in general. Our system model is different to those proposed in [36], [37], and [38], where bi-directional multi-user communication via a single AF multi-antenna relay is considered.

6.2 Signal model

Let us assume a relay network with frequency-flat fading channels, R AF relays, and a total number of $2M$ transceivers grouped in M pairs, as discussed in Chapter 2.2.2. The M transceiver pairs are organized in N subgroups where each pair is assigned to one subgroup. In the nth MAC phase, the members of the nth subgroup send their information-bearing symbols to the relays. Note that we propose to use to multiple transmission phases from the terminals to the relays to avoid MUI. After

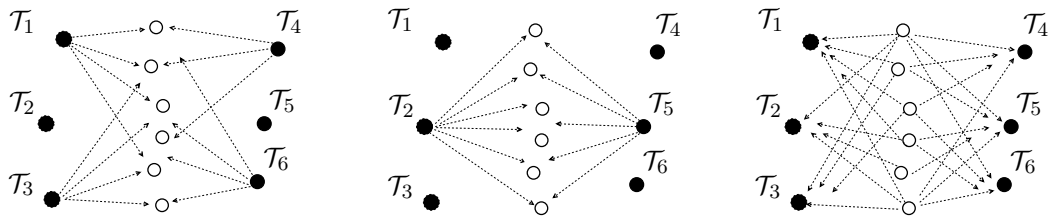

First time slot. Second time slot. Third time slot.

Figure 6.1: Example: $M = 3$, $N = 2$, $\mathcal{Q}_1 = \{1, 3, 4, 6\}$, $\mathcal{Q}_2 = \{2, 5\}$, $\circ$: Relay, $\bullet$: Transceiver.

N uplink phases follows a single broadcast phase where the relays forward their received signals to the respective destinations. In Figure 6.1, we illustrate an example for $M = 3$ and $N = 2$.

Let $\mathcal{Q}_n \subset \{1, 2, \ldots, N\}$ denote the index set containing the indices of the transceiver pairs of the nth subgroup, $n = 1, \ldots, N$. According to (5.13), the vector
$\mathbf{x}(n) \triangleq [x_1(n), \ldots, x_R(n)]^T$ of the signals received by the relay in the nth MAC phase is given by

$$\mathbf{x}(n) = \sum_{k \in \mathcal{Q}_n} \left(\sqrt{P_k} \mathbf{f}_k s_k + \sqrt{P_{M+k}} \mathbf{g}_k s_{M+k} \right) + \boldsymbol{\eta}(n), \tag{6.1}$$

where $\boldsymbol{\eta}(n) \triangleq [\eta_1(n), \eta_2(n), \ldots, \eta_{R,n}]^T$ is the relay noise vector of the nth MAC phase. In the $(N+1)$th time slot, the relays forward the signals received in the N MAC phases to their respective destinations. To generate the transmit signal, the relay $\mathcal{R}_r$ multiplies the nth received signal by a complex weight and sends the superposition of all scaled and phase-adjusted signals to the transceivers in the single downlink phase. Let $\mathbf{w}_n$ denote the complex $R \times 1$ relay weight vector for the signals received by the relays in the nth MAC phase. The vector of transmitted signals at the relays can be expressed as

$$\mathbf{t} = \sum_{n=1}^{N} \mathbf{W}_n \mathbf{x}(n), \tag{6.2}$$

where $\mathbf{W}_n \triangleq \mathrm{diag}(\mathbf{w}_n^H)$. According to (2.9), (6.1), and (6.2), the signal y_m received at transceiver $\mathcal{T}_m$, $m \leq M$, is given by

$$y_m = \mathbf{f}_m^T \mathbf{t} + \nu_m = \sum_{n=1}^{N} \mathbf{f}_m^T \mathbf{W}_n \left(\sum_{k \in \mathcal{Q}_n} \left(\sqrt{P_k} \mathbf{f}_k s_k + \sqrt{P_{M+k}} \mathbf{g}_k s_{M+k} \right) + \boldsymbol{\eta}(n) \right) + \nu_m.$$

Exploiting the identity $\mathbf{a}^T \mathrm{diag}(\mathbf{b}) = \mathbf{b}^T \mathrm{diag}(\mathbf{a})$, we have $\mathbf{f}_m^T \mathbf{W}_n = \mathbf{w}_n^H \mathbf{F}_m$ and $\mathbf{f}_m^T \mathbf{W}_n \boldsymbol{\eta}(n) = \mathbf{w}_n^H \mathbf{F}_m \boldsymbol{\eta}(n)$, where $\mathbf{F}_m \triangleq \mathrm{diag}(\mathbf{f}_m)$. Let us define the relay channels between transceiver $\mathcal{T}_m$ and

transceiver $\mathcal{T}_k$ as

$$\mathbf{h}_{m,k} \triangleq \begin{cases} \mathbf{F}_m \mathbf{f}_k & \text{if} \quad m,k \leq M \\ \mathbf{G}_m \mathbf{g}_k & \text{if} \quad m,k > M \\ \mathbf{G}_m \mathbf{f}_k & \text{if} \quad m > M, k \leq M \\ \mathbf{F}_m \mathbf{g}_k & \text{if} \quad m \leq M, k > M \end{cases} \tag{6.3}$$

Note that

$$\mathbf{h}_{m,k} = \mathbf{h}_{k,m} \tag{6.4}$$

holds true due to the reciprocity assumption.

Let us rewrite y_m for $M \geq m \in \mathcal{Q}_n$ as

$$\begin{aligned} y_m = & \underbrace{\sqrt{P_{M+m}}\mathbf{w}_n^H \mathbf{h}_{m,M+m} s_{M+m}}_{y_{m,\mathrm{S}}} + \underbrace{\sqrt{P_m}\mathbf{w}_n^H \mathbf{h}_{m,m} s_m}_{y_{\mathrm{SI},m}} \\ & + \underbrace{\sum_{n=1}^{N} \mathbf{w}_n^H \left(\sum_{\substack{k \in \mathcal{Q}_n \\ k \neq m}} \sqrt{P_k}\mathbf{h}_{m,k} s_k + \sqrt{P_{k+M}}\mathbf{h}_{m,k+M} s_{k+M} \right)}_{y_{m,\mathrm{MUI}}} + \underbrace{\sum_{n=1}^{N} \mathbf{w}_n^H \mathbf{F}_m \boldsymbol{\eta}(n) + \nu_m}_{y_{m,\mathrm{N}}}, \end{aligned} \tag{6.5}$$

where $y_{m,\mathrm{S}}$, $y_{\mathrm{SI},m}$, $y_{m,\mathrm{MUI}}$, and $y_{m,\mathrm{N}}$ is the desired signal, the SI caused by the own transmitted signal, the MUI caused by the remaining transceiver pairs and the noise at transceiver $\mathcal{T}_m$, respectively. Note that it is straightforward to obtain the corresponding formulations of (6.5) for even $m > M$.

Assuming that the complex scalar $\mathbf{w}_n^H \mathbf{h}_{m,m}$ is known at transceiver $\mathcal{T}_m$, the SI term $\sqrt{P_m}\mathbf{w}_n^H \mathbf{h}_{m,m} s_m$ can be subtracted from the received signal, as it has been proposed in (5.14) for the single-user case. SI cancellation is possible since the transceiver $\mathcal{T}_m$ knows its own transmitted symbol. The resulting received signal is $\hat{y}_m = y_m - \sqrt{P_m}\mathbf{w}_n^H \mathbf{h}_{m,m} s_m$.

6.3 SINR maximization

In this section, we design the weight vectors to maximize the QoS of the transceivers quantified in terms of the received SINR at each transceiver. It is assumed that there are constraints on the individual power of each relay and a constraint on the sum power consumed by the relays. According to (2.16), the max-min fair beamformer design problem can be expressed as

$$\begin{aligned} \max_{\substack{\mathbf{w}_n \\ n \in \{1,\ldots,N\}}} \min_m \mathrm{SINR}_m \quad \text{s.t.} \quad & p_r \leq p_{r,\max}, \quad r = 1, \ldots, R, \\ & \sum_{r=1}^{R} p_r \leq P_{\mathrm{R,max}}. \end{aligned} \tag{6.6}$$

Note that SINR_m denotes the SINR after the SI cancellation applied at transceiver $\mathcal{T}_m$. Using (6.5) and assuming $M \geq m \in \mathcal{Q}_n$

$$\mathbf{w} \triangleq [\mathbf{w}_1^T, \mathbf{w}_2^T, \ldots, \mathbf{w}_L^T]^T, \tag{6.7}$$

$$\mathbf{h}_m \triangleq \left[\mathbf{0}^{(m-1)R}, \mathbf{h}_{m,M+m}, \mathbf{0}^{(N-n)R}\right]^T, \tag{6.8}$$

$$\mathbf{Q}_{m,\text{S}} \triangleq P_{M+m}\mathbf{h}_m\mathbf{h}_m^H, \tag{6.9}$$

$$\mathbf{Q}_{m,n,\text{I+N}} \triangleq \sum_{\substack{k\in\mathcal{Q}_n \\ k\neq m}} P_k\mathbf{h}_{m,k}\mathbf{h}_{m,k}^H + P_{M+k}\mathbf{h}_{m,M+k}\mathbf{h}_{m,M+k}^H + \sigma^2\mathbf{F}_m\mathbf{F}_m^H, \tag{6.10}$$

$$\mathbf{Q}_{m,\text{I+N}} \triangleq \text{blkdiag}([\mathbf{Q}_{m,1,\text{I+N}}, \mathbf{Q}_{m,2\text{I+N}}, \ldots, \mathbf{Q}_{m,L,\text{I+N}}]), \tag{6.11}$$

such that $\text{E}\{|y_{m,\text{S}}|^2\} = \mathbf{w}^H\mathbf{Q}_{m,\text{S}}\mathbf{w}$, $\text{E}\{|y_{m,\text{MUI}}|^2\} + \text{E}\{|y_{\text{N},m}|^2\} = \mathbf{w}^H\mathbf{Q}_{m,\text{I+N}}\mathbf{w} + \sigma^2$. With the above definitions, the SINR at transceiver $\mathcal{T}_m$ is given by

$$\text{SINR}_m(\mathbf{w}) = \frac{\mathbf{w}^H\mathbf{Q}_{m,\text{S}}\mathbf{w}}{\mathbf{w}^H\mathbf{Q}_{m,\text{I+N}}\mathbf{w} + \sigma^2}. \tag{6.12}$$

Making use of (6.1) and (6.2), we find

$$\begin{aligned} p_r \triangleq \text{E}\{|[\mathbf{t}]_r|^2\} &= \sum_{n=1}^{N} |[\mathbf{w}_n]_r|^2 \left(\sum_{k\in\mathcal{Q}_n} P_k|f_{k,r}|^2 + P_{M+k}|g_{r,k}|^2 + \sigma^2\right) \\ &= \sum_{n=1}^{N} \mathbf{w}_n^H\mathbf{D}_{r,n}\mathbf{w}_n \triangleq \mathbf{w}^H\mathbf{D}_r\mathbf{w}, \end{aligned} \tag{6.13}$$

where $\mathbf{D}_{r,n}$ is the $R \times R$ matrix having $\sum_{k\in\mathcal{Q}_n} P_k|f_{k,r}|^2 + P_{M+k}|g_{r,k}|^2 + \sigma^2$ as its rth diagonal entry and zeros elsewhere and $\mathbf{D}_r \triangleq \text{diag}([\mathbf{D}_{r,1}, \mathbf{D}_{r,2}, \ldots, \mathbf{D}_{r,N}])$. The relay sum power in (6.6) can be expressed as

$$\sum_{r=1}^{R} p_r = \sum_{r=1}^{R} \mathbf{w}^H\mathbf{D}_r\mathbf{w} = \mathbf{w}^H\mathbf{D}\mathbf{w}, \tag{6.14}$$

where $\mathbf{D} \triangleq \sum_{r=1}^{R} \mathbf{D}_r$ is a diagonal matrix. According to (2.17), the max-min fairness problem in (6.6) can be equivalently rewritten as

$$\max_{\mathbf{w},\gamma} \gamma \quad \text{s.t.} \quad \mathbf{w}^H\mathbf{Q}_{m,\text{S}}\mathbf{w} \geq \gamma\mathbf{w}^H\mathbf{Q}_{m,\text{I+N}}\mathbf{w} + \gamma\sigma^2, \quad m = 1, \ldots, 2M, \tag{6.15a}$$

$$\mathbf{w}^H\mathbf{D}_r\mathbf{w} \leq p_{r,\max}, \quad r = 1, \ldots, R, \tag{6.15b}$$

$$\mathbf{w}^H\mathbf{D}\mathbf{w} \leq P_{\text{R},\max}. \tag{6.15c}$$

The matrices $\{\mathbf{D}_r\}_{r=1}^R$ and $\mathbf{D}$ are positive semidefinite. Therefore, the power constraints (6.15b) and (6.15c) in (6.15) are convex and the reformulated SINR constraint (6.15a) are non-convex.

6.3.1 Solution to the max-min fairness problem for $N < M$

In this section, we propose an iterative algorithm on the basis of a local convex approximation of the non-convex SINR constraints in (6.15) around a feasible point $(\mathbf{w}^{(\kappa)}, \gamma^{(\kappa)})$. The proposed algorithm is similar to the CCCP-based algorithm proposed in Chapter 4.3.2, even though the approximations are coarser. As the proposed algorithm solves a convex problem in each iteration step, it belongs to the class of sequential convex programming algorithms.

Let us replace $\mathbf{w}$ by $\mathbf{w}^{(\kappa)} + \Delta\mathbf{w}$ and γ by $\gamma^{(\kappa)} + \Delta\gamma$ in (6.15), where we define $\Delta\mathbf{w}$ and $\Delta\gamma$ as the design variables and consider $\mathbf{w}^{(\kappa)}$ and $\gamma^{(\kappa)}$ to be constant. Then, the objective function and the power constraints are still convex and the SINR constraint functions of (6.15a) are given by

$$\begin{aligned}
&\underbrace{\gamma^{(\kappa)}\mathbf{w}^{(\kappa)H}\mathbf{Q}_{m,\mathrm{I+N}}\mathbf{w}^{(\kappa)} + \gamma^{(\kappa)}\sigma^2 - \mathbf{w}^{(\kappa)H}\mathbf{Q}_{m,\mathrm{S}}\mathbf{w}^{(\kappa)}}_{\triangleq c_m^{(\kappa)}(\mathbf{w}^{(\kappa)},\gamma^{(\kappa)})} \\
&+ \underbrace{\Delta\gamma(\sigma^2 + \mathbf{w}^{(\kappa)H}\mathbf{Q}_{m,\mathrm{I+N}}\mathbf{w}^{(\kappa)}) + \gamma^{(\kappa)}\Delta\mathbf{w}^H\mathbf{Q}_{m,\mathrm{I+N}}\Delta\mathbf{w} + 2\Re\{\Delta\mathbf{w}^H(\gamma^{(\kappa)}\mathbf{Q}_{m,\mathrm{I+N}} - \mathbf{Q}_{m,\mathrm{S}})\mathbf{w}^{(\kappa)}\}}_{\text{convex}} \\
&+ \underbrace{\Delta\gamma(\Delta\mathbf{w}^H\mathbf{Q}_{m,\mathrm{I+N}}\Delta\mathbf{w} + 2\Re\{\Delta\mathbf{w}^H\mathbf{Q}_{m,\mathrm{I+N}}\mathbf{w}^{(\kappa)}\}) - \Delta\mathbf{w}^H\mathbf{Q}_{m,\mathrm{S}}\Delta\mathbf{w}}_{\text{non-convex}},
\end{aligned} \tag{6.16}$$

where $c_m^{(\kappa)}(\mathbf{w}^{(\kappa)}, \gamma^{(\kappa)})$ is a constant that represents the value of the mth SINR constraint function at point $(\mathbf{w}^{(\kappa)}, \gamma^{(\kappa)})$. It is clear that the constraint function in (6.16) becomes convex if the non-convex terms are dropped. As these terms are quadratic and cubic, neglecting them in (6.16) leads to a tight approximation of the original constraint function if $\|\Delta\mathbf{w}\|$ and $\Delta\gamma$ are sufficiently small. On this view, the feasible set of the problem in (6.15) is approximated around the point $(\mathbf{w}^{(\kappa)}, \gamma^{(\kappa)})$ by a convex set, leading to the convex approximation of the problem in (6.15) given by

$$\begin{aligned}
\max_{\Delta\mathbf{w},z} \; z \quad \text{s.t.} \quad & c_m^{(\kappa)}(\mathbf{w}^{(\kappa)}, \gamma^{(\kappa)}) + z + \gamma^{(\kappa)}\Delta\mathbf{w}^H\mathbf{Q}_{m,\mathrm{I+N}}\Delta\mathbf{w} + \\
& 2\Re\{\Delta\mathbf{w}^H(\gamma^{(\kappa)}\mathbf{Q}_{m,\mathrm{I+N}} - \mathbf{Q}_{m,\mathrm{S}})\mathbf{w}^{(\kappa)}\} \le 0, \quad m = 1, \ldots, 2M, \\
& (\mathbf{w}^{(\kappa)} + \Delta\mathbf{w})^H\mathbf{D}_r(\mathbf{w}^{(\kappa)} + \Delta\mathbf{w}) \le p_{r,\max}, \; r = 1, \ldots, R \\
& (\mathbf{w}^{(\kappa)} + \Delta\mathbf{w})^H\mathbf{D}(\mathbf{w}^{(\kappa)} + \Delta\mathbf{w}) \le P_{\mathrm{R,max}},
\end{aligned} \tag{6.17}$$

where we have made use of the definition $z \triangleq \Delta\gamma(\sigma^2 + \mathbf{w}^{(\kappa)H}\mathbf{Q}_{m,\mathrm{I+N}}\mathbf{w}^{(\kappa)})$ and have dropped the constant term $\gamma^{(\kappa)}$ and the scaling factor $1/(\sigma^2 + \mathbf{w}^{(\kappa)H}\mathbf{Q}_{m,\mathrm{I+N}}\mathbf{w}^{(\kappa)})$ in the objective function $\gamma^{(\kappa)} + z/(\sigma^2 + \mathbf{w}^{(\kappa)H}\mathbf{Q}_{m,\mathrm{I+N}}\mathbf{w}^{(\kappa)})$, leading to the objective function z.

Theorem 4. *Let $\mathbf{w}^{(\kappa)}$ be feasible for the constraints of (6.15), let $\gamma^{(\kappa)} = \min_m \mathrm{SINR}_m(\mathbf{w}^{(\kappa)})$ and assume that $(\Delta\mathbf{w}, z)$ is a solution to (6.17). Then $\mathbf{w}^{(\kappa+1)} \triangleq \mathbf{w}^{(\kappa)} + \Delta\mathbf{w}$ will also be feasible for (6.15) and $\min_m \mathrm{SINR}_m(\mathbf{w}^{(\kappa+1)}) \ge \min_m \mathrm{SINR}_m(\mathbf{w}^{(\kappa)})$.*

Therefore, any weight vector $\mathbf{w}^{(\kappa+1)}$ that is a solution to (6.17) is feasible and the smallest SINR is at least as great as the smallest SINR of the previous weight vector $\mathbf{w}^{(\kappa)}$.

Proof. As the variable pair $(\Delta\mathbf{w} = \mathbf{0}, z = 0)$ is feasible for (6.17), $z \geq 0$ is true for any solution of (6.17). From the constraints of (6.17), we derive

$$\begin{aligned} 0 \geq & c_m^{(\kappa)}(\mathbf{w}^{(\kappa)}, \gamma^{(\kappa)}) + z + \gamma^{(\kappa)}\Delta\mathbf{w}^H\mathbf{Q}_{m,\mathrm{I+N}}\Delta\mathbf{w} + 2\Re\{\Delta\mathbf{w}^H(\gamma^{(\kappa)}\mathbf{Q}_{m,\mathrm{I+N}} - \mathbf{Q}_{m,\mathrm{S}})\mathbf{w}^{(\kappa)}\} \\ \geq & c_m^{(\kappa)}(\mathbf{w}^{(\kappa)}, \gamma^{(\kappa)}) + z + \gamma^{(\kappa)}\Delta\mathbf{w}^H\mathbf{Q}_{m,\mathrm{I+N}}\Delta\mathbf{w} + 2\Re\{\Delta\mathbf{w}^H(\gamma^{(\kappa)}\mathbf{Q}_{m,\mathrm{I+N}} - \mathbf{Q}_{m,\mathrm{S}})\mathbf{w}^{(\kappa)}\} \\ & - \Delta\mathbf{w}^H\mathbf{Q}_{m,\mathrm{S}}\Delta\mathbf{w}, \end{aligned}$$

where it is exploited that $\mathbf{Q}_{m,\mathrm{S}}$ is positive semidefinite. Reformulating the above inequality results in

$$\underbrace{\frac{\mathbf{w}^{(\kappa+1)H}\mathbf{Q}_{m,\mathrm{S}}\mathbf{w}^{(\kappa+1)}}{\mathbf{w}^{(\kappa+1)H}\mathbf{Q}_{m,\mathrm{I+N}}\mathbf{w}^{(\kappa+1)} + \sigma^2}}_{\mathrm{SINR}_m(\mathbf{w}^{(\kappa+1)})} \geq \underbrace{\gamma^{(\kappa)}}_{\substack{= \\ \min_m \mathrm{SINR}_m(\mathbf{w}^{(\kappa)})}} + \underbrace{\frac{z}{\mathbf{w}^{(\kappa+1)H}\mathbf{Q}_{m,\mathrm{I+N}}\mathbf{w}^{(\kappa+1)} + \sigma^2}}_{\geq 0},$$

and, as the above inequality is true for all m, we have

$$\min_m \mathrm{SINR}_m(\mathbf{w}^{(\kappa+1)}) \geq \min_m \mathrm{SINR}_m(\mathbf{w}_k),$$

completing the proof. □

Repeating the update $\mathbf{w}^{(\kappa+1)} = \mathbf{w}^{(\kappa)} + \Delta\mathbf{w}, \kappa = 0, 1, 2, \ldots$, where $\Delta\mathbf{w}$ is found by solving (6.17), leads to a sequence of weight vectors with a monotonically increasing value of $\min_m \mathrm{SINR}_m(\mathbf{w}^{(\kappa)})$. As a stopping criterion, it is proposed that the iterative algorithm breaks if the relative progress ρ in terms of the minimum SINR is smaller than the predefined value ϵ.

The computational effort of the algorithm is to solve the problem in (6.17) that is a convex QCQP. Convex QCQPs are solved with interior point methods at the complexity of $\mathcal{O}(l^{1/2}(l+q)q^2)$, where $l = 2M + R + 1$ is the number of constraints and $q = NR$ is the number of variables [135]. On the other hand, the SDR-based algorithm of Chapter 3 solves an SDP of the complexity $\mathcal{O}(R^6 l^{1/2})$ in each iteration of a bisection search.

6.3.2 Solution to the max-min fairness problem for $N = M$

If $N = M$, each transceiver pair is a member of a unique group and, therefore, each MAC phase is assigned to a single pair. It is assumed that $m \equiv \mathcal{Q}_m$ and, consequently, transceiver $\mathcal{T}_m$ and transceiver $\mathcal{T}_{M+m}$ are assigned to the mth MAC phase. Note that the constraints of the problem in (6.15) are not affected if the weight vector $\mathbf{w}_m$ is multiplied by the complex number $e^{j\phi_m}$, where ϕ_m is arbitrary. Using this phase-rotation, we choose $\mathbf{w}_m$ such that $\mathbf{w}_m^H\mathbf{h}_{m,M+m}$ is real-valued. As a

consequence, $\mathbf{w}^H\mathbf{h}_m = \mathbf{w}^H\mathbf{h}_{M+m}$ is also real-valued according to (6.4) and (6.8). Since each weight vector $\mathbf{w}_m$ is assigned exclusively to the mth transceiver pair, and, using the definitions

$$\begin{aligned}
\tilde{\mathbf{w}} &\triangleq \left[\mathbf{w}^T, 1\right]^T, \\
\tilde{\mathbf{h}}_m &\triangleq \left[\mathbf{h}_m^T, 0\right]^T, m = 1, \dots 2M, \\
\tilde{\mathbf{Q}}_{m,\mathrm{I+N}} &\triangleq \mathrm{diag}([\mathbf{Q}_{m,\mathrm{I+N}}, \sigma^2])^{1/2}, m = 1, \dots 2M, \\
\tilde{\mathbf{D}}_r &\triangleq \mathrm{diag}([\mathbf{D}_r, 0]), r = 1, \dots R, \qquad \tilde{\mathbf{D}} \triangleq \mathrm{diag}([\mathbf{D}, 0]),
\end{aligned}$$

we reformulate the problem in (6.15) to the equivalent problem

$$\begin{aligned}
\max_{\tilde{\mathbf{w}},\gamma} \gamma \quad \text{s.t.} \quad & \Re\{\tilde{\mathbf{w}}^H\tilde{\mathbf{h}}_m\} \geq \sqrt{\gamma}\|\tilde{\mathbf{Q}}_{m,\mathrm{I+N}}\tilde{\mathbf{w}}\|, \quad m = 1, \dots, 2M \\
& \Im\{\tilde{\mathbf{w}}^H\tilde{\mathbf{h}}_m\} = 0, \quad m = 1, \dots, 2M \\
& \tilde{\mathbf{w}}^H\tilde{\mathbf{D}}_r\tilde{\mathbf{w}} \leq p_{r,\max}, \quad r = 1, \dots, R, \\
& \tilde{\mathbf{w}}^H\tilde{\mathbf{D}}\tilde{\mathbf{w}} \leq P_{\mathrm{R,max}}, \quad [\tilde{\mathbf{w}}]_{L\cdot R+1} = 1.
\end{aligned} \tag{6.18}$$

Note that the feasibility problem of computing a weight vector $\mathbf{w}$ for some fixed γ that satisfies the constraints of (6.18) is convex and belongs to the class of second order cone problems. Similar to bisection search combined with the SDR method explained in Chapter 3.3.2, the maximum objective value of (6.18) can be found by a simple bisection search on γ.

We remark that, in general, the assumption that $\mathbf{w}^H\mathbf{h}_m$ is real-valued restricts the feasible set and may lead to a suboptimal solution if $N < M$.

6.4 Simulation results

A network consisting of 15 relays is considered, where the noise and channel vectors $\{\mathbf{f}_m\}_{m=1}^M$ and $\{\mathbf{g}_m\}_{m=1}^M$ are generated in each of the 100 simulation runs as complex zero mean circular Gaussian distributed random variables with unit variance. The proposed algorithm is initialized with a random vector that is created as a complex zero mean circular Gaussian distributed random variable and choose $\epsilon = 10^{-4}$.

In the first example, we consider the case of $L = 1$. In this case, our scheme comprises two time slots and all transceivers are members of a single group. We set $p_{r,\max} = P_{\mathrm{R,max}}/10$ for $r = 1, \dots, R$ and the transmit powers of the transceivers $\{P_m\}_{m=1}^{2M}$ are 10dB above the noise power. We compare the rate achieved by the proposed two time slot scheme to the rate achieved by the one-directional multi-user p2p scheme proposed in [24], using two transmissions, resulting in four

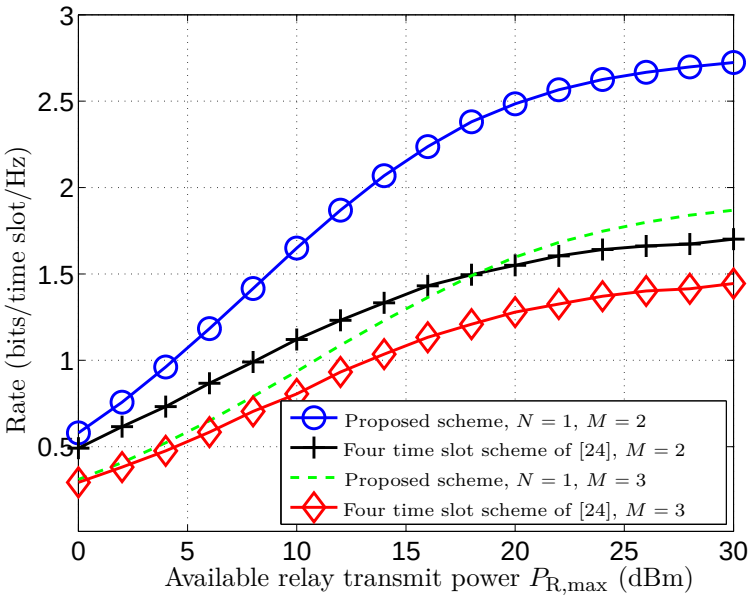

Figure 6.2: First example, $N = 1$. Minimal rate versus the available relay transmit power.

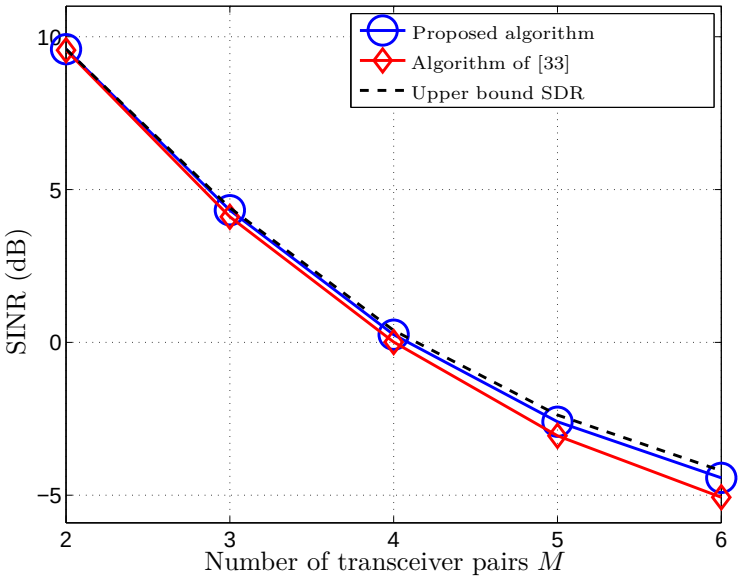

Figure 6.3: First example, $N = 1$. Minimal SINR versus the number of transceiver pairs M.

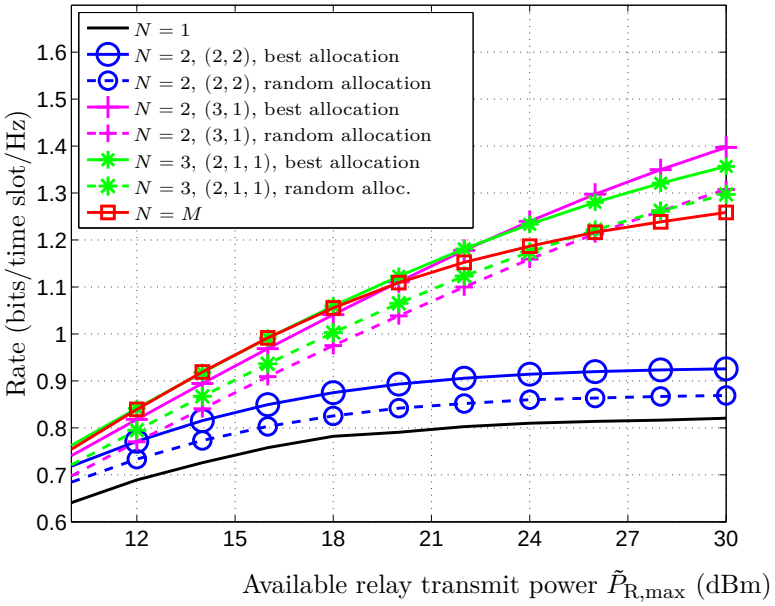

Figure 6.4: Second example. Minimal rate versus the relay transmit power.

time slots. The rate is defined as $1/2 \cdot \log_2(1 + \mathrm{SINR})$ for the proposed two time slot scheme and $1/4 \cdot \log_2(1 + \mathrm{SINR})$ for the one-directional multi-user p2p scheme, where the prefactors $1/2$ and $1/4$ take the number of time slots into account. For the one-directional p2p scheme, we consider the joint optimization of two weight vectors of the two sequential transmissions. As the optimization problem of maximizing the minimum SINR has the same structure as (6.6), the proposed algorithm is used to compute the weight vectors. Note that the transceiver powers and the bounds on the sum power and the individual relay powers are set twice as high as the corresponding values for the two time slot scheme since the number of time slots is doubled.

In Figure 6.2, the minimum rate is depicted versus the maximum relay transmit power $P_{\mathrm{R,max}}$ for $M = 2$ and $M = 3$ transceiver pairs. The proposed two time slot scheme outperforms the four time slot scheme for both $M = 2$ and $M = 3$ transceiver pairs.

In Figure 6.3, we compare the proposed algorithm to the SDR-based Algorithm 1 of Chapter 3.3.1 and the theoretical upper bound which is obtained as a byproduct of the SDR method. Figure 6.3 depicts the minimum SINR versus the number of transceiver pairs for fixed $P_{\mathrm{R,max}} = 10\mathrm{dBm}$. The minimum SINR decreases with the increase of M. For $M = 2$ and $M = 3$, the proposed algorithm and the SDR-based algorithm of [33] perform similarly and achieve almost the upper bound on the minimum SINR obtained by the SDR-based algorithm. Therefore, the performance of this scheme

cannot be substantially improved by a rank-two beamforming scheme as proposed in Chapter 4. For $M = 5$ and $M = 6$, the proposed algorithm performs better than the that of [33]. We observe that the SINR increases significantly with a growing number of user pairs.

In the second example, $M = 4$ transceiver pairs are considered. We set $p_{r,\max} = P_{\mathrm{R},\max}/4$ for $r = 1, \ldots, R$ and the transmit powers of the transceivers $\{P_m\}_{m=1}^{2M} = 10 \cdot (L+1)$. We compare the rate achieved by the proposed schemes which is defined as $1/(L+1) \cdot \log_2(1 + \mathrm{SINR})$, where the prefactors take the number of time slots into account.

In Figure 6.4, the minimum rate is depicted versus the maximum relay transmit power $\tilde{P}_{\mathrm{R},\max}$ where $P_{\mathrm{R},\max} = (L+1)\tilde{P}_{\mathrm{R},\max}$. We indicate the allocation of the transceivers by $(a, b, \ldots)$, where we have one group of a transceivers, one group of b etc.. As the allocation of the transceivers into the groups is not unique (except for the cases $L = M$ and $L = 1$) and as the allocation may influence the performance, we display the allocation that achieves the highest rate (best allocation) and a random allocation of the transceivers. Note that the best allocation is found by testing all possible combinations.

6.5 Conclusion

In this chapter, bi-directional distributed beamforming for the p2p communication of multiple transceiver pairs is considered. In contrast to a single transceiver pair of Chapter 5, the multi-user environment leads to MUI. As a consequence, the gain of the two time-slot scheme of Figure 1.1 (c) to the four time slot scheme of Figure 1.1 (a) in terms of transmission gain is lower as compared with the single transceiver pair case. We have proposed a class of novel TDMA schemes to provide a trade-off between spectral efficiency and the number of degrees of freedom in the beamformer design. The simulation results demonstrate the impact of the choice of the TDMA scheme. Furthermore, an iterative algorithm based on inner approximations is proposed that yields a performance close to the upper bound obtained by SDR.

In this chapter, we have considered a relatively small number of users where the considered rank-one beamforming scheme performs already close to the theoretical bound that cannot improved by using higher rank beamforming schemes. For a large number of users, MUI excessively impairs the communication. In this case, it is desirable to separate the various transmit signals not only in the spatial domain by using beamforming but also in the time domain by using multiple access schemes.

Chapter 7

Differential beamforming

7.1 Introduction

In the previous chapters, we have assumed that the CSI is perfectly known and solved power minimization problems or max-min fairness problems to compute the relay weight vectors. Moreover, we have assumed that the computation of weight vectors and power scaling factors is performed by a central processing node. In this chapter, we propose a novel DBF scheme that computes the relay weight without explicit knowledge of the CSI. To establish relay communication without CSI, differential techniques [114]–[123] and non-differential techniques [124], [125] for single-antenna relays have been proposed. The developed DBF scheme exploits implicit CSI contained in previously received signal vectors to perform receive and transmit beamforming. Note that the DBF scheme does not require a central processing node as each parameter is derived at its respective node. This is different to the previous chapter, where we have assumed that all CSI is accumulated at one node to compute the network parameters.

We consider the bi-directional communication between two terminals in the four time slot scheme illustrated in Figure 1.1 (a). In contrast to Chapter 5, where multiple single-antenna relays form a distributed beamforming system, a single multi-antenna AF relay is regarded.

In our theoretical analysis, we derive an expression for the approximated SNR achieved by the proposed DBF scheme for time-invariant channels. Our simulations demonstrate that the latter approximation is highly accurate in the medium to high-power regime. Based on this approximation, we propose to distribute the total power among the terminals and the relay such that max-min fairness is achieved. The proposed power allocation scheme requires only the knowledge of the noise powers at the RS and the terminals but no CSI. In the simulations, we consider time-variant channels using the model of [138] and compare the BER of the proposed DBF scheme with state of

the art approaches known from the literature for different terminal velocities. The simulation results demonstrate that the proposed DBF scheme dramatically outperforms the differential single-antenna relaying scheme of [123] as well as the multi-antenna relaying scheme of [133], which requires the knowledge of the second order statistics of the CSI.

The contributions of chapter are:

- We propose a novel DBF scheme for bi-directional AF relaying that does not require CSI at any node.
- We derive an approximation expression for the SNR at each terminal which is accurate for medium and high transmit powers.
- We derive a simple power allocation scheme that achieves almost optimum performance.
- We test our proposed DBF scheme under realistic high mobility scenarios using numerical simulations and demonstrate that the proposed scheme outperforms existing schemes.

7.2 Signal model

We consider a wireless single carrier network with two single-antenna transceivers $\mathcal{T}_1$ and $\mathcal{T}_2$ and one multi-antenna AF relay comprising N_R antennas. We assume frequency flat fading channels and that direct link between the transceivers is not available. We further assume that reciprocity holds for transmissions from the terminals to the RS and vice versa. We consider in our derivations a block fading channel model in which the channels remain constant during two consecutive transmission blocks. This assumption is however relaxed in the simulations, where we consider both time-variant and time-invariant channels.

The bi-directional communication between $\mathcal{T}_1$ and $\mathcal{T}_2$ is organized in consecutive blocks, where in each block a four time slot protocol according to Figure 1.1 (a) is used.

In the first time slot of the nth transmission block, terminal $\mathcal{T}_1$ transmits the signal $\sqrt{P_1}v_1(n)$ to the relay, where P_1 is the transmit power of terminal $\mathcal{T}_1$ and $v_1(n)$ is the transmitted data symbol of the nth transmission block. We denote $\mathbf{f}$ and $\mathbf{g}$ as the $R \times 1$ vectors containing the channel coefficients characterizing the transmission in the nth and $(n-1)$th transmission block between terminal $\mathcal{T}_1$ and the relay and between the relay and terminal $\mathcal{T}_2$, respectively. Then, the signals received at the relay in the first time slot can be expressed as the vector $\mathbf{x}(n,1) = [x_1(n,1), \ldots, x_{N_R}(n,1)]^T$, given by

$$\mathbf{x}(n,1) = \sqrt{P_1}v_1(n)\mathbf{f} + \boldsymbol{\eta}(n,1), \tag{7.1}$$

where $\boldsymbol{\eta}(n,t) = [\eta_1(n)(n,t), \ldots, \eta_{N_R}(n,t)]^T$ and where $\eta_r(n,t)$ denotes the noise at the rth relay antenna in the nth transmission block at time slot $t \in \{1,2,3,4\}$. The received signal vector $\mathbf{x}(n,1)$ is weighted by the $N_R \times N_R$ beamforming matrix $\mathbf{W}(2)$ and the resulting $R \times 1$ signal vector

$$\mathbf{t}(n,2) = \mathbf{W}(2)\mathbf{x}(n,1) \tag{7.2}$$

is transmitted to terminal $\mathcal{T}_2$ in the second time slot of the nth transmission block. The corresponding received signal at terminal $\mathcal{T}_2$ is then given by

$$y_2(n) = \mathbf{g}^T\mathbf{t}(n,2) + \nu_2(n) = \mathbf{g}^T\mathbf{W}(2)\mathbf{x}(n,1) + \nu_2(n), \tag{7.3}$$

where $\nu_2(n)$ is the noise at terminal $\mathcal{T}_2$.

Let us assume that the noise in the network can be modeled as a spatially and temporally uncorrelated random processes with zero mean and variance $\mathrm{E}\{|\eta_{r,t}(n)|^2\} = \sigma_R^2$, $\mathrm{E}\{|\nu_2(n)|^2\} = \sigma_2^2$, $\mathrm{E}\{|\nu_4(n)|^2\} = \sigma_1^2$, $\forall r, m, t$. Moreover, we assume without any loss of generality that $\mathrm{E}\{|v_1(n)|^2\} = \mathrm{E}\{|v_2(n)|^2\} = 1$.

We first regard the ideal case that full CSI is available at the relay. The optimization problem of designing $\mathbf{W}(2)$ such that the SNR at terminal $\mathcal{T}_2$ is maximized has been treated in [132]. It has been shown that the ideal AF beamforming matrix is given by

$$\mathbf{W}^\star(2) = c_2\mathbf{g}^*\mathbf{f}^H, \tag{7.4}$$

where $c_2 = \sqrt{P_{\mathrm{R},2} / \left(\left(\sigma_R^2 + P_1\|\mathbf{f}\|^2\right)\|\mathbf{f}\|^2\|\mathbf{g}\|^2\right)}$ is a power scaling factor to ensure an *average* transmit power of $P_{\mathrm{R}}(2)$ at the relay. Note that $\mathbf{W}^\star(2)$ contains the vectors $\mathbf{f}$ and $\mathbf{g}$ that are respectively the matched filter solutions for receive and transmit beamforming at the relay. The ideal matrix leads to a maximum SNR of

$$\mathrm{SNR}^\star(2) = \frac{P_1 P_{\mathrm{R}}(2)\|\mathbf{f}\|^2\|\mathbf{g}\|^2}{\sigma_R^2\sigma_2^2 + \sigma_2^2 P_1\|\mathbf{f}\|^2 + \sigma_R^2 P_{\mathrm{R}}(2)\|\mathbf{g}\|^2}. \tag{7.5}$$

In the third and the fourth time slot, the communication from terminal $\mathcal{T}_2$ to terminal $\mathcal{T}_1$ is accomplished. In the third time slot, terminal $\mathcal{T}_2$ transmits the signal $\sqrt{P_2}v_2(n)$ to $\mathcal{T}_1$, where P_2 denotes the transmit power of terminal $\mathcal{T}_2$ and $v_2(n)$ is the transmitted data symbol. Similar as in (7.1), the received $N_R \times 1$ signal vector at the relay in the third time slot of the nth transmission block is given by

$$\mathbf{x}(n,3) = \sqrt{P_2}v_2(n)\mathbf{g} + \boldsymbol{\eta}(n,3). \tag{7.6}$$

Following the relaying procedure for the second time slot given in (7.2) - (7.5), the relay weights $\mathbf{x}(n,3)$ by the $N_R \times N_R$ beamforming matrix $\mathbf{W}(4)$ and transmits the $N_R \times 1$ signal vector $\mathbf{t}(n,4)$,

given by $\mathbf{t}(n,4) = \mathbf{W}(4)\mathbf{x}(n,3)$ to terminal $\mathcal{T}_1$ in the fourth time slot. The ideal relay weight matrix $\mathbf{W}(4)^\star$ is given by $\mathbf{W}(4)^\star = c_4\mathbf{f}^*\mathbf{g}^H$, where
$c_4 = \sqrt{P_{\mathrm{R}}(4) / \left(\left(\sigma_R^2 + P_2\|\mathbf{g}\|^2\right)\|\mathbf{g}\|^2\|\mathbf{f}\|^2\right)}$ is a constant and $P_{\mathrm{R}}(4)$ is the transmit power of the relay.

Utilizing the ideal relay beamforming matrices requires the perfect knowledge of the instantaneous channel vectors $\mathbf{f}$ and $\mathbf{g}$. Here, we address the problem of choosing the beamforming matrices in the case that CSI is not available.

7.3 The differential beamforming scheme

In this section, we present the DBF scheme which does not require knowledge of the CSI neither at the relay nor at the terminals.

At the terminals, we apply differential phase shift keying (PSK) where the transmitted data symbols $v_1(n)$ and $v_2(n)$ are generated from the information bearing symbols $s_1(n)$ and $s_2(n)$ by differential coding as [137]

$$v_1(n) = v_1(n-1)s_1(n), \qquad v_2(n) = v_2(n-1)s_2(n). \tag{7.7}$$

$v_1(n-1)$ and $v_2(n-1)$ are the transmitted data symbols of the transmission block $n-1$, and $s_1(n)$ and $s_2(n)$ are drawn from PSK constellations $\mathcal{M}_1$ and $\mathcal{M}_2$, respectively. We assume, without loss of generality, that $|s_1(n)|^2 = |s_2(n)|^2 = 1$ holds true for all n and that the DBF scheme is initialized with the symbols $v_1(0) = 1$ and $v_2(0) = 1$. Then, it follows by induction that $|v_1(n)|^2 = |v_2(n)|^2 = 1$ holds true for all $n \geq 1$.

In the second time slot of the nth transmission block, the goal is to approximate the ideal beamforming matrix $\mathbf{W}^\star(2)$ of (7.4) by approximating the beamforming vectors $\mathbf{f}$ and $\mathbf{g}$. We first aim to approximate the receive beamforming vector $\mathbf{f}$ by considering the Maximum-Likelihood (ML) detection problem of finding the transmitted data symbols from the received signal vectors $\mathbf{x}(n-1,1)$ and $\mathbf{x}(n,1)$ at the relay. Let us define $\mathbf{h} = \sqrt{P}_1\mathbf{f}$, where $\mathbf{h}$ is unknown. Then, the ML problem corresponds to the following Least Squares problem [126]

$$\min_{\mathbf{h}, v_1(n)\in\mathcal{M}_1, v_1(n-1)\in\mathcal{M}_1} \|\mathbf{h}v_1(n) - \mathbf{x}(n,1)\|^2 + \|\mathbf{h}v_1(n-1) - \mathbf{x}(n-1,1)\|^2. \tag{7.8}$$

For given $v_1(n)$ and $v_1(n-1)$, $\hat{\mathbf{h}} = \frac{1}{2}\left(\mathbf{x}(n,1)v_1^*(n) + \mathbf{x}(n-1,1)v_1^*(n-1)\right)$ is a solution to (7.8) with respect to $\mathbf{h}$. Inserting $\hat{\mathbf{h}}$ into the problem in (7.8) and applying (7.7) results in

$$\max_{s_1(n)\in\mathcal{M}_1} \Re\{s_1^*(n)\mathbf{x}^H(n-1,1)\mathbf{x}(n,1)\},$$

which leads to the *soft decoded* symbol at the relay

$$\hat{s}_{1,\mathrm{R}}(n) = \mathbf{x}^H(n-1,1)\mathbf{x}(n,1) = \sum_{r=1}^{N_R} x_r^*(n-1,1)x_r(n,1) \tag{7.9}$$

Remark 1. The vector $\hat{\mathbf{f}} \triangleq \mathbf{x}(n-1,1)$ in (7.9) can be interpreted as a receive beamforming vector and is the optimal linear receive filter under the condition that the instantaneous CSI is not known but implicitly given from differential encoding. From (7.1), we see that $\hat{\mathbf{f}}$ is equal to $\mathbf{f}$ up to the complex factor $z_f \triangleq \sqrt{P_1}v_1(n-1)$ if the noise is neglected. The concept of using a receive signal vector to perform beamforming has also been proposed in [126]–[128], however in a different context where receive beamforming has been applied to detect differentially encoded symbols.

Remark 2. From (7.9), it is easy to adapt the proposed DBF scheme which uses the AF relaying protocol to a decode-and-forward relaying scheme. The relay can decode the information symbol $s_1(n)$ from (7.9) and then retransmit it. Another alternative is to transmit a block of symbols from terminal $\mathcal{T}_1$ to the relay and then apply error correction to the received signals if additional channel coding is used. The decoded symbols can then be re-encoded and transmitted to terminal $\mathcal{T}_2$.

To transmit $\hat{s}_{1,\mathrm{R}}(n)$ from the relay to terminal $\mathcal{T}_2$, we follow a similar approach as for the derivation of $\hat{\mathbf{f}}$ and approximate the transmit beamforming vector $\mathbf{g}$ contained in the beamforming matrix of (7.4) by $\hat{\mathbf{g}} \triangleq \mathbf{x}(n-1,3)$. From (7.6), we observe that $\hat{\mathbf{g}}$ is equal to $\mathbf{g}$ up to the complex factor $z_g \triangleq \sqrt{P_2}v_2(n-1)$ if the noise is neglected. We remark that using the receive signal vectors to recover CSI for transmit beamforming in TDD systems has been proposed in [129]–[131].

Then, using (7.1) and (7.6), the approximated beamforming matrix is given by

$$\hat{\mathbf{W}}^\star(2) = \hat{c}_2\hat{\mathbf{g}}^*\hat{\mathbf{f}}^H = \hat{c}_2\Big(\sqrt{P_1P_2}(v_1(n-1)v_2^*(n-1)\mathbf{g}^*\mathbf{f}^H + \mathbf{N}(n,2)\Big), \tag{7.10}$$

$$= z_w\mathbf{W}^\star(n) + \hat{c}_2\mathbf{N}(n,2) \tag{7.11}$$

where

$$\hat{c}_2 = \sqrt{P_{\mathrm{R}}(2)}/\|\hat{\mathbf{g}}^*\hat{\mathbf{f}}^H\mathbf{x}(n,1)\|, \tag{7.12}$$

$$\begin{aligned}\mathbf{N}(n,2) =& \boldsymbol{\eta}^*(n-1,3)\boldsymbol{\eta}^H(n-1,1) + v_2^*(n-1)\sqrt{P_2}\mathbf{g}^*(\boldsymbol{\eta}(n-1,1))^H \\ &+ v_1^*(n-1)\sqrt{P_1}\boldsymbol{\eta}^*(n-1,3)\mathbf{f}^H,\end{aligned} \tag{7.13}$$

$$z_w = \hat{c}_2 z_f z_g / c_2. \tag{7.14}$$

Here, $\hat{c}_2$ is a scaling factor such that the *instantaneous* transmit power at the relay results in $\|\mathbf{t}(n,2)\|^2 = P_{\mathrm{R}}(2)$. This is different to the ideal relaying scheme of Section 7.2, where $P_{\mathrm{R}}(2)$ is the average transmit power. Comparing (7.4) and (7.11) we observe that in the noise free case the

approximation (7.11) is exact up to the complex scaling factor z_w which depends on the transmitted symbols $v_1(n-1)$ and $v_2(n-1)$.

The transmit signal vector $\mathbf{t}(n,2)$ at the relay is given by

$$\mathbf{t}(n,2) = \hat{\mathbf{W}}^{\star}(2)\mathbf{x}(n,1). \tag{7.15}$$

Making use of (7.1) - (7.3) and (7.10) - (7.15), the signal $y_2(n)$ received at terminal $\mathcal{T}_2$ in the second time slot of the nth transmission block is given by

$$y(n,2) = \mathbf{g}^T\hat{\mathbf{W}}^{\star}(2)\mathbf{x}(n,1) + \nu_2(n) = \underbrace{d(n,2)v_2^*(n-1)s_1(n)}_{\text{desired signal}} + \underbrace{\tilde{\nu}_2(2)}_{\text{noise signal}}, \tag{7.16}$$

where we have used the definitions

$$d(n,2) = \hat{c}_2 P_1\sqrt{P_2}\|\mathbf{f}\|^2\|\mathbf{g}\|^2, \tag{7.17}$$

$$\tilde{\nu}_2(2) = \mathbf{g}^T\hat{\mathbf{W}}^{\star}(2)\boldsymbol{\eta}(n,1) + \hat{c}_2\sqrt{P_1}v_1(n)\mathbf{g}^T\mathbf{N}(n,2)\mathbf{f} + \nu_2(n). \tag{7.18}$$

Note that according to (7.7), the product $v_1(n)\cdot v_1^*(n-1)$ in (7.16) results in $s_1(n)$.

The desired signal in (7.16) contains the transmitted symbol $v_2(n-1)$ of terminal $\mathcal{T}_2$. This is a consequence of using $\hat{\mathbf{g}} = \mathbf{x}(n-1,3)$ of (7.6) as the transmit beamforming vector at the relay. However, similar as in the analog network coding techniques of [114] and [118], terminal $\mathcal{T}_2$ can cancel the unwanted phase shift of the desired signal caused by $v_2^*(n-1)$ as this symbol is known at terminal $\mathcal{T}_2$. Towards this goal, terminal $\mathcal{T}_2$ multiplies its received signal by $v_2(n-1)$, since $v_2^*(n-1)v_2(n-1) = |v_2(n-1)|^2 = 1$ and obtains

$$\hat{s}_{1,\mathcal{T}_2}(n) = y(n,2)v_2(n-1) = d(n,2)s_1(n) + \tilde{\nu}_2(2)v_2(n-1). \tag{7.19}$$

$\hat{s}_{1,\mathcal{T}_2}(n)$ can be viewed as the *soft decoded* symbol at terminal $\mathcal{T}_2$. From (7.19), the symbol $\hat{s}_1(n)$ is detected as

$$\hat{s}_1(n) = \arg\min_{s\in\mathcal{M}_1} \left|\hat{s}_{1,\mathcal{T}_2}(n)/|\hat{s}_{1,\mathcal{T}_2}(n)| - s\right|.$$

The signal vector transmitted at the relay in the fourth time slot of the nth transmission block can be expressed as $\mathbf{t}(n,4) = \hat{\mathbf{W}}_4^{\star}\mathbf{x}(n,3)$, where $\hat{\mathbf{W}}_4^{\star} = \hat{c}_4(\mathbf{x}^*(n,1))\mathbf{x}^H(n-1,3)$ and $\hat{c}_4 = \sqrt{P_{\mathrm{R}}(4)}/\|(\mathbf{x}^*(n,1))\mathbf{x}^H(n-1,3)\mathbf{x}(n,3)\|$. Similarly as in (7.19), the signal received at terminal $\mathcal{T}_1$ is multiplied by $v_1(n-1)$ before the symbol detection.

Remark 3. The DBF scheme can easily be modified to a *one-directional* two-time-slot scheme, where data is transferred from terminal $\mathcal{T}_1$ to terminal $\mathcal{T}_2$. In the one-directional communication, $\mathbf{g}$ can be estimated at the relay when $\mathcal{T}_2$ transmits pilot symbols to the relay.

7.4 Analysis for the high power regime and power allocation

In this section, approximate expressions for the SNRs at the terminals are derived. These expressions are utilized to develop a simple power allocation scheme. We assume that the block fading assumption of the previous section is valid and that the transmit powers of the terminals are large as compared with the noise power. Our simulations carried out in Section 7.5 will demonstrate that this approximate expression is also accurate for moderate transmit powers.

If the CSI is available and for $P_1, P_2, P_{\mathrm{R}}(2) \to \infty$, the maximum achievable SNR at terminal $\mathcal{T}_2$ is well approximated by the expression

$$\overline{\mathrm{SNR}}^{\star}(2) = \frac{P_1 P_{\mathrm{R}}(2)\|\mathbf{f}\|^2\|\mathbf{g}\|^2}{\sigma_2^2 P_1\|\mathbf{f}\|^2 + \sigma_R^2 P_{\mathrm{R}}(2)\|\mathbf{g}\|^2}, \tag{7.20}$$

where we have dropped the term $\sigma_R^2\sigma_2^2$ in the denominator of $\mathrm{SNR}^{\star}(2)$ given in (7.5) as $\sigma_R^2\sigma_2^2 \ll \sigma_2^2 P_1\|\mathbf{f}\|^2 + \sigma_R^2 P_{\mathrm{R},2}\|\mathbf{g}\|^2$.

To derive an asymptotic approximation of the performance of the proposed DBF scheme, let us focus on the scaling factor $\hat{c}_2$ of (7.12) contained in the relay weight matrix $\hat{\mathbf{W}}^{\star}(2)$. Neglecting the noise terms in the vectors $\mathbf{x}(n-1,3) = \sqrt{P_2}v_2(n-1)\mathbf{g} + \boldsymbol{\eta}(n,3)$, $\mathbf{x}(n-1,1) = \sqrt{P_1}v_1(n-1)\mathbf{f} + \boldsymbol{\eta}(n-1,1)$, and $\mathbf{x}(n,1) = \sqrt{P_1}v_1(n)\mathbf{f} + \boldsymbol{\eta}(n,1)$, we obtain

$$\hat{c}_2 \approx \sqrt{P_{\mathrm{R}}(2)} \Big/ \left(P_1\sqrt{P_2}\|\mathbf{g}\|\|\mathbf{f}\|^2\right), \tag{7.21}$$

where we have made use of the fact that $|v_1(n-1)| = |v_2(n-1)| = |v_1(n)| = 1$. Then, using (7.10) - (7.19) and (7.21) leads to

$$d(n,2) \approx \sqrt{P_{\mathrm{R}}(2)}\|\mathbf{g}\|, \tag{7.22}$$

$$\begin{aligned}\tilde{\nu}_2(2)v_2(n-1) \approx \sqrt{P_{\mathrm{R}}(2)}\Bigg(&\frac{n_1(n-1)\|\mathbf{g}\|\mathbf{f}^H\boldsymbol{\eta}(n,1)}{\sqrt{P_1}\|\mathbf{f}\|^2} + \frac{v_1(n)\|\mathbf{g}\|\boldsymbol{\eta}^H(n-1,1)\mathbf{f}}{\sqrt{P_1}\|\mathbf{f}\|^2} \\ &+ \frac{s_1(n)\mathbf{g}^T\boldsymbol{\eta}^*(n-1,3)x_2(n-1)}{\sqrt{P_2}\|\mathbf{g}\|} + \nu_2(n)x_2(n-1).\end{aligned} \tag{7.23}$$

From (7.22) and (7.23), we observe that the proposed differential scheme approximately achieves an SNR given by

$$\hat{\mathrm{SNR}}_2 = \frac{P_1 P_2 P_{\mathrm{R}}(2)\|\mathbf{f}\|^2\|\mathbf{g}\|^2}{\sigma_R^2\left(2P_{\mathrm{R}}(2)P_2\|\mathbf{g}\|^2 + P_{\mathrm{R}}(2)P_1\|\mathbf{f}\|^2\right) + \sigma_2^2 P_1 P_2\|\mathbf{f}\|^2}. \tag{7.24}$$

Similar to the derivation of $\hat{\mathrm{SNR}}_2$, one can show that the SNR at terminal $\mathcal{T}_1$ is approximately given by

$$\hat{\mathrm{SNR}}_4 = \frac{P_1 P_2 P_{\mathrm{R}}(4)\|\mathbf{f}\|^2\|\mathbf{g}\|^2}{\sigma_R^2\left(2P_{\mathrm{R}}(4)P_1\|\mathbf{f}\|^2 + P_{\mathrm{R}}(4)P_2\|\mathbf{g}\|^2\right) + \sigma_1^2 P_1 P_2\|\mathbf{g}\|^2}. \tag{7.25}$$

Based on the SNR expressions in (7.24) and (7.25), we propose to distribute an amount of total power P_{T} among the relay and the terminals to solve the max-min fairness problem in (2.16) which can be formulated as

$$\begin{aligned} &\max_{P_1,P_2,P_{\mathrm{R}}(2),P_{\mathrm{R}}(4)} \quad \min(\hat{\mathrm{SNR}}_2, \hat{\mathrm{SNR}}_4) \\ &\text{s.t.} \quad P_1+P_2+P_{\mathrm{R}}(2)+P_{\mathrm{R}}(4) \leq P_{\mathrm{T}}, \end{aligned} \tag{7.26}$$

where $P_1, P_2, P_{\mathrm{R}}(2)$, and $P_{\mathrm{R}}(4)$ are the optimization variables and where the constraint guarantees that the sum power does not exceed P_{T}. It is easy to show that at an optimum point of the problem in (7.26), i) $\hat{\mathrm{SNR}}_2 = \hat{\mathrm{SNR}}_4$ holds true; ii) the inequality constraint is satisfied with equality and $P_{\mathrm{R}}(2)+P_{\mathrm{R}}(4) = P_{\mathrm{T}}-P_2-P_1$ holds true. Based on the properties i) and ii), we derive a simple but generally suboptimal solution to (7.26).

Let us define $P_{\mathrm{R}} = P_{\mathrm{R}}(2)+P_{\mathrm{R}}(4)$ and introduce the power allocation factor $0 \leq \alpha \leq 1$ such that $P_{\mathrm{R}}(2) = \alpha P_{\mathrm{R}}$ and $P_{\mathrm{R}}(4) = (1-\alpha)P_{\mathrm{R}}$. For the sake of simplicity, let us first assume that P_1 and P_2 are fixed. Then, the power allocation can be found by solving the equation $\hat{\mathrm{SNR}}_2 = \hat{\mathrm{SNR}}_4$ which results in solving the quadratic form

$$\begin{aligned} &\alpha^2 P_{\mathrm{R}}\sigma_{\mathrm{R}}^2 \left(P_2\|\mathbf{g}\|^2 - P_1\|\mathbf{f}\|^2\right) + \alpha\Big(P_{\mathrm{R}}\sigma_{\mathrm{R}}^2 \left(P_1\|\mathbf{f}\|^2 - P_2\|\mathbf{g}\|^2\right) \\ &+ \sigma_2^2 P_1 P_2\|\mathbf{f}\|^2 + \sigma_1^2 P_1 P_2\|\mathbf{g}\|^2\Big) - \sigma_2^2 P_1 P_2\|\mathbf{f}\|^2 = 0. \end{aligned} \tag{7.27}$$

For the symmetric (but generally non-optimal) case

$$P_1 = P_{\mathrm{R}}\sigma_{\mathrm{R}}^2/(2\sigma_1^2), \qquad P_2 = P_{\mathrm{R}}\sigma_{\mathrm{R}}^2/(2\sigma_2^2), \tag{7.28}$$

$$P_{\mathrm{R}} = P_{\mathrm{T}}/\left(1 + \sigma_{\mathrm{R}}^2/(2\sigma_1^2) + \sigma_{\mathrm{R}}^2/(2\sigma_2^2)\right), \tag{7.29}$$

the solution to (7.27) is given by $\alpha = 1/2$ leading to

$$P_{\mathrm{R}}(2) = P_{\mathrm{R}}(4) = P_{\mathrm{R}}/2. \tag{7.30}$$

Interestingly, inserting (7.28) - (7.30) in (7.20) and (7.24), we obtain

$$\hat{\mathrm{SNR}}(2) = \overline{\mathrm{SNR}}^{\star}(2)/2. \tag{7.31}$$

We observe from (7.31) that the proposed DBF scheme achieves approximately half the SNR of the ideal AF beamforming scheme if the communication channels remain constant during two consecutive transmission blocks and if we use (7.28) - (7.30). The latter 3dB performance loss is common in differential schemes [137].

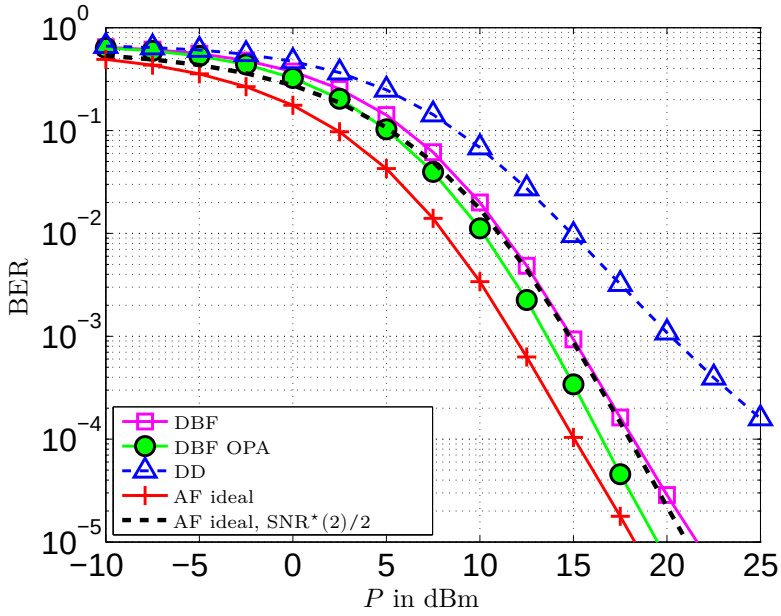

Figure 7.1: BER versus transmit power P for differential and non-differential schemes using QPSK in an urban micro scenario, v =0 km/h.

In general, the power allocation according to (7.28) - (7.30) is not the optimum solution to the problem in (7.26). However, the optimization problem in (7.26) is highly non-linear and difficult to solve exactly in reasonable time. Furthermore, the optimum power allocation (OPA) depends on the channel vectors $\mathbf{f}$ and $\mathbf{g}$ and has to be recomputed if $\mathbf{f}$ and $\mathbf{g}$ change. The advantage of the *constant* power allocation in (7.28) - (7.30) is that it does not depend on the time-variant channel vectors but only on the constant noise powers and the total available power P_{T}. Therefore, it is sufficient to compute (7.28) - (7.30) once at the relay using $\sigma_1^2, \sigma_2^2, \sigma_{\mathrm{R}}^2$ and P_{T}.

7.5 Simulation Results

Throughout our simulations, we consider a relay equipped with $R=5$ antennas arranged in a uniform linear array in which neighboring antennas have a distance of two wavelengths. The information bearing symbols are taken from a QPSK constellation. We set the noise powers $\sigma_R^2=\sigma_1^2=\sigma_2^2=-132$ dBm and divide the transmit power such that $P \triangleq P_1=P_2=P_{\mathrm{R}}(2)=P_{\mathrm{R}}(4)=P_{\mathrm{T}}/4$. This choice satisfies (7.28) - (7.30). To test our scheme under realistic conditions, the channel coefficients are created by using the urban micro scenario of [138]. We do not regard shadowing effects in our simulations to avoid that the simulation results are dominated by a few runs of deep fading that

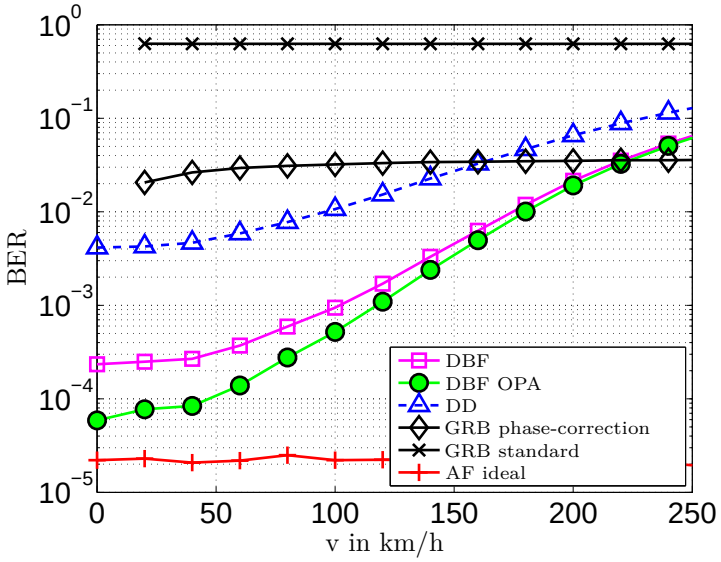

Figure 7.2: BER versus velocity v for differential and non-differential schemes using QPSK in an urban micro scenario, $P = 17$dBm.

are caused by the strong fluctuations in the channel strengths. The following system parameters are chosen according to the simulation requirements used in 3gpp for the LTE standard [2]. The system operates at a carrier frequency of 1800 MHz and we set $T_S = 66.7\mu$sec as the symbol duration and the duration of one time slot. Then, the bandwidth is given by $1/T_S$ which corresponds to the bandwidth of a subcarrier in a multi-carrier LTE system. Our simulation results are averaged over 20000 runs and each simulation run comprises $M = 300$ transmission blocks.

We compare the DBF scheme ("DBF") with the ideal AF relaying scheme ("AF ideal"), the ideal AF relaying scheme where P_{T} is scaled such that the SNR at terminal $\mathcal{T}_2$ is halved ("AF ideal, SNR$^\star(2)/2$"), the distributed differential (DD) scheme of [123] ("DD"), where every relay transmits with the power P/R, and the general rank beamforming (GRB) scheme proposed in [133]. The GRB scheme is suitable for time-variant channels as it does not use the instantaneous CSI. In the GRB scheme, beamformers are designed based on the channel covariance matrices corresponding to $\mathbf{f}$ and $\mathbf{g}$. In practice, the channel covariance matrices are estimated by using training symbols. In the simulations, we use $1/(4M)\sum_{m=1}^{M}\sum_{t=1}^{4}\mathbf{f}(m,t)\mathbf{f}^H(m,t)$ and $1/(4M)\sum_{m=1}^{M}\sum_{t=1}^{4}\mathbf{g}(m,t)\mathbf{g}^H(m,t)$ as estimates of the channel covariance matrices where $\mathbf{f}_{m,t}$ and $\mathbf{g}_{m,t}$ denote channel vectors in the tth time slot of the nth transmission block for the channels between terminal $\mathcal{T}_1$ and the relay and between the relay and terminal $\mathcal{T}_2$, respectively. Note that the GRB scheme does not explicitly regard a phase correction in the desired signal at the terminals. We examine the GRB scheme

of [133] without correcting a phase shift ("GRB standard") and the GBR scheme where terminals know and correct the phase shift perfectly ("GRB phase-correction"). Moreover, we compare our results to the DBF scheme with OPA ("DBF OPA") where P_{T} is divided by solving (7.26) via grid search. To model time-variant channels we consider motion of the terminals with different velocities v including the case of $v = 0$ km/h in which the channels remain constant. As the GRB scheme for constant channels leads to the ideal AF relaying scheme, we regard the GRB scheme if $\mathrm{v} > 0$ km/h.

Fig. 7.1 depicts the BER at terminal $\mathcal{T}_2$ versus P for v = 0 km/h and, therefore, for time-invariant channels. The proposed DBF scheme achieves the performance of the ideal AF relaying scheme at $\mathrm{SNR}^{\star}(2)/2$ which confirms the theoretical result of (7.31). The approximation of (7.31) is highly accurate, especially for $P > 5$dBm. For time-variant channels, the DBF scheme outperforms the GRB scheme with perfect phase correction at velocities below 220 km/h, see Fig. 7.2. The GRB scheme without phase correction is not practical. From Fig. 7.1 and Fig. 7.2, we observe that the centralized DBF scheme offers significant performance gains compared with the DD system. Moreover, the DBF scheme with OPA performs slightly better than the DBF scheme with constant power allocation.

7.6 Conclusion

In this chapter, we have introduced a novel DBF scheme for the bi-directional communication between two terminals via a multi-antenna relay. The scheme does not require CSI at any node in the network and it is therefore particularly suitable for environments with time-variant channels. For time-invariant channels, we have shown that the performance of the DBF scheme degrades by approximately 3dB compared with the ideal AF relaying scheme which requires perfect knowledge of the CSI. In the simulations, this analytical result is highly accurate for transmit powers above 5dBm. For time-variant channels, the simulation results demonstrate that the proposed scheme dramatically outperformed the covariance based beamforming scheme of the literature for velocities below 220 km/h.

Chapter 8

Conclusions and future work

In this thesis, novel schemes for relaying have been developed. In particular, novel schemes for one- and bi-directional relaying for single-user communication, multi-user p2p communication, multi-user downlink transmissions and multicasting have been proposed. Conclusions are drawn in Section 8.1 and an outlook on future work is given in Section 8.2.

8.1 Conclusions

One-directional relaying schemes were developed in Chapter 3 and 4.

In Chapter 3, we developed novel FF relaying schemes in environments with frequency-selective channels. Two multi-user scenarios were considered. First, we regarded the multi-user downlink scenario, where a single source transmits individual messages to several destinations via FF relays. The second scenario was a multi-user p2p relaying scenario that can be regarded as a special case of the multi-user downlink scenario. In both scenarios, FF relaying substantially improved the system performance compared with AF relaying, especially for large relay filter lengths. To avoid communication overhead, however, small relay filter lengths are desirable. In the multi-user downlink scenario, large filter lengths at the relays could be avoided by using precoding at the source.

To compute relay filter coefficients for p2p relaying, we applied SDR-based optimization methods which yielded in most of the simulation scenarios the optimum solution to the power minimization and SINR maximization problems. The latter optimization method is an outer approximation technique that replaces the original variable vector of QCQPs by a positive definite matrix and is especially powerful if the number of constraints is small. A drawback of the SDR technique is that the SDR solution matrix is only feasible for the original problem if its rank is one. Otherwise, the

SDR some provides only a bound to the optimum value of the QCQP.

In the FF multiuser downlink scenario, the mathematical optimization was more complicated compared with the p2p scenario as the optimization included not only relay but also source and destination filter coefficients. To solve the highly non-linear problem to maximize the minimum SINR, we proposed an alternating algorithm. The latter algorithm aims to optimize one set of filter coefficients after another. As the respective optimization problems are non-convex and therefore still difficult to solve directly, we propose to use an inner approximation method. The key idea of the latter CCCP approach was to decompose the non-convex constraint functions into convex and a concave functions. Then, an inner approximation is obtained by linearization of the concave functions. The proposed alternating algorithm is generally suboptimal as it does not consider the joint optimization of all filter coefficients but has the property to improve the minimum SINR in each iteration. Note that embedding the SDR method in an alternating algorithm is difficult since it is not guaranteed to obtain a feasible rank-one solution matrix in every run. In this case, even though it is possible to create feasible (but non optimum) points via randomization methods, improving the target function cannot be ensured.

In Chapter 4, we developed a novel rank-two beamforming technique for which SDR solution matrices with rank one and two are feasible. In the proposed AF single group multicasting scheme, two two different weight vectors are used to increase the degrees of freedom with respect to the rank-one multicasting scheme of the literature that uses a single weight vector. The goal was to choose the proper relay weights and the ideal power allocation in the network to maximize the minimum SNR at the destinations. We combined the SDR method with a 2D search to find optimum power allocation. As the latter technique is computationally costly, we proposed a CCCP-based iterative algorithm. This algorithm is faster than the SDR-based algorithm and yields a performance close to the theoretical upper bound. For a high number of destinations, the SDR solution matrices tend to have a rank higher than two and the CCCP algorithm performs better than the SDR-based algorithm. Comparing the proposed rank-two multicasting scheme with the rank-one scheme of the literature, simulation results demonstrated that the increased number of degrees of freedom substantially improved the system performance.

Bi-directional relaying schemes were investigated in Chapters 5–7. In Chapter 5, we compared different bi-directional AF schemes for a single user pair to the one-directional AF relaying scheme. In the analysis it was shown that the maximum rate of the two time slot scheme was approximately twice the rate of the one-directional scheme. Furthermore, the two time slot scheme outperformed

the bi-directional schemes with three and four time slots.

In Chapter 6, we generalized the bi-directional scheme with two time slots for a single user pair to a TDMA scheme with multiple user pairs, using two or more time slots. To compute the relay weights, we proposed an iterative algorithm. The simulation results demonstrated that the system throughput was substantially dependent on the choice of the TDMA scheme. We proposed an algorithm based on inner approximations that offers a better performance than the SDR-based algorithm and close to the theoretical upper bound. Therefore, we cannot expect that higher rank beamforming schemes lead to substantial improvements.

For a large number of users, MUI excessively impairs the communication. In this case, it is desirable to separate the various transmit signals not only in the spatial domain by using beamforming but also in the time domain by using multiple access schemes. The proposed algorithm can be seen as an earlier version of the CCCP-based algorithm of Chapter 4 and uses a coarser inner approximation.

From the results on inner and outer approximation methods, we can conclude:

- The SDR-method is especially suitable in scenarios where the arising optimization problems have the QCQP structure and the number of users and consequently, the number of QoS constraints, is small. Then, the SDR solution is highly likely to be feasible.
- For the traditional (rank-one) beamforming methods, the SDR solution matrix is only feasible if its rank is one. The feasibility range can however be increased by applying rank-two beamforming methods for which also rank-two matrices are feasible.
- In the case of single-group multicasting, where relay and destination noise is the only impairment of the communication, higher rank beamforming methods can substantially improve the system performance if the number of users is high. This is true for both inner and outer approximation methods.
- Inner approximation methods perform better than the SDR method if the rank of the solution matrices is high. Typically this is the case if the number of users is high.
- The number of variables for the SDR method is roughly squared, which leads to higher computational cost compared with inner approximation methods. Inner approximations keep the number of variables.
- Inner approximation methods are more flexible as compared with the SDR method which addresses QCQPs. The extension to more general optimization problems is generally possible

but leads to additional computational complexity. In contrast, inner approximation methods can be directly applied to the much more general form of optimization problems referred to as DC problems. Moreover, inner approximation methods can easily be embedded in alternating algorithms where the optimization variables are divided into subsets and the subsets are updated one after another.

- In scenarios where MUI occurs, inner approximation methods combined with rank-one beamforming yield a performance close to the theoretical bound obtained by SDR if the number of users is low. In these scenarios, the performance of a relaying scheme cannot be substantially improved by using higher rank beamforming schemes. For high user numbers, the parallel communication of all users is not practical. To avoid strong MUI, it is therefore necessary to separate the various signals by TDMA and frequency division multiple access schemes.

In Chapter 7, we proposed a novel DBF scheme for bi-directional multi-antenna relaying of one user pair. The scheme does not require explicit CSI, is easy to implement and robust to time selective channels. However, this scheme cannot be easily extended to multiple user pairs.

8.2 Future work

In Chapters 3–6, it was assumed that the full CSI is available at one processing node in the considered network. The processing node uses the CSI to compute the variables such as weight coefficients and transmit power of the respective transceiver. The drawback of this approach is the costly acquisition of CSI at the processing node which requires the estimation of the channel coefficients and feedback channels. Moreover, the computation of the variables requires processing power and each variable needs to be communicated to its respective node. Differential techniques, such as the DBF scheme in Chapter 7, do not need to estimate or to communicate CSI and there is no processing node in the network. Due to the simplicity of differential schemes, it is therefore desirable to develop differential counterparts to already existing relaying schemes that require CSI.

We can identify the following challenges in differential relaying that have not been addressed in the thesis and in the current literature.

- *Differential techniques for multi-user scenarios.* The challenge is to avoid MUI by separating signals without knowing their spatial signature. Differential schemes for multi-user scenarios are desirable as the number of channels that have to be estimated and communicated grows

with the number of users. Consequently, the overhead to communicate the CSI to a processing node is high if the number of users is large. One promising candidate for a generalization of the proposed DBF scheme to the multi-user case is the bi-directional multi-user p2p scheme of Chapter 6. Especially, TDMA can be exploited to separate different signals in the time domain.

- *Differential techniques for bi-directional relaying in two and three time slot schemes.* To increase the spectral efficiency it is desirable to adapt the four time slot DBF scheme to two or three time slots. The adaptation to the three time slot scheme is straightforward, however, the adaptation to the two time slot scheme is challenging.

- *Low complexity algorithms for relay network optimization.* Even though the proposed iterative algorithms of Chapters 3.2, 4 and 6, provide a high performance, a nonlinear optimization problem has to be solved in every iteration. To reduce the computational burden, it is possible to use inaccurate solutions in each iteration as it has been proposed in [103] for power minimization. For max-min fairness beamforming in the context of multi-antenna relaying, it has been proposed to use the Levenberg-Marquardt method in every step of an iterative algorithm [70].

Appendix A

DC programming theorem

Let us derive the following theorem on iterative approximations in DC programming. For further information on DC programming see [140]–[144] and references therein.

Consider the optimization problem

$$\min_{\mathbf{x}} \Phi_0(\mathbf{x}) \quad \text{s.t.} \quad \Phi_m(\mathbf{x}) \leq 0, m = 1, \ldots, M, \tag{A.1}$$

where $\mathbf{x}$ is the vector of variables, $\Phi_0(\mathbf{x})$ is the objective function and $\Phi_m(\mathbf{x})$ are the constraint functions. It is assumed that the objective function and the constraint functions are the difference of two convex functions such that $\Phi_m(\mathbf{x}) = \Lambda_m(\mathbf{x}) - \Psi_m(\mathbf{x}), \quad m = 1, \ldots, M$, where $\{\Lambda_m(\mathbf{x})\}_{m=0}^{M}$ and $\{\Psi_m(\mathbf{x})\}_{m=0}^{M}$ are convex functions and $\{\Psi_m(\mathbf{x})\}_{m=0}^{M}$ are two times continuously differentiable.

Let us assume that $\mathbf{x}_0$ is feasible for the problem in (A.1) and let us rewrite the original optimization problem into the equivalent optimization problem

$$\min_{\Delta\mathbf{x}} \Phi_0(\mathbf{x}_0 + \Delta\mathbf{x}) \quad \text{s.t.} \quad \Phi_m(\mathbf{x}_0 + \Delta\mathbf{x}) \leq 0, \quad m = 1, \ldots, M, \tag{A.2}$$

where $\Delta\mathbf{x}$ is the new vector of variables and $\mathbf{x}_0$ is fixed. The problem in (A.2) is approximated by the convex problem

$$\min_{\Delta\mathbf{x}} \hat{\Phi}_0(\mathbf{x}_0 + \Delta\mathbf{x}) \quad \text{s.t.} \quad \hat{\Phi}_m(\mathbf{x}_0 + \Delta\mathbf{x}) \leq 0, \quad m = 1, \ldots, M, \tag{A.3}$$

where the approximated functions are given by

$$\hat{\Phi}_m(\mathbf{x}_0 + \Delta\mathbf{x}) = \Lambda_m(\mathbf{x}_0 + \Delta\mathbf{x}) - \Psi_m(\mathbf{x}_0) - [\nabla\Psi_m(\mathbf{x}_0)]\,\Delta\mathbf{x}, \tag{A.4}$$

where $[\nabla\Psi_m(\mathbf{x}_0)]$ is the gradient of Ψ_m at $\mathbf{x}_0$. $\hat{\Phi}_m(\mathbf{x}_0+\Delta\mathbf{x})$ is convex, as it is the summation of the convex function Λ_m, the constant $-\Psi_m(\mathbf{x}_0)$ and the (convex) linear term $-[\nabla\Psi_m(\mathbf{x}_0)]\,\Delta\mathbf{x}$. Note that in (A.4), Ψ_m has been replaced by its first order Taylor approximation.

DC Programming Theorem 5. *Let $\mathbf{x}_0$ be feasible for (A.2). Then there is a feasible solution $\Delta\mathbf{x}^\star$ for (A.3) and $\mathbf{x}=\mathbf{x}_0+\Delta\mathbf{x}^\star$ is feasible for (A.2) and $\Phi_0(\mathbf{x}_0+\Delta\mathbf{x}^\star)\leq\Phi_0(\mathbf{x}_0)$.*

Proof. The existence of a solution $\Delta\mathbf{x}^\star$ is guaranteed as $\Delta\mathbf{x}=\mathbf{0}$ is feasible for (A.3).

We prove

$$\Phi_m(\mathbf{x}_0+\Delta\mathbf{x})\leq\hat{\Phi}_m(\mathbf{x}_0+\Delta\mathbf{x}) \tag{A.5}$$

for $m=0,1,\ldots,M$. From (A.5), it follows feasibility for any solution $\Delta\mathbf{x}^\star$ of (A.3) to (A.2) since $\Phi_m(\mathbf{x}_0+\Delta\mathbf{x}^\star)\leq\hat{\Phi}_m(\mathbf{x}_0+\Delta\mathbf{x}^\star)\leq 0$. From (A.5) it follows $\Phi_0(\mathbf{x}_0+\Delta\mathbf{x}^\star)\leq\hat{\Phi}_0(\mathbf{x}_0+\Delta\mathbf{x}^\star)\leq\hat{\Phi}_0(\mathbf{x}_0)=f_0(\mathbf{x}_0)$ and $\Phi_0(\mathbf{x}_0+\Delta\mathbf{x}^\star)\leq\Phi_0(\mathbf{x}_0)$.

We prove (A.5), using Taylor's theorem. According to Taylor's theorem there is a $t\in[0,1]$ such that

$$\Psi_m(\mathbf{x}_0+\Delta\mathbf{x})=\Psi_m(\mathbf{x}_0)+[\nabla\Psi_m(\mathbf{x}_0)]\,\Delta\mathbf{x}+1/2\Delta\mathbf{x}^T\left[\nabla^2\Psi_m(\mathbf{x}_0+t\Delta\mathbf{x})\right]\Delta\mathbf{x},$$

where $\left[\nabla^2\Psi_m(\mathbf{x}_0+t\Delta\mathbf{x})\right]$ is the Hessian matrix of Ψ_m at $\mathbf{x}_0+t\Delta\mathbf{x}$. Due to the convexity, the Hessian is positive semidefinite for any t and $\Delta\mathbf{x}^T\left[\nabla^2\Psi_m(\mathbf{x}_0)+t\Delta\mathbf{x}\right]\Delta\mathbf{x}\geq 0$. Therefore

$$\begin{aligned}
\Phi_m(\mathbf{x}_0+\Delta\mathbf{x}^\star)&=\Lambda_m(\mathbf{x}_0+\Delta\mathbf{x}^\star)-\Psi_m(\mathbf{x}_0+\Delta\mathbf{x}^\star)\\
&=\Lambda_m(\mathbf{x}_0+\Delta\mathbf{x}^\star)-\Psi_m(\mathbf{x}_0)-[\nabla\Psi_m(\mathbf{x}_0)]\,\Delta\mathbf{x}^\star\\
&\quad -1/2(\Delta\mathbf{x}^\star)^T\left[\nabla^2\Psi_m(\mathbf{x}_0)+t\Delta\mathbf{x}^\star\right]\Delta\mathbf{x}^\star\\
&\leq\Lambda_m(\mathbf{x}_0+\Delta\mathbf{x}^\star)-\Psi_m(\mathbf{x}_0)-[\nabla\Psi_m(\mathbf{x}_0)]\,\Delta\mathbf{x}^\star\\
&=\hat{\Phi}_m(\mathbf{x}_0+\Delta\mathbf{x}^\star),
\end{aligned}$$

and (A.5) follows.

□

From inequality (A.5) it follows that the approximation by replacing the problem in (A.2) by the problem in (A.3) is an *inner approximation* as the set relation

$$\{\Delta\mathbf{x}|\hat{\Phi}_m(\mathbf{x}_0+\Delta\mathbf{x})\leq 0\}\subset\{\Delta\mathbf{x}|\Phi_m(\mathbf{x}_0+\Delta\mathbf{x})\leq 0\}$$

holds true. Therefore the feasible set of (A.3) is a subset of (A.2).

Appendix B

Convolution matrices

Consider an FIR multiple-input-multiple-output (MIMO) system where $\mathbf{x}(n)$ is the $N \times 1$ input vector and $\mathbf{y}(n)$ is the $M \times 1$ output vector in time n. Let $\mathbf{H}_l$, $l = 0, \ldots, L-1$, the lth filter matrix such that

$$\mathbf{y}(n) = \sum_{l=0}^{L-1} \mathbf{H}_l \mathbf{x}(n-l).$$

This equation can be equivalently formulated as

$$\mathbf{y}(n) = \mathbf{H}\tilde{\mathbf{x}}(n),$$

where $\mathbf{H} = [\mathbf{H}_0, \mathbf{H}_1, \ldots, \mathbf{H}_{L-1}]$ and $\tilde{\mathbf{x}}(n) = [\mathbf{x}^T(n), \ldots, \mathbf{x}^T(n-L+1)]^T$.

Let $\mathbf{K}_l$, $l = 0, \ldots, L-1$, be the filter matrices of a second FIR MIMO system such that

$$\mathbf{z}(n) = \sum_{l=0}^{L-1} \mathbf{K}_l \mathbf{y}(n-l) = \mathbf{K}\tilde{\mathbf{y}}(n),$$

where $\mathbf{y}(n)$ is the $M \times 1$ input vector and $\mathbf{z}(n)$ is the $Q \times 1$ output vector in time slot n and where $\mathbf{K} = [\mathbf{K}_0, \ldots, \mathbf{K}_{L-1}]$ and $\tilde{\mathbf{y}}(n) = [\mathbf{y}^T(n), \ldots, \mathbf{y}^T(n-L+1)]^T$.

Consider that the second MIMO system with channel matrix $\mathbf{K}$ is affiliated to the first MIMO system with channel matrix $\mathbf{H}$. We want a simple input-output relationship of the output vector $\mathbf{z}(n)$ and the input vectors $\mathbf{x}(n), \ldots, \mathbf{x}(n-2L+2)$.

Let us define the $LM \times N(2L-1)$ block Toeplitz matrix $\underline{\mathbf{H}}_{(L,N)}$ where use the definitions

$$\underline{\mathbf{H}}_{(L,N)} = [\tilde{\mathbf{H}}_0^T, \ldots, \tilde{\mathbf{H}}_{L-1}^T]^T, \tag{B.1a}$$

$$\tilde{\mathbf{H}}_l = [\mathbf{0}_{M \times lN}, \mathbf{H}, \mathbf{0}_{M \times (L-l-1)N}]. \tag{B.1b}$$

Let $\hat{\mathbf{x}}(n) = [\mathbf{x}^T(n), \ldots, \mathbf{x}^T(n - 2L_k + 2)]^T$, then

$$\mathbf{z}(n) = \mathbf{K}\underline{\mathbf{H}}_{(L,N)}\hat{\mathbf{x}}(n) \tag{B.2}$$

holds true. We remark that there is the selection matrix $\mathbf{Z}_{(L,N,M)}$ that relates the vectorization of the matrix $\mathbf{H}$ to the vectorization of the corresponding convolution matrix $\underline{\mathbf{H}}_{(L,N)}$ of (B.1) such that

$$\mathrm{vec}\{\underline{\mathbf{H}}_{(L,N)}\} = \mathbf{Z}_{(L,N,M)}\mathrm{vec}\{\mathbf{H}\} \tag{B.3}$$

where

$$\mathbf{Z}_{(L,N,M)} = [\mathbf{Z}_1^T, \mathbf{Z}_2^T, \ldots, \mathbf{Z}_{(2L-1)N}^T]^T, \tag{B.4a}$$

$$\mathbf{Z}_k = [\mathbf{Z}_{k,0}^T, \mathbf{Z}_{k,1}^T, \ldots, \mathbf{Z}_{k,L-1}^T]^T, \quad k = 1, 2, \ldots, (2L-1)N, \tag{B.4b}$$

$$\mathbf{Z}_{k,l} = (\mathbf{I}_M \otimes \tilde{\mathbf{Z}}_{k,l}), \quad k = 1, 2, \ldots, (2L-1)N, \quad l = 0, 1, \ldots, L-1, \tag{B.4c}$$

$$\tilde{\mathbf{Z}}_{k,l} = [\delta(k - lN - 1), \delta(k - lN - 2), \ldots, \delta(k - lN - (NL))],$$
$$k = 1, 2, \ldots, (2L-1)N, \quad l = 0, 1, \ldots, L-1. \tag{B.4d}$$

Let

$$\mathbf{K} \triangleq \mathbf{k}^T \tag{B.5}$$

be the $1 \times LM$ channel matrix of an FIR MISO system, $Q = 1$. We are interested in an equivalent representation of (B.2) that depends on the vectorization of $\mathbf{H}$. Then, from the identity

$$\mathbf{k}^T\underline{\mathbf{H}}_{(L,N)} = \mathrm{vec}^T\{\underline{\mathbf{H}}_{(L,N)}\}\left(\mathbf{I}_{N(2L-1)} \otimes \mathbf{k}\right) = \mathrm{vec}\{\mathbf{H}\}^T\mathbf{Z}_{(L,N,M)}^T\left(\mathbf{I}_{N(2L-1)} \otimes \mathbf{k}\right),$$

and using the definition of

$$\overline{\mathbf{k}}_{(L,N)} \triangleq \mathbf{Z}_{(L,N,M)}^T\left(\mathbf{I}_{N(2L-1)} \otimes \mathbf{k}\right) \tag{B.6}$$

it can readily be verified that

$$\mathbf{k}^T\underline{\mathbf{H}}_{(L,N)} = \mathrm{vec}^T\{\mathbf{H}\}\overline{\mathbf{k}}_{(L,N)}. \tag{B.7}$$

Then from (B.2), (B.5) and (B.7) follows

$$\mathbf{z}(n) = \mathbf{K}\underline{\mathbf{H}}_{(L,N)}\hat{\mathbf{x}}(n) = \mathbf{k}^T\underline{\mathbf{H}}_{(L,N)}\hat{\mathbf{x}}(n) = \mathrm{vec}^T\{\mathbf{H}\}\overline{\mathbf{k}}_{(L,N)}\hat{\mathbf{x}}(n).$$

Let us furthermore assume that $M = N = R \cdot N_R$ and that the matrices
$\mathbf{H}_l = \mathrm{blkdiag}([\mathbf{H}_{1,l}^H, \ldots, \mathbf{H}_{R,l}^H])$, $l = 0, \ldots, L-1$, have a block diagonal structure, where $\mathbf{H}_{r,l}$, $r = 1, \ldots, R$, are $N_R \times N_R$ matrices. Let us define

$$\mathbf{h} = [\mathbf{h}_0^T, \ldots, \mathbf{h}_{L-1}^T]^T,$$
$$\mathbf{h}_l = [\mathrm{vec}\{\mathbf{H}_{1,l}^T\}^T, \ldots, \mathrm{vec}\{\mathbf{H}_{R,l}^T\}^T]^T$$

then

$$\text{vec}^T\{\mathbf{H}\} = \mathbf{h}^H \mathbf{T}_{(L,R,N_R)}, \tag{B.8}$$

where

$$\mathbf{T}_{(L,R,N_R)} = [\hat{\mathbf{I}}_0, \hat{\mathbf{I}}_1, \ldots, \hat{\mathbf{I}}_{L-1}], \tag{B.9a}$$

$$\hat{\mathbf{I}}_l = [\mathbf{0}^T_{lRN_R^2, R^2N_R^2}, \tilde{\mathbf{I}}^T, \mathbf{0}^T_{(L-l-1)RN_R^2, R^2N_R^2}]^T, \tag{B.9b}$$

$$\tilde{\mathbf{I}} = [\tilde{\mathbf{I}}_1^T, \tilde{\mathbf{I}}_2^T, \ldots, \tilde{\mathbf{I}}_R^T]^T, \tag{B.9c}$$

$$\tilde{\mathbf{I}}_r = [\Big(\mathbf{e}_r^T \otimes \Big((\mathbf{I}_{N_R} \otimes \mathbf{e}_r^T) \otimes \mathbf{I}_{N_R}\Big)\Big)]^T. \tag{B.9d}$$

Appendix C

Power and matrix calculation

C.1 Power and matrix calculation for Chapter 3

C.1.1 Relay transmit power as a function of the filter weight vector

Using (3.13) - (3.20), the power $\tilde{p}_q$ transmitted at the qth relay antenna is given by

$$\begin{aligned}\tilde{p}_q &= \mathrm{E}\left\{|t_q(n)|^2\right\} \\ &= \mathrm{E}\left\{\mathbf{e}_q^T\left(\mathbf{W}\mathbf{F}_{\mathfrak{W}}\mathbf{v}_{\mathfrak{W}}(n)\right)\left(\mathbf{W}\mathbf{F}_{\mathfrak{W}}\mathbf{v}_{\mathfrak{W}}(n)\right)^H\mathbf{e}_q\right\} \\ &\quad +\mathrm{E}\left\{\mathbf{e}_q^T\mathbf{W}\boldsymbol{\eta}_{\mathfrak{W}}(n)\left(\boldsymbol{\eta}_{\mathfrak{W}}(n)\right)^H\mathbf{W}^H\mathbf{e}_q\right\}. \end{aligned} \tag{C.1}$$

The power p_r transmitted at relay $\mathcal{R}_r$ is given by

$$p_r = \sum_{q=(r-1)N_R+1}^{rN_R}\tilde{p}_q. \tag{C.2}$$

using the identity $\mathbf{e}_q^T\mathbf{W} = \mathrm{vec}(\mathbf{W})\left(\mathbf{I}_{RN_RL_w}\otimes\mathbf{e}_q\right)$, equations (3.15), (3.16), (3.50), (3.51), and using the definition of $\mathbf{T}_{(L_w,R,N_R)}$ according to (B.9) such that
$\mathrm{vec}^T(\mathbf{W}) = \mathbf{w}^H\mathbf{T}_{(L_w,R,N_R)}$, we have

$$\mathbf{e}_q^T\mathbf{W} = \mathbf{w}^H\mathbf{T}_{(L_w,R,N_R)}\left(\mathbf{I}_{RN_RL_w}\otimes\mathbf{e}_q\right). \tag{C.3}$$

Using (C.1) and (C.3), we can express p_r in (C.2) as

$$\begin{aligned} p_r &= \sum_{q=(r-1)N_R+1}^{rN_R} \mathbf{w}^H \Big(\mathbf{T}_{(L_w,R,N_R)} \left(\mathbf{I}_{RN_RL_w} \otimes \mathbf{e}_q \right) \mathbf{F}_{\mathfrak{W}} \Big) \mathbf{C} \Big(\mathbf{T}_{(L_w,R,N_R)} \left(\mathbf{I}_{RN_RL_w} \otimes \mathbf{e}_q \right) \mathbf{F}_{\mathfrak{W}} \Big)^H \mathbf{w} \\ &+ \sum_{q=(r-1)N_R+1}^{rN_R} \sigma^2 \mathbf{w}^H \mathbf{T}_{(L_w,R,N_R)} \left(\mathbf{I}_{RN_RL_w} \otimes \mathbf{e}_q \right) \Big(\left(\mathbf{I}_{RN_RL_w} \otimes \mathbf{e}_q \right) \mathbf{T}_{(L_w,R,N_R)} \Big)^H \mathbf{w}, \end{aligned} \tag{C.4}$$

where $\mathbf{C} = \mathrm{E}\{\mathbf{v}_{\mathfrak{W}}(n) \left(\mathbf{v}_{\mathfrak{W}}(n)\right)^H\}$ is the covariance matrix of the transmitted source symbols and where the assumption

$$\mathrm{E}\left\{ \boldsymbol{\eta}_{\mathfrak{W}}(n) \left(\boldsymbol{\eta}_{\mathfrak{W}}(n)\right)^H \right\} = \sigma^2 \mathbf{I}_{RN_RL_w} \tag{C.5}$$

has been used. The relay sum power P_{R} can then be expressed as

$$P_{\mathrm{R}} = \sum_{r=1}^{R} p_r = \mathbf{w}^H \left(\sum_{r=1}^{R} \mathbf{D}_r \right) \mathbf{w} = \mathbf{w}^H \mathbf{D} \mathbf{w}, \tag{C.6}$$

where

$$\begin{aligned} \mathbf{D}_r &\triangleq \sum_{q=(r-1)N_R+1}^{rN_R} \Big(\mathbf{T}_{(L_w,R,N_R)} \left(\mathbf{I}_{RN_RL_w} \otimes \mathbf{e}_q \right) \mathbf{F}_{\mathfrak{W}} \Big) \mathbf{C} \Big(\mathbf{T}_{(L_w,R,N_R)} \left(\mathbf{I}_{RN_RL_w} \otimes \mathbf{e}_q \right) \mathbf{F}_{\mathfrak{W}} \Big)^H \\ &+ \sum_{q=(r-1)N_R+1}^{rN_R} \sigma^2 \mathbf{T}_{(L_w,R,N_R)} \left(\mathbf{I}_{RN_RL_w} \otimes \mathbf{e}_q \right) \Big(\left(\mathbf{I}_{RN_RL_w} \otimes \mathbf{e}_q \right) \mathbf{T}_{(L_w,R,N_R)} \Big)^H, \end{aligned} \tag{C.7}$$

$$\mathbf{D} \triangleq \sum_{r=1}^{R} \mathbf{D}_r. \tag{C.8}$$

and contains the signal covariance matrix given by $\mathbf{C} = \sum_{m=1}^{M} \underline{\mathbf{A}_m}_{(L_w+L-1,1)} \underline{\mathbf{A}_m}_{(L_w+L-1,1)}^H$ due to (3.4) and (3.5).

C.1.2 Relay transmit power as a function of the precoding weights

From (C.1) and (C.2), we have

$$p_{r,\eta} \triangleq \sigma^2 \sum_{q=(r-1)N_R+1}^{rN_R} \mathbf{e}_q^T \mathbf{W} \mathbf{W}^H \mathbf{e}_q, \quad r = 1, \ldots, R. \tag{C.9}$$

Let us define

$$\mathbf{D}_{r,\mathfrak{A}} \triangleq \sum_{q=(r-1)N_R+1}^{rN_R} \mathbf{I}_M \otimes \left(\overline{\mathbf{d}_{q,\mathfrak{A}}}_{(L_w+L-1,1)} \left(\overline{\mathbf{d}_{q,\mathfrak{A}}}_{(L_w+L-1,1)} \right)^H \right), \quad r = 1, \ldots, R, \tag{C.10}$$

$$\mathbf{d}_{q,\mathfrak{A}} \triangleq \mathbf{e}_q^T \mathbf{W} \mathbf{F}_{\mathfrak{W}}, \quad q = 1, \ldots, N_R R. \tag{C.11}$$

Note that in (C.10), we have defined $\overline{\mathbf{d}_{q,\mathfrak{A}}}_{(L_w+L-1,1)}$ according to (B.6) to exploit the identity

$$\mathbf{e}_q^T\mathbf{W}\mathbf{F}_{\mathfrak{W}}\mathbf{A}_{m,\mathfrak{W}} = \mathbf{e}_q^T\mathbf{W}\mathbf{F}_{\mathfrak{W}}\underline{\mathbf{A}_m}_{(L_w+L-1,1)} = \mathbf{a}_m^H\overline{\mathbf{d}_{q,\mathfrak{A}}}_{(L_w+L-1,1)}, \tag{C.12}$$

which follows from (B.7). Then, recalling (C.1) and (C.2) and using the definitions (3.47), (3.48), and (C.11), equation (3.52) follows from (C.12).

C.1.3 Covariance matrices for the destination filter weights

For convenience, let us define $\mathbf{S}_{m,k,\mathfrak{U}} \triangleq \mathbf{G}_{m,\mathfrak{U}}\mathbf{W}_{\mathfrak{U}}\mathbf{F}_{\mathfrak{U}}\mathbf{A}_{k,\mathfrak{U}}$ and

$$\mathbf{h}_{m,\mathfrak{U}} \triangleq \left[\mathbf{S}_{m,m,\mathfrak{U}}\right]_{:,L_u}, \quad m = 1,\ldots,M, \tag{C.13}$$

$$\mathbf{Q}_{m,\mathfrak{U}} \triangleq \mathbf{Q}_{m,\mathrm{ISI},\mathfrak{U}} + \mathbf{Q}_{m,\mathrm{MUI},\mathfrak{U}} + \mathbf{Q}_{m,\mathrm{N},\mathfrak{U}}, \quad m = 1,\ldots,M, \tag{C.14}$$

$$\mathbf{Q}_{m,\mathrm{ISI},\mathfrak{U}} \triangleq \mathbf{S}_{m,m,\mathfrak{U}}\check{\mathbf{E}}_{L_u}\mathbf{S}_{m,m,\mathfrak{U}}^H, \quad m = 1,\ldots,M, \tag{C.15}$$

$$\mathbf{Q}_{m,\mathrm{MUI},\mathfrak{U}} \triangleq \sum_{k=1,k\neq m}^{M} \mathbf{S}_{m,k,\mathfrak{U}}\mathbf{S}_{m,k,\mathfrak{U}}^H, \quad m = 1,\ldots,M, \tag{C.16}$$

$$\mathbf{Q}_{m,\mathrm{N},\mathfrak{U}} \triangleq \sigma^2\left(\mathbf{G}_{m,\mathfrak{U}}\mathbf{W}_{\mathfrak{U}}\right)\left(\mathbf{G}_{m,\mathfrak{U}}\mathbf{W}_{\mathfrak{U}}\right)^H + \sigma^2\mathbf{I}_{L_u}, \quad m = 1,\ldots,M. \tag{C.17}$$

Then, inserting (C.13) - (C.17) in (3.41) - (3.45), we have $\mathrm{E}\{|z_{m,\mathrm{S}}|^2\} = |\mathbf{u}_m^H\mathbf{h}_{m,\mathfrak{U}}|^2$, $\mathrm{E}\{|z_{m,\mathrm{ISI}}|^2\} = \mathbf{u}_m^H\mathbf{Q}_{m,\mathrm{ISI},\mathfrak{U}}\mathbf{u}_m$, $\mathrm{E}\{|z_{m,\mathrm{MUI}}|^2\} = \mathbf{u}_m^H\ \mathbf{Q}_{m,\mathrm{MUI},\mathfrak{U}}\mathbf{u}_m$, and $\mathrm{E}\{|z_{m,\mathrm{N}}|^2\} = \mathbf{u}_m^H\ \mathbf{Q}_{m,\mathrm{MUI},\mathfrak{N}}\mathbf{u}_m$.

C.1.4 Covariance matrices for the precoding filter weights

Making use of (B.6) to define $\overline{(\mathbf{u}_m^H\mathbf{G}_{m,\mathfrak{U}}\mathbf{W}_{\mathfrak{U}}\mathbf{F}_{\mathfrak{U}})^T}_{(L_u+L_w+2L-4,1)}$, we introduce the compact notation

$$\mathbf{S}_{m,\mathfrak{U}} \triangleq \overline{(\mathbf{u}_m^H\mathbf{G}_{m,\mathfrak{U}}\mathbf{W}_{\mathfrak{U}}\mathbf{F}_{\mathfrak{U}})^T}_{(L_u+L_w+2L-4,1)} \tag{C.18}$$

$$\tilde{\mathbf{h}}_{m,\mathfrak{A}} \triangleq \left[\mathbf{S}_{m,\mathfrak{A}}\right]_{:,L_u}, \tag{C.19}$$

$$\mathbf{h}_{m,\mathfrak{A}} \triangleq [\mathbf{0}_{(m-1)N_SL_a}^T, \tilde{\mathbf{h}}_{m,\mathfrak{A}}^T, \mathbf{0}_{(M-m)N_SL_a}^T]^T, \tag{C.20}$$

$$\tilde{\mathbf{Q}}_{m,\mathrm{ISI},\mathfrak{A}} \triangleq \mathbf{S}_{m,\mathfrak{A}}\check{\mathbf{E}}_{L_u}\mathbf{S}_{m,\mathfrak{A}}^H, \tag{C.21}$$

$$\tilde{\mathbf{Q}}_{m,\mathrm{MUI},\mathfrak{A}} \triangleq \mathbf{S}_{m,\mathfrak{A}}\mathbf{S}_{m,\mathfrak{A}}^H, \tag{C.22}$$

$$\mathbf{Q}_{m,\mathfrak{A}} \triangleq \mathrm{blkdiag}([\underbrace{\tilde{\mathbf{Q}}_{m,\mathrm{MUI},\mathfrak{A}},\ldots,\tilde{\mathbf{Q}}_{m,\mathrm{MUI},\mathfrak{A}}}_{m-1\text{ blocks}}, \tilde{\mathbf{Q}}_{m,\mathrm{ISI},\mathfrak{A}}\ \underbrace{\tilde{\mathbf{Q}}_{m,\mathrm{MUI},\mathfrak{A}},\ldots,\tilde{\mathbf{Q}}_{m,\mathrm{MUI},\mathfrak{A}}}_{M-m\text{ blocks}}]), \tag{C.23}$$

$$\sigma_{m,\mathfrak{A}}^2 \triangleq \mathrm{E}\{|z_{m,\mathrm{N}}|^2\}. \tag{C.24}$$

Applying the identity

$$\mathbf{q}_{m,k}^H = \mathbf{a}_k^H\mathbf{S}_{m,\mathfrak{A}} \tag{C.25}$$

which follows from (3.3), (3.31), (3.47), (C.18) and (B.7) and using the definitions (3.40) - (3.45), (3.48), (C.18) - (C.24), we have $\mathrm{E}\{|z_{m,\mathrm{S}}|^2\} = |\mathbf{a}^H\mathbf{h}_{m,\mathfrak{A}}|^2$, $\mathrm{E}\{|z_{m,\mathrm{ISI}}|^2\} = \mathbf{a}^H\,\mathbf{Q}_{m,\mathrm{ISI},\mathfrak{A}}\mathbf{a}$, $\mathrm{E}\{|z_{m,\mathrm{MUI}}|^2\} = \mathbf{a}^H\,\mathbf{Q}_{m,\mathrm{MUI},\mathfrak{A}}\mathbf{a}$, and $\mathrm{E}\{|z_{m,\mathrm{N}}|^2\} = \mathbf{a}^H\,\mathbf{Q}_{m,\mathrm{N},\mathfrak{A}}\mathbf{a}$.

Covariance matrices for the relay filter weights

Let us define

$$\mathbf{h}_{m,\mathfrak{W}} \triangleq [\mathbf{S}_{m,\mathfrak{W}}\mathbf{F}_{\mathfrak{U}}\mathbf{A}_{m,\mathfrak{U}}]_{:,L_u}, \tag{C.26}$$

$$\mathbf{Q}_{m,\mathfrak{W}} \triangleq \mathbf{Q}_{m,\mathrm{ISI},\mathfrak{W}} + \mathbf{Q}_{m,\mathrm{MUI},\mathfrak{W}} + \mathbf{Q}_{m,\mathrm{N},\mathfrak{W}}, \tag{C.27}$$

$$\mathbf{Q}_{m,\mathrm{ISI},\mathfrak{W}} \triangleq \mathbf{S}_{m,\mathfrak{W}}\mathbf{F}_{\mathfrak{U}}\mathbf{A}_{m,\mathfrak{U}}\check{\mathbf{E}}_{L_u}(\mathbf{S}_{m,\mathfrak{W}}\mathbf{F}_{\mathfrak{U}}\mathbf{A}_{m,\mathfrak{U}})^H, \tag{C.28}$$

$$\mathbf{Q}_{m,\mathrm{MUI},\mathfrak{W}} \triangleq \sum_{l=1,l\neq m}^{M} \mathbf{S}_{m,\mathfrak{W}}\mathbf{F}_{\mathfrak{U}}\mathbf{A}_{m,\mathfrak{U}}(\mathbf{S}_{m,\mathfrak{W}}\mathbf{F}_{\mathfrak{U}}\mathbf{A}_{m,\mathfrak{U}})^H, \tag{C.29}$$

$$\mathbf{Q}_{m,\mathrm{N},\mathfrak{W}} \triangleq \sigma^2\mathbf{S}_{m,\mathfrak{W}}\mathbf{S}_{m,\mathfrak{W}}^H, \tag{C.30}$$

$$\mathbf{S}_{m,\mathfrak{W}} \triangleq \mathbf{T}_{(L_w,R,1)}\overline{(\mathbf{u}_m^H\mathbf{G}_{m,\mathfrak{U}})^T}_{(L_u+L-1,N_RR)}, \tag{C.31}$$

we have made use of (B.6) to define $\overline{(\mathbf{u}_m^H\mathbf{G}_{m,\mathfrak{U}})^T}_{(L_u+L-1,N_RR)}$ and (B.9) to define $\mathbf{T}_{(L_w,R,1)}$. Then, the identity

$$\mathbf{w}^H\mathbf{S}_{m,\mathfrak{W}} = \mathbf{u}_m^H\mathbf{G}_{m,\mathfrak{U}}\mathbf{W}_{\mathfrak{U}} \tag{C.32}$$

follows from (3.15), (3.16), (3.51), (3.50), (B.7), and (B.8). Inserting (C.26) - (C.31) in (3.40) - (3.45) and using (C.32), we have $\mathrm{E}\{|z_{m,\mathrm{S}}|^2\} = |\mathbf{w}^H\mathbf{h}_{m,\mathfrak{W}}|^2$, $\mathrm{E}\{|z_{m,\mathrm{ISI}}|^2\} = \mathbf{w}^H\,\mathbf{Q}_{m,\mathrm{ISI},\mathfrak{W}}\mathbf{w}$, $\mathrm{E}\{|z_{m,\mathrm{MUI}}|^2\} = \mathbf{w}^H\,\mathbf{Q}_{m,\mathrm{MUI},\mathfrak{W}}\mathbf{w}$, and $\mathrm{E}\{|z_{m,\mathrm{N}}|^2\} = \mathbf{w}^H\,\mathbf{Q}_{m,\mathrm{N},\mathfrak{W}}\mathbf{w} + \sigma^2$.

C.2 Power and matrix calculation for Chapter 4

Using equations (4.1) and (4.6), the power $p_r(\mathbf{w}, a)$ transmitted at the rth relay in the third time slot can be expressed as

$$\begin{aligned}
p_r(\mathbf{w}, a) &= E\{|t_{3,r}|^2\} \\
&= E\{|\alpha_1 w_{r,1}^* f_r s_1 + w_{r,1}^*\eta_{1,r} + \alpha_1^* w_{2,r}^* f_r^* s_2 + w_{r,2}^*\eta_{2,r}^*|^2\} \\
&= \left(|w_{r,1}|^2 + |w_{r,2}|^2\right)\left(|\alpha_1 f_r|^2 + \sigma_\eta^2\right) \\
&= \tilde{\mathbf{w}}_1^H\tilde{\mathbf{D}}_r\tilde{\mathbf{w}}_1/a + \tilde{\mathbf{w}}_2^H\tilde{\mathbf{D}}_r\tilde{\mathbf{w}}_2/a + \tilde{\mathbf{w}}_1^H\tilde{\mathbf{E}}_r\tilde{\mathbf{w}}_1 + \tilde{\mathbf{w}}_2^H\tilde{\mathbf{E}}_r\tilde{\mathbf{w}}_2 \\
&= \mathbf{w}^H\mathbf{D}_r\mathbf{w}/a + \mathbf{w}^H\mathbf{E}_r\mathbf{w}
\end{aligned} \tag{C.33}$$

where we have used the assumption that the data symbols are mutually uncorrelated with zero mean and unit variance, where for $r = 1, \ldots, R$, the $(R+1) \times (R+1)$ matrices $\tilde{\mathbf{D}}_r$ and $\tilde{\mathbf{E}}_r$ have respectively $|f_r|^2$ and σ_η^2 as their rth diagonal entry and zeros elsewhere and where $\mathbf{D}_r \triangleq \text{blkdiag}([\tilde{\mathbf{D}}_r, \tilde{\mathbf{D}}_r])$ and $\mathbf{E}_r \triangleq \text{blkdiag}([\tilde{\mathbf{E}}_r, \tilde{\mathbf{E}}_r])$. It can be easily seen that for the relay power in the fourth time slot $E\{|t_{4,r}|^2\} = p_r(\mathbf{w}, a)$ holds true. Due to the symmetry in the transmission scheme the relay power in the fourth time slot is equivalent to the relay power in the third time slot, i.e., $p_r(w, a) = E\{t_3, r\} = E\{t_4, r\}$. Hence $p_r(w, a)$ represents the relay power consumed in each time slot in which the relays transmit. As $p_r(\mathbf{w}, a)$ is the transmit power in the third and the fourth time slot, we will refer to $p_r(\mathbf{w}, a)$ as the transmit power of one time slot. Note that the constraint $p_r(\mathbf{w}, a) \leq p_{r,\max}$ in (4.43) is convex as $p_r(\mathbf{w}, a)$ in (C.33) is expressed as the sum of the convex quadratic form $\mathbf{w}^H \mathbf{E}_r \mathbf{w}$ and the fraction of the convex quadratic form $\mathbf{w}^H \mathbf{D}_r \mathbf{w}$ and the linear term a, which is a convex function [73]. The same holds true for the condition $\sum_{r=1}^{R} p_r(\mathbf{w}, a) \leq P_{\text{R,max}}$ in (4.44), as the summation of convex functions leads to a convex function. The transmit power of the source during the four time slots is given by

$$\begin{aligned} P_{\text{S}}(\mathbf{w}, a) &= E\{|\alpha_1 s_1|^2\} + E\{|\alpha_1 s_2^*|^2\} + E\{|\alpha_3 s_1 + \alpha_4 s_2|^2\} \\ &\quad + E\{|-\alpha_4 s_1^* + \alpha_3 s_2^*|^2\} = 2/a + 2|\alpha_3|^2 + 2|\alpha_4|^2 \\ &= 2/a + \tilde{\mathbf{w}}_1^H \tilde{\mathbf{S}} \tilde{\mathbf{w}}_1 / a + \tilde{\mathbf{w}}_2^H \tilde{\mathbf{S}} \tilde{\mathbf{w}}_2 / a \\ &= 2/a + \mathbf{w}^H \mathbf{S} \mathbf{w} / a, \end{aligned} \tag{C.34}$$

where $\tilde{\mathbf{S}}$ is an $(R+1) \times (R+1)$ matrix, having 2 as its $R+1$th entry and zeros elsewhere and where $\mathbf{S} \triangleq \text{blkdiag}([\tilde{\mathbf{S}}, \tilde{\mathbf{S}}])$. Note that $P_{\text{S}}(\mathbf{w}, a)$ is a convex function of $\mathbf{w}$ and a.

As the sum powers of the relays in third and the fourth time slot are equal, the total transmit power of the relays and source $\mathcal{S}$ during four time slots is given by

$$P_{\text{T}}(\mathbf{w}, a) = P_{\text{S}}(\mathbf{w}, a) + 2 \sum_{r=1}^{R} p_r(\mathbf{w}, a). \tag{C.35}$$

Bibliography

[1] H. Yanikomeroglu, "Cellular multihop communications: infrastructure-based relay network architecture for 4G wireless systems," *Proceedings of the 22nd Biennial Symposium on Communications,* Queen's University, Kingston, Canada, June 2004.

[2] E. Dahlman, S. Parkvall, and J. Sköld, "LTE/LTE-Advanced for Mobile Broadband," Academic Press, 2011.

[3] T. Wirth, L. Thiele, T. Haustein, O. Braz, and J. Stefanik, "LTE amplify and forward relaying for indoor coverage extension," *IEEE 72nd Vehicular Technology Conference Fall,* vol. 147, pp. 1–5, Oct. 2010.

[4] V. Venkatkumar, T. Wirth, T. Haustein, and E. Schulz, "Relaying in long term evolution: Indoor full frequency reuse," *European Wireless (EW),* vol. 149, pp. 298–302, May 2009.

[5] T. Wirth, V. Venkatkumar, T. Haustein, E. Schulz, and R. Halfmann, "LTE-advanced relaying for outdoor range extension," *VTC2009- Fall,* Anchorage, USA, pp. 1–4, Sep. 2009.

[6] F. Fitzek, D. Angelini, G. Mazzini, and M. Zorzi, "Design and performance of an enhanced IEEE802.11 MAC protocol for ad hoc networks and coverage extension for wireless networks," *IEEE Wireless Communications,* vol. 10, no. 6, pp. 30 – 39, Dec. 2003.

[7] V. Stankovic, A. Host-Madsen, and Z. Xiong, "Cooperative diversity for wireless ad hoc networks," *IEEE Signal Process. Mag.,* vol. 23, pp. 37–49, Sep. 2006.

[8] I. Akyildiz, W. Su, Y. Sankarasubramaniam, and E. Cayirci, "Wireless sensor networks: a survey," *Computer Networks,* vol. 38, pp. 393–422, 2002.

[9] J. Carle and D. Simplot, "Energy efficient area monitoring by sensor networks," *IEEE computer,* vol. 37, pp. 40–46, Feb. 2004.

[10] I. F. Akyildiz, W. Su, Y. Sankarasubramaniam, and E. Cayirci, "A survey on sensor networks, *IEEE Commun. Mag.,* vol. 40, no. 8, pp. 102–114, Aug. 2002.

[11] M. Dohler and Y. Li, "Cooperative Communications: Hardware, Channel & PHY," Wiley and Sons, Feb. 2010.

[12] S. Chen, M. A. Beach, and J. P. McGeehan, "Division-free duplex for wireless applications," *Electronics Letters,* vol. 34, pp. 147–148, Jan. 22, 1998.

[13] J. N. Laneman, D. N. C. Tse, and G. W. Wornell, "Cooperative diversity in wireless networks: Efficient protocols and outage behavior," *IEEE Trans. Inform. Theory*, vol. 50, pp. 3062–3080, Dec. 2004.

[14] A. Sedonaris, E. Erkip, and B. Aazhang, "User cooperation diversity — Part I. System description," *IEEE Trans. Commun.*, vol. 51, pp. 1927–1938, Nov. 2003.

[15] A. Sedonaris, E. Erkip, and B. Aazhang, "User cooperation diversity — Part II. Implementation aspects and performance analysis," *IEEE Trans. Commun.*, vol. 51, pp. 1927–1938, Nov. 2003.

[16] Y. Jing and B. Hassibi, "Distributed space-time coding in wireless relay networks," *IEEE Trans. Wireless Commun.*, vol. 5, pp. 3524–3536, Dec. 2006.

[17] Y. Jing and H. Jafarkhani, "Distributed differential space-time coding for wireless relay networks," *IEEE Trans. Commun.*, vol. 56, pp. 1092–1100, July 2008.

[18] H. Mheidat, M. Uysal, and N. Al-Dhahir, "Equalization techniques for distributed space-time block codes with amplify-and-forward relaying," *IEEE Trans. Signal Process.*, vol. 55, pp. 1839–1852, May 2007.

[19] Y. Jing and H. Jafarkhani, "Network beamforming using relays with perfect channel information," *IEEE Trans. Inf. Theory,* vol. 55, no. 6, pp. 2499–2517, June 2009.

[20] G. Zheng, K.-K. Wong, A. Paulraj, and B. Ottersten, "Collaborative-relay beamforming with perfect CSI: Optimum and distributed implementations," *IEEE Signal Process. Lett.*, vol. 16, pp. 257–260, April 2009.

[21] P. Larsson, "Large-scale cooperative relaying network with optimal combining under aggregate relay power constraint," *Proc. of Future Telecommunications Conference*, 2003

[22] E. Koyuncu, Y. Jing, and H. Jafarkhani, "Distributed beamforming in wireless relay networks with quantized feedback," *IEEE J. Sel. Areas Commun.*, vol. 26, pp. 1429–1439, Oct. 2008.

[23] V. Havary-Nassab, S. Shahbazpanahi, A. Grami, and Z.-Q. Luo, "Distributed beamforming for relay networks based on second-order statistics of the channel state information," *IEEE Trans. Signal Process.*, vol. 56, pp. 4306–4316, Sept. 2008.

[24] S. Fazeli-Dehkordy, S. Shahbazpanahi, and S. Gazor, "Multiple peer-to-peer communications using a network of relays," *IEEE Trans. Signal Process.*, vol. 57, pp. 3053–3062, Aug. 2009.

[25] C. Hoymann, W. Chen, J. Montojo, A. Golitschek, C. Koutsimanis, and X. Shen, "Relaying operation in 3GPP, LTE: challenges and solutions," *IEEE Commun. Mag.* 50(2), pp. 156 –162, 2012.

[26] V. Havary-Nassab, S. Shahbazpanahi, and A. Grami, "Optimal distributed beamforming for two-way relay networks," *IEEE Trans. Signal Process.*, vol. 58, pp. 1238–1250, Mar. 2010.

[27] S. Shahbazpanahi and M. Dong, "A semi-closed form solution to the SNR balancing problem of two-Way telay network beamforming," *Proc. ICASSP'10*, Dallas, USA, Mar. 2010

[28] M. Zaeri-Amirani, S. Shahbazpanahi, T. Mirfakhraie, and K. Ozdemir, "Performance tradeoffs in amplify-and-forward bidirectional network beamforming," *IEEE Trans. Signal Process.*, vol. 60, no. 8, pp. 4196–4209, Aug. 2012.

[29] Z. Ding, W. H. Chin, and K. K. Leung "Distributed beamforming and power allocation for cooperative networks," *IEEE Trans. Wireless Commun.,* vol. 7, no. 5, pp.1817–1822, 2008.

[30] K. Phan, T. Le-Ngoc, S. A. Vorobyov, and C. Tellambura, "Power allocation in wireless multi-user relay networks," *IEEE Trans. Wireless Commun.,* vol. 8, no. 5, pp. 2535–2545, 2009.

[31] Yong Cheng and Marius Pesavento, "Joint Optimization of Source Power Allocation and Distributed Relay Beamforming in Multiuser Peer-to-Peer Relay Networks," *IEEE Trans. on Signal Processing,*, vol. 60, no. 6, pp. 2962 – 2973, June 2012.

[32] A. Schad, A.B. Gershman, and S. Shahbazpanahi, "Capacity maximization for distributed beamforming in one- and bi-directional relay networks," *Proceedings of the International Conference on Acoustics, Speech, and Signal Processing (ICASSP'11), Prague, Czech Republic,* pp. 2804–2807, May 2011.

[33] A. Schad and M. Pesavento, "Multiuser bi-directional communications in cooperative relay networks," *Proc. IEEE CAMSAP'11*, pp. 217 – 220, San Juan, Puerto Rico, Dec. 2011.

[34] A. Schad and M. Pesavento, "Time Division Multiple Access Methods in Bi-Directional Cooperative Relay Networks," *Proceedings of the IEEE Sensor Array and Multichannel Signal Processing Workshop,* pp. 89–92, Hoboken, USA, June 2012.

[35] C. Wang, H. Chen, Q. Yin, A. Feng, and A. Molisch, "Multi-user two-way relay networks with distributed beamforming," *IEEE Trans. Wireless Commun.,* vol. 10, no. 10, pp. 3460–3471, Oct 2011.

[36] A. Amah and A. Klein, "Pair-aware transceive beamforming for nonregenerative multi-user two-way relaying," *Proceedings of the International Conference on Acoustics, Speech, and Signal Processing (ICASSP'11), Prague, Czech Republic,* Mar. 2010, pp. 2506–2509.

[37] G. Sidhu, F. Gao, W. Chen, and A. Nallanathan, "A joint resource allocation scheme for multiuser two-way relay networks," *IEEE Trans. Commun.,* vol. 59, no. 11, pp. 2970–2975, Nov 2011.

[38] J. Joung and A. H. Sayed, "Multiuser two-way amplify-and-forward relay processing and power control methods for beamforming systems," *IEEE Transactions on Signal Processing,* vol. 58, pp. 1833–1846, Mar. 2010.

[39] A. Schad, K. Law, and M. Pesavento, "A convex inner approximation technique for rank-two beamforming in multicasting relay networks," *Proc. Eur. Signal Process. Conf.,* pp. 1369–1373, Aug. 2012.

[40] A. Abdelkader, M. Pesavento, and A.B. Gershman, "Orthogonalization Techniques for Single Group Multicasting in Cooperative Amplify-And-Forward Networks," *Proceedings of the Fourth International Workshop on Computational Advances in Multi-Sensor Adaptive Processing (CAMSAP2011),* San Juan, Puerto Rico, pp. 225–228, December 2011.

[41] N. Bornhorst, M. Pesavento, and A.B. Gershman, "Distributed Beamforming for Multi-group Multicasting Relay Networks," *IEEE Trans. on Signal Process.*, vol. 60, no. 1, pp. 221 – 232, 2011.

[42] J. Luo, R. S. Blum, L. J. Cimini, L. J. Greenstein, and A. M. Haimovich, "Decode-and-forward cooperative diversity with power allocation in wireless networks," *IEEE Trans. Wireless Commun.*, vol. 6, pp. 793–799, March 2007.

[43] T. Wang, A. Cano, G. B. Giannakis, and N. Laneman, "High- performance cooperative demodulation with decode-and-forward relays," *IEEE Trans. Commun.,* vol. 55, no. 7, pp. 1427–1438, July 2007.

[44] 3GPP TR 36.814 v9.0.0, "Further Advancements for EUTRA (Physical Layer Aspects)," Mar. 2010.

[45] D. Tse and P. Viswanath, "Fundamentals of wireless communication," Cambridge: Cambridge University Press, 2005.

[46] R. Wang and M. Tao, "Joint source and relay precoding design for MIMO two-way relaying based on MSE criteria," *IEEE Transactions on Signal Processing,* vol. 6, no. 3, pp. 1352–1365, Mar. 2012.

[47] R. Zhang, Y.-C. Liang, C. C. Chai, and S. Cui, "Optimal beamforming for two-way multi-antenna relay channel with analogue network coding," *IEEE Journal on Selected Areas in Communications,* vol. 27, no. 5, pp. 699–712, June 2009.

[48] X. Wang and X.-D. Zhang, "Optimal beamforming in MIMO two-way relay channels," *Proceedings IEEE Global Telecommunications Conference,* pp. 1–5, Miami, USA, 2010.

[49] F. Roemer and M. Haardt, "Algebraic Norm-Maximizing (ANOMAX) transmit strategy for Two-Way relaying with MIMO amplify and forward relays," *IEEE Signal Processing Letters,* vol. 16, pp. 909–912, Oct. 2009.

[50] F. Roemer and M. Haardt "A low-complexity relay transmit strategy for two-way relaying with MIMO amplify and forward relays," *Proceedings IEEE International Conference on Acoustics, Speech and Signal Processing (ICASSP'10),* pp. 3254–3257, Dallas, TX, Mar. 2010.

[51] J. Zhang, F. Roemer, and M. Haardt, "Beamforming design for multi-user two-way relaying with mimo amplify and forward relays," *Proceedings IEEE International Conference on Acoustics, Speech and Signal Processing (ICASSP'11),* pp. 2824–2827, Prague, Czech Republic, May 2011.

[52] A. Khabbazibasmenj, F. Roemer, S. A. Vorobyov, and M. Haardt, "Sum-rate maximization in two-way AF MIMO relaying: polynomial time solutions to a class of DC programming problems," *IEEE Transactions on Signal Processing,* vol. 60, no. 10, pp. 5478–5493, Oct. 2012.

[53] G. Li, Y. Wang, and P. Zhang, "Optimal linear MMSE beamforming for two way multi-antenna relay systems," *IEEE Communications Letters,* vol. 15, no. 5, pp. 533–535, May 2011.

[54] M. Zeng, R. Zhang, and S. Cui, "On design of collaborative beamforming for two-way relay networks," *IEEE Transactions on Signal Processing,* vol. 59, no. 5, pp. 2284–2295, May 2011.

[55] C. Li, L. Yang, and W.-P. Zhu, "Two-way MIMO relay precoder design with channel state information," *IEEE Transactions on Communications,* vol. 58, no. 12, pp. 3358–3363, Dec. 2010.

[56] K.-J. Lee, K. W. Lee, H. Sung, and I. Lee, "Sum-rate maximization for two-way MIMO amplify-and-forward relaying systems," *Proceedings IEEE Vehicular Technology Conference (VTC'09),* pp. 1–5, Spring, 2009.

[57] C. Shannon and W. Weaver, "The mathematical theory of communication," Univ. of IL Press, 1949.

[58] H. Chen, A. Gershman, and S. Shahbazpanahi, "Filter-and-forward distributed beamforming for relay networks in frequency selective fading channels," *Proc. ICASSP'09*, Taipei, Apr. 2009, pp. 2269–2272.

[59] H. Chen, A. B. Gershman, and S. Shahbazpanahi, "Filter-and-forward distributed beamforming in relay networks with frequency selective fading," *IEEE Trans. Signal Process.*, vol. 58, pp. 1251–1262, March 2010.

[60] Z. Zhou, S. Zhou, J. Cui, and S. Cui, "Energy-efficient cooperative communication based on power control and selective single-relay in wireless sensor networks," *IEEE Transactions on Wireless Communications,* vol. 7, no. 8, pp. 3066–3078, 2008.

[61] H. Al-Shatri and T. Weber, "Optimizing power allocation in interference channels using D.C. programming," *Proceedings of the Int. Symp. Modeling Optimization Mobile, Ad Hoc Wireless Netw.,* pp. 367–373, June 2010.

[62] K. Eriksson, S. Shi, N. Vucic, M. Schubert, and E. G. Larsson, "Global optimal resource allocation for achieving maximum weighted sum rate," in Proc. 2010 IEEE Global Telecommun. Conf.

[63] H. H. Kha, H. D. Tuan, and H. H. Nguyen, "Fast global optimal power allocation in wireless networks by local d.c. programming," *IEEE Trans. Wireless Commun.,* vol. 11, pp. 510–515, Feb. 2012.

[64] B. Song, Y.-H. Lin, and R. Cruz, "Weighted max-min fair beamforming, power control, and scheduling for a MISO downlink," *IEEE Trans. Wireless Commun.,* vol. 7, pp. 464–469, Feb. 2008.

[65] A. Khabbazibasmenj, S. A. Vorobyov, F. Roemer, and M. Haardt, "Polynomial-time DC (POTDC) for sum-rate maximization in two-way AF MIMO relaying," *Proc. IEEE ICASSP'12,* Kyoto, Japan, pp. 2889–2892, Mar. 2012.

[66] A. Khabbazibasmenj, F. Roemer, S. A. Vorobyov, and M. Haardt, "Sum-rate maximization in two-way AF MIMO relaying: Polynomial time solutions to a class of DC programming problems," *IEEE Trans. Signal Process.,* vol. 60, no. 10, pp. 5478–5493, 2012.

[67] H. H. Kha, H. D. Tuan, H. H. Nguyen, and T. T. Pham, "Optimization of Cooperative Beamforming for SC-FDMA Multi-user Multi-relay networks by tractable D.C. programming," *IEEE Trans. on Signal Process.,* vol. 61, pp. 467–479, Jan. 2013.

[68] A. H. Phan, H. D. Tuan, and H. H. Kha, "D.C. Iterations for SINR Maximin Multicasting in Cognitive radio," *Proc. IEEE ICSPCS'12,* pp. 1–5, Dec. 2012.

[69] G. Dartmann, E. Zandi, and G. Ascheid, "A modified Levenberg-Marquardt method for the bidirectional relay channel," available on http://arxiv.org/abs/1307.3121, Jul. 2013.

[70] G. Dartmann and G. Ascheid, "Equivalent quasi-convex form of the multicast max-min beamforming problem," *IEEE Trans. on Vehicular Tech.,* vol. 62, no. 9, pp. 4643–4648, Nov. 2013.

[71] A. B. Gershman, N. D. Sidiropoulos, S. Shahbazpanahi, M. Bengtsson, and B. Ottersten, "Convex optimization-based beamforming: From receive to transmit and network designs," *IEEE Signal Processing Magazine*, vol. 27, no. 3, pp. 62–75, May 2010.

[72] S. Shahbazpanahi, A. B. Gershman, Z-Q. Luo, and K. M. Wong, "Robust adaptive beamforming for general-rank signal models," *IEEE Trans. Signal Process.*, vol. 51, pp. 2257–2269, Sept. 2003.

[73] S. Boyd and L. Vandenberghe, *Convex Optimization*, Cambridge University Press, 2004.

[74] J. F. Sturm, "Using SeDuMi 1.02, a Matlab toolbox for optimization over symmetric cones,"*Optimization Methods and Software, Special issue on Interior Point Methods*, vol. 11/12, pp. 625–653, 1999.

[75] M. Grant, S. Boyd, and Y. Ye, "CVX: Matlab software for disciplined convex programming," available on http://www.stan- ford.edu/ boyd/cvx.

[76] "The MOSEK optimization toolbox for MATLAB manual. Version 7.0 (Revision 103)," available on http://docs.mosek.com/7.0/toolbox/.

[77] *MATLAB Optimization Toolbox.* U.K.: The Math Works Press, Aug. 2010, Release 2010 b.

[78] M. Bengtsson and B. Ottersten, "Optimal and suboptimal transmit beamforming," in *Handbook of Antennas in Wireless Communications*, L. C. Godara, Ed. Boca Raton, FL: CRC Press, ch. 18, Aug. 2001.

[79] W. K. Ma, T. Davidson, K. M. Wong, Z.-Q. Luo, and P. C. Ching, "Quasi-ML multiuser detection using semi-definite relaxation with application to synchronous CDMA," *IEEE Trans. Signal Process.*, vol. 50, pp. 912–922, Apr. 2002.

[80] L. Lei, J. P. Lie, A. B. Gershman, and C. M. S. See, "Robust adaptive beamforming in partly calibrated sparse sensor arrays," *IEEE Trans. Signal Process.*, vol. 58, pp. 1661–1667, March 2010.

[81] A. Beck and Y. C. Eldar, "Strong duality in noncovex quadratic optimization with two quadratic constraints," *SIAM J. Optimization*, vol. 17, No. 3, pp. 844–860, 2006.

[82] T. Rappaport *Wireless Communications: Principles and Practice*, Second Edition, Prentice Hall, 2002.

[83] Y. Liang, A. Ikhlef, W. Gerstacker, and R. Schober, "Cooperative filter-and-forward beamforming for frequency-selective channels with equalization," *IEEE Trans. Wireless Commun.,* vol. 10, no. 1, pp. 228– 239, Jan. 2011.

[84] Y. Liang, A. Ikhlef, W. Gerstacker, and R. Schober, "Filter-and-forward beamforming for multiple multi-antenna relays," *Proc. Int. ICST Conf. Commun. Netw. China (CHINACOM),* pp. 1–8, 2010.

[85] H. Chen, A. B. Gershman, and S. Shahbazpanahi, "Filter-and-forward distributed beamforming for two-way relay networks with frequency selective channels," *IEEE Proc. GlOCOM'2010,* pp. 1–5, Jan. 2010.

[86] Y. Liang, A. Ikhlef, W. Gerstacker, and R. Schober, "Two-way filter-and-forward beamforming for frequency-selective channels," *IEEE Trans, Wireless Commun.* vol. 10, pp. 4172–4183, Dec. 2011.

[87] H. Pilaram, M. Kiamari, B. H. Khalaj, "Distributed beamforming and base station post-processing in uplink relay OFDMA Comp asynchronous networks," to appear in *IEEE Proc. VTC Spring*, Dresden, Jun. 2013.

[88] D. Kim, J. Seo, and Y. Sung, "Filter-and-Forward Transparent Relay Design for OFDM Systems," submitted to *IEEE Trans. on Vehicular Technology,* Nov. 2012.

[89] S. M. Alamouti, "A simple transmitter diversity scheme for wireless communications," *IEEE J. Select. Areas Commun.,* vol. 16, pp.1451 – 1458, 1998.

[90] V. Tarokh, H. Jafarkhani, and A.R. Chalderbank, "Space Time Block Codes from orthogonal designs," *IEEE Trans. Information Theory,* vol. 45, no.5, pp. 1456–1467, July 1999.

[91] E.G. Larsson, P. Stoica, "Space-time block coding for wireless communications," Cambridge University Press, 2003.

[92] P. Viswanath, D. Tse, and R. Laroia, "Opportunistic beamforming using dumb antennas," *IEEE Trans. Inform. Theory,* vol. 48, pp. 1277–1294, Jun. 2002.

[93] M. Schubert and H. Boche, "Solution of the Multiuser Downlink Beamforming Problem with Individual SINR Constraints," *IEEE Trans. Vehic. Tech.*, vol. 53, Jan. 2004, pp. 18 – 28.

[94] N.D. Sidiropoulos, T.N. Davidson, and Z.-Q. Luo, "Transmit beamforming for physical-layer multicasting," *IEEE Trans. on Signal Process.*, vol. 54, no. 6, pp. 2239 – 2251, Jun. 2006.

[95] E. Karipidis, N. D. Sidiropoulos, and Z.-Q. Luo, "Quality of service and max-minfair transmit beamforming to multiple co-channel multicast groups,"*IEEE Trans. Signal Processing*, vol. 56, pp. 1268 – 1279, Mar. 2008.

[96] S.X. Wu, A.M. So, and W. Ma, "Rank-two transmit beamformed Alamouti space-time coding for physical-layer multicasting," *Proc. IEEE ICASSP'12*, pp. 2793 – 2796, Kyoto, Japan, Mar. 2012.

[97] S. Ji, S. X. Wu, A. M. So, and W. K. Ma, "Multi-Group Multicast Beamforming in Cognitive Radio Networks via Rank-Two Transmit Beamformed Alamouti Space-Time Coding," *Proc. ICASSP'13,* pp. 4409–4413, 2013.

[98] X. Wu, W. K. Ma, and A. M. So, "Physical-layer multicasting by stochastic transmit beamforming and Alamouti space-time coding," *IEEE Trans. on Signal Process.*, Vol. 61, No. 17, Sep. 2013.

[99] K. L. Law, X. Wen, and M. Pesavento, "General-rank Transmit Beamforming for Multi-group Multicasting Networks Using OSTBC", *Proc. IEEE SPAWC'13,* pp. 475–479, June 2013.

[100] X. Wen, K. L. Law, S. J. Alabed, and M. Pesavento, "Rank-two beamforming for single-group multicasting networks using OSTBC," *Proc. IEEE SAM'012*, pp. 69 – 72, Hoboken, USA, June 2012.

[101] Y. Silva and A. Klein, "Linear Transmit Beamforming Techniques for the Multigroup Multicast Scenario," *IEEE Trans. Vehicular Techn.* , vol. 58, pp. 4353 – 4367, 2009.

[102] A. Abdelkader, A.B. Gershman, and N. Sidiropoulos, N, "Multiple-Antenna Multicasting Using Channel Orthogonalization and Local Refinement," *IEEE Trans. Signal Processing*, vol. 58, pp. 3922 – 3927, 2010.

[103] N. Bornhorst, P. Davarmanesh, and M. Pesavento, "An extended interior-point method for transmit beamforming in multi-group multicasting," *Proc. EUSIPCO'12*, Bucharest, Romania, August 2012.

[104] Z.-Q. Luo and T.-H. Chang, "SDP relaxation of homogeneous quadratic optimization: Approximation bounds and applications," *in Convex Opt. in Signal Processing and Comm.,* D. P. Palomar and Y. C. Eldar, Eds. Cambridge University Press, ch. 4, pp. 117–162, 2010.

[105] Y. Jing and H. Jafarkhani, "Using orthogonal and quasi-orthogonal designs in wireless relay networks," *IEEE Trans. Inform. Theory,* vol. 53, pp. 4106–4118, Nov. 2007.

[106] J. M. Paredes, B. H. Khalaj, and A. B. Gershman, "Cooperative Transmission for Wireless Relay Networks Using Limited Feedback," *IEEE Trans. on Signal Process.*, vol. 58, pp. 3828–3841, 2010.

[107] B. Maham, A. Hjørungnes, and G. Abreu, "Distributed GABBA spacetime codes in amplify-and-forward relay networks," *IEEE Trans.Wireless Commun.,* vol. 8, no. 4, pp. 2036–2045, Apr. 2009.

[108] A. Schad, H. Chen, A.B. Gershman, and S. Shahbazpanahi, "Filter-and-forward peer-to-peer beamforming in relay networks with frequency selective channels,"*Proceedings of the International Conference on Acoustics, Speech, and Signal Processing (ICASSP'10),* Dallas, TX, USA, pp. 3246–3249 March 2010.

[109] A. Schad, B. Khalaj, and M. Pesavento, "Precoding in Relay Networks with Frequency Selective Channels," *Proceedings of the Asilomar Conference on Signals, Systems and Computers,* Pacific Grove, CA, Nov. 2012.

[110] H. Boche and M. Schubert, "Resource allocation in multi-antenna systems – Achieving max–min fairness by optimizing a sum of inverse SIR," *IEEE Trans. Signal Process.,* vol. 54, no. 6, pp. 1990–1997, Jun. 2006.

[111] W. Xu, X. Dong, and W.-S. Lu, "MIMO relaying broadcast channels with linear precoding and quantized channel state information feedback," *IEEE Trans. Signal Process.,* vol. 58, no. 10, pp. 5233–5245, Oct. 2010.

[112] S. J. Alabed, J. M. Paredes, and A. B. Gershman, "A simple distributed space-time coded strategy for two-way relay channels," *IEEE Trans. Wireless Comm.,* vol. 11, no. 4, pp. 1260 – 1265, Feb. 2012.

[113] T. Cui, F. Gao, T. Ho, and A. Nallanathan, "Distributed space-time coding for two-way wireless relay networks," *IEEE Trans. Signal Process.,* vol. 57, pp. 658–671, May 2009.

[114] S. Alabed, M. Pesavento, and A. Klein, "Non-coherent distributed space-time coding techniques for two-way wireless relay networks," *EURASIP special issue on Sensor Array Processing,* Jan. 2013.

[115] Y. Jing and H. Jafarkhani, "Distributed differential space-time coding in wireless relay networks," *IEEE Transactions on Wireless Communications,* vol. 56, pp. 1092–1100, July 2008.

[116] Z. Utkovski, G. Yammine, and J. Lindner, "A distributed differential space-time coding scheme for two-way wireless relay networks," *Proceedings IEEE International Symposium on Information Theory (ISIT'09),* Seoul, Korea, pp. 779–783, Jun. 2009.

[117] S. J. Alabed, M. Pesavento, and A. B. Gershman, "Distributed differential space-time coding techniques for two-way wireless relay networks," *Proceedings IEEE International Workshop on Computational Advances in Multi-Sensor Adaptive Processing (CAMSAP'11)*, San Juan, Puerto Rico, Dec. 2011.

[118] S. Alabed, M. Pesavento, and A. Klein, "Distributed differential space-time coding for two-way relay networks using analog network coding," *Proceedings IEEE European Signal Processing Conference (EUSIPCO'13),* Marrakech, Morocco, March 2013.

[119] T. Himsoon, W. Siriwongpairat, W. Su, and K. Liu, "Differential modulations for multinode cooperative communications," IEEE Transactions on Signal Processing, vol. 56, no. 7, July 2008.

[120] T. Himsoon, W. Su, and K. Liu, "Differential modulation for multi-node amplify-and-forward wireless relay networks," Wireless Communications and Networking Conference, vol. 2, pp. 1195–1200, 2006.

[121] T. Himsoon, W. Su, and K. Liu, "Differential transmission for amplify-and-forward cooperative communications," *IEEE Signal Processing Letters,* vol. 12, no. 9, Sep. 2005.

[122] Q. Zhao and H. Li, "Differential modulation for cooperative wireless systems," *IEEE Transactions on Signal Processing,* vol. 55, pp. 2273–2283, May 2007.

[123] S. J. Alabed and M. Pesavento, "A Simple Distributed Differential Transmit Beamforming Techniques for Two-Way Wireless Relay Networks," *Proc. IEEE/ITG Workshop Smart Antennas (WSA 2012),* pp. 243–247, Dresden, Mar. 2012.

[124] Q. Liu, W. Zhang, X. Ma, and G. T. Zhou, "A practical amplify-and-forward relaying strategywith an intentional peak power limit," *ICASSP'10,* pp. 2518–2521, Dallas, TX, Mar. 2010.

[125] Q. Liu, W. Zhang, and X. Ma, "Practical and general amplify-and-forward designs for cooperative networks," *INFOCOM'2010*, pp. 1999–2007, San Diego, CA, Mar. 2010.

[126] M. K. Varanasi, "A Systematic Approach to the Design and Analysis of Optimum DPSK Receivers for Generalized Diversity Communications over Rayleigh Fading Channels," *IEEE Transactions on Communications,* vol. 47, No. 9, pp. 1365–1375 Sept. 1999.

[127] F. Adachi, "Postdetection optimal diversity combiner for DPSK differential detection," *IEEE Transactions on Vehicular Technology,* vol. 42, pp. 326–337, Aug. 1993.

[128] C. Chung, "Differentially amplitude and phase-encoded QAM for the correlated Rayleigh-fading channel with diversity reception," *IEEE Transactions on Communications,* vol. 45, pp. 309–321, Mar. 1997.

[129] H. Liu and G. Xu, "Multiuser blind channel estimation and spatial channel pre-equalization," *Proc. ICASSP'95,* pp. 1756–1759, Detroit, MI, May 1995.

[130] G. G. Raleigh, S. D. Diggavi, V. K. Jones, and A. Paulraj, "A blind adaptive transmit antenna algorithm for wireless communications," *in Proc. ICC'95,* vol. 3, p. 1949, 1995.

[131] P. Mongensen, F. Frederiksson, J. Wigard, and S. Peterson, "A research study of antenna diversity and data receivers for DECT," *Proc. Nordic Radio Symp.,* Slatsjobaden, Sweden, Apr. 1995.

[132] B. Khoshnevis, W. Yu, and R. Adve, "Grassmannian beamforming for MIMO amplify-and-forward relaying," *IEEE J. Sel. Areas Commun.,* vol. 26, no. 8, pp. 1397–1407, Oct. 2008.

[133] V. Havary-Nassab, S. Shahbazpanahi, and A. Grami, "Joint receive-transmit beamforming for multi-antenna relaying schemes," *IEEE Trans. Signal Process.,* vol. 58, pp. 4966–4972, Sep. 2010.

[134] J. R. Taylor, An Introduction to Error Analysis. Mill Valley, CA: Univ. Science Books, 1982.

[135] Y. Nesterov and A. Nemirovskii, *Interior-point polynomial methods in convex programming,* PA: SIAM, 1994.

[136] M. Grant and S. Boyd, *cvx Users' guide,* http://cvxr.com/cvx/cvx_usrguide.pdf, Apr. 2011.

[137] J. Boccuzzi, "Signal Processing for Wireless Communications," McGraw Hill, New York, 2008.

[138] D. S. Baum, J. Hansen, and J. Salo, "An interim channel model for beyond-3G systems: Extending the 3GPP spatial channel model," in *Proc. IEEE Veh. Technol. Conf.,* vol. 5, pp. 3132–3136, Jun. 2005.

[139] J. C. Haartsen, "Impact of non-reciprocal channel conditions in broadband TDD systems,"*Proc. IEEE PIMRC'08,* pp. 1–5, Sep. 2008.

[140] R. Horst and N. V. Thoai, "Dc programming: Overview," *J. Optim. Theory Appl.,* vol. 103, no. 1, pp. 1–43, Oct. 1999.

[141] B. K. Sriperumbudur and G. R. G. Lanckriet, "On the convergence of the concave-convex procedure," *Neural Inf. Process. Syst.,* pp. 1–9, 2009.

[142] H. A. Le-Thi and T. Pham-Dinh, "Large scale molecular optimization from distance matrix by a d.c. optimization approach," *SIAM J. Optim.,* vol. 14, pp. 77–117, Jan. 2003.

[143] L. T. H. An and P. D. Tao "The DC (difference of convex functions) programming and DCA revisited with DC models of real world nonconvex optimization problems," *133. Annals of Operations Research,* pp. 23–46, 2005.

[144] H. Tuy, "Convex Analysis and Global Optimization," Boston: Kluwer Academic Publishers, 1998.

Curriculum Vitae

Personal

Name:	Adrian Schad
Date and place of birth:	27.07.1982, Schweinfurt, Germany

Education

10.2003–10.2008	Diploma in Electrical Engineering, Friedrich-Alexander-Universität Erlangen-Nürnberg, Germany. *Thesis*: "Optimization of the Least-Squares Frequency-Invariant Beamformer (LS-FIB) Design".
10.2007–03.2008	Prediploma in Mathematics, Friedrich-Alexander-Universität Erlangen-Nürnberg, Germany.
04.2009–10.2011	Diploma in Mathematics, Technische Universität Darmstadt, Germany. *Thesis*: "Solutions to the broadcasting problem".
02.2009–03.2014	PhD student, Communication Systems Group, Technische Universität Darmstadt.

Award

Finalist of the best student paper contest for the paper "Time Division Multiple Access Methods in Bi-Directional Cooperative Relay Networks," 7th IEEE Sensor Array and Multichannel Signal Processing Workshop, Hoboken New Jersey, pp. 89–92, June 2012.